AN ABSTRACT OF THE THESIS OF

Xiao Li for the degree of Doctor of Philosophy. in Mechanical Engineering presented on September 3, 1996.

Title: Design Of Advanced Aluminum Silicon Alloy Compositions And Processing

Redacted for Privacy

Abstract approved: _____

Michael E. Kassner

Part I discusses the development of an aluminum-magnesium-silicon alloy that may combine strength, extrudability, favorable corrosion resistance with low cost and scrap compatibility. The first part of the study determined the effects of small composition, heat treatment and mechanical processing changes on the ambient temperature tensile properties of the alloy. A combination of magnesium and silicon of about 2%, 1% copper, 0.2% chromium and 0.1% vanadium can produce a T6 alloy with significant higher strength, fatigue and corrosion fatigue properties for both ingot and extrusion than those of 6061 but with only a modest increase in cost. The new alloy has been designated as AA6069. The second part of the study determined the T6 properties of 6069 alloy. The tensile test results of cold and hot extrusions of hollow, solid bars, and high pressure cylinders indicate that the T6 properties ranged from 55-70 ksi (380-490 MPa) UTS, 50-65 ksi (345-450 MPa) yield strength, and 10-18% elongation. It also appears that the fracture toughness and general corrosion resistance in saline environment are comparable or better than those of 6061 T6.

Part II attempted to evaluate the formation, formability, thermal and mechanical properties of semi-solid A356, A357 and modified aluminum silcon semi-solid alloys. The semi-solid alloy microstructure was produced in this study by purely thermal treatment rather than conventional and expensive electromagnetic or mechanical stirring. Three heat-up stages in semi-solid treatment were evaluated. Stage I is related to the heating of the alloy in the solid state. Stage II is related to the eutectic reaction. Stage III is related to the heating of the semi-solid slurry. Stage II requires the longest time of the three heat-up stages due to the endothermic reaction on heating. An increase of furnace temperature can greatly reduce the time of stage II. The atmosphere (vacuum, air, argon) of the semi-solid treatment does not appear to greatly affect the T6 properties of semi-solid alloys. The microstructure and T6 properties of semi-solid A356 do not appear sensitive to the homogenization treatments before semi-solid treatment. The porosity of semi-solid ingots and pressed parts increases as the cooling rate decreases in unformed and subsequent-to-moderate pressure forming. The T6 properties basically appear sensitive to voids, with a degradation of properties as the void concentration increases. The formability of A357 may be improved as the spheroidal particle size decreases. Hence, formability may improve with decreasing ingot grain size. The mechanism of coarsening of the solid phase at isothermal temperatures is related to Ostwald ripening and/or "merging" of particles. The mechanical properties of die-casting parts show that the method of thermal treatment to produce a spheroidal microstructure is an effective method for industrial production of semi-solid aluminum-silicon alloys.

Design Of Advanced Aluminum Silicon Alloy Compositions And Processing

by

Xiao Li

A THESIS

submitted to

Oregon State University

in partial fulfillment of
the requirements for the
degree of

Doctort of Philosophy

Completed Semptember 3, 1996

Commencement June 1997

Doctor of Philosophy thesis of Xiao Li presented on Septemper 3 , 1996

APPROVED:

Redacted for Privacy

Major Professor, representing Mechanical Engineering

Redacted for Privacy

Head of Department of Mechanical Engineering

Redacted for Privacy

Dean of Graduate School

I understand that my thesis will become part of the permanent collection of Oregon State University libraries. My signature below authorizes release of my thesis to any reader upon request.

Redacted for Privacy

Xiao Li, Author

ACKNOWLEDGMENTS

This study was supported by the Northwest Aluminum Company through the Oregon Metals Initiative which has received funds from the Oregon Economic Development Department, U.S. Bureau of Mines and OJGSE. Discussions and help from other members of our research group, especially fatigue and corrosion fatigue tests performed by Mr. Michael Delos-Reyes, Mr. Troy Hayes and Ms. Robyn Faber, are highly appreciated. I would like to thank my wife Jun Xiao for her enduring support over the duration of this study. Finally, I am extremely thankful to Prof. M.E. Kassner for his all warm guidance and help to me with which this thesis was made possible.

TABLE OF CONTENTS

TABLE OF CONTENTS (CONTINUED)

LIST OF FIGURES

LIST OF FIGURES (CONTINUED)

LIST OF FIGURES (CONTINUED)

LIST OF FIGURES (CONTINUED)

LIST OF FIGURES (CONTINUED)

LIST OF FIGURES (CONTINUED)

LIST OF TABLES

LIST OF TABLES (CONTINUED)

LIST OF TABLES (CONTINUED)

Design Of Advanced Aluminum Silicon Alloy Composition And Processing

Chapter I.

INTRODUCTION

A unique combination of properties makes aluminum and its alloys the second most widely used material, after iron and its alloys, in the world. 6xxx aluminum alloys, possessing the common good characters such as high strength-weight ratio, good electrical and thermal conductivity, favorable corrosion resistance and good workability, have become one of the most important commercial alloys in the aluminum industry. 6xxx aluminum alloys, consisting of magnesium and silicon (principal alloy elements) and other additional elements (copper, iron, chromium, titanium and vanadium), usually require heat-treatment to obtain optimum properties. Fig.1 illustrates the common production process of 6xxx aluminum alloys [1-3]. Alloying, homogenization and heat treatment are main factors that affect the mechanical properties of the alloy [4-7].

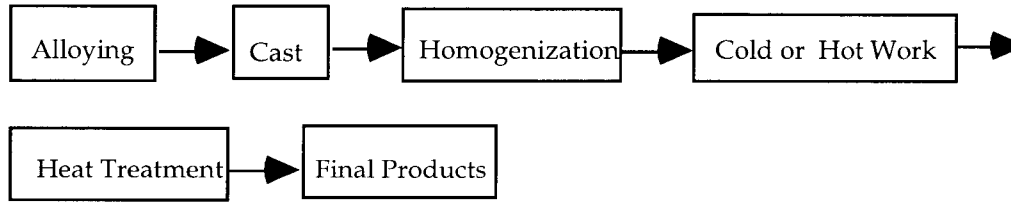

Fig.1 The production process of 6xxx Al alloys

Alloying. The predominant reason for alloying is to increase the strength of materials [8-15].

Al-Mg_2Si: 6xxx aluminum alloys contain up to 1.5% each of magnesium and silicon in the approximate ratio of 1.73:1 (wt %) to form incoherent Mg_2Si which is the main hardening phase in the alloys. The maximum solubility of Mg_2Si in aluminum matrix

is 1.85 wt%. Precipitation, upon age hardening, occurs by formation of G-P zones followed by fine incoherent precipitation, which increases the strength of 6xxx group. 6xxx alloys can be divided into three groups. In the first group, the total amount of magnesium and silicon does not exceed 1.5 wt%. Typical of this group is 6063, which is widely used in extruded architectural sections. Because of its low solution heat-treating temperature and low quench sensitivity, this alloy does not need a separate solution treatment after hot extrusion but may be air-quenched and artificially aged to obtain the required properties. The second group nominally contains 1.5 wt% or more magnesium and silicon which has a higher strength compared to first group. Because of a higher amount of alloying elements, this group requires a separate solution treatment followed by rapid quenching and artificial aging. Typical of this group is structural alloy 6061. The third group contains an amount of Mg_2Si overlapping the first two but with a substantial excess silicon. An excess of Si (for example, 0.2 wt%) increases the strength as second phase particle. Larger amount of excess silicon are less beneficial because segregation of silicon to the grain boundaries causes intergranular fracture in the alloys. The typical alloys of this group are 6009, 6010 and 6351.

Copper: Small amount of copper (up to 0.3 wt%) is added to increase the strength by coherent precipitation hardening (usually as $CuAl_2$) in 6xxx aluminum alloys. Copper additions generally increase cost.

Iron: The solubility of iron in aluminum is very low (about 0.05 wt%). Therefore, most of the iron present in aluminum over this amount appears as an intermetallic second phase in combination with aluminum and often other elements, which provides a slight increase in strength and better mechanical properties at moderately elevated temperature.

Chromium: Chromium has a low diffusion rate and forms finely dispersed phase in wrought products. Therefore, chromium can be used to prevent grain growth and recrystallization during hot working or heat treatment and slightly increase strength of 6xxx groups.

Titanium: Titanium is used primarily as grain refiner of aluminum castings and ingots.

Vanadium: Vanadium and aluminum can combine as the intermetallic VAl_{11}, which has a grain-refining effect during solidification. The recrystallization temperature is also raised by vanadium.

Beryllium: Beryllium is used in aluminum alloys containing magnesium to reduce oxidation at elevated temperatures. Oxidation and discoloration of wrought aluminum products are greatly reduced by small amounts of beryllium because of the diffusion of beryllium to the surface and formation of an oxide.

Homogenization. The initial thermal operation applied to ingots prior to hot working is referred to as "ingot preheating" or "homogenization" and has one or more purposes depending on the alloy, product, and fabricating process as involved. It consists of three steps: heating to homogenization temperature, a soak at the homogenization temperature, and cooling to ambient temperature. The principal objective of homogenization for 6xxx aluminum alloys is to improve hot workability by eliminating the initial cast structure. The microstructure of aluminum-magnesium-silicon alloys in the as-cast condition is a cored dendritic structure. As-cast structures generally have inferior workability and heterogeneous distribution of alloying elements. Solution of the intermetallic phases rejected interdendritically during solidification by the homogenization operation is only one step toward providing maximum workability. Because most of the solute is in solid solution after heating and soaking, further softening and improvement in workability can be obtained by slow cooling, to reprecipitate and coalesce the solute as fairly large particles [16,17]. Greatly extended homogenizing periods result in a higher rate of extrusion and in an improved surface appearance of extruded products. Therefore, the soaking temperature and time as well as cooling rate greatly affect the workability of 6xxx aluminum alloys [5]. Although the study of homogenization is very important, the methods used to study homogenization of cast structures for improved workability were developed

chiefly by empirical methods, correlated with optical metallographic examinations, to determine the time and temperature required to minimize coring and dissolve the second-phase particles. Because of the differences in alloy composition and casting methods, it is necessary to find optimum homogenization cycle for each alloy and processing method.

Heat Treatments. In general, heat treatments determine the final mechanical properties of these materials. Solution heat treating, quenching and aging are basic heat treatments for 6xxx aluminum alloys. The proper selection of these heat treatments can achieve optimum combination of strength and ductility of the material.

A. Solution Heat Treating. The purpose of solution heat treatment is to put the maximum practical amount of hardening solutes such as magnesium, silicon, and copper into solid solution in the aluminum matrix. For 6xxx alloys, the solution temperature at which the maximum amount is soluble corresponds to a eutectic temperature. Overheating and partial melting must be avoided. The time required for solution heating depends on the type of product, alloy elements, casting or fabricating procedure used and thickness insofar as it influences the pre-existing microstructure. The main consideration is the coarseness of the microstructure and the diffusion distances required to bring about a satisfactory degree of homogeneity.

B. Quenching. Quenching is another important step in the sequence of the heat treating operation. The purpose of quenching is to preserve the solid solution formed at the solution heat treating temperature by rapidly cooling to some lower temperature, usually near room temperature. Quenching not only retains solute atoms in solid solution, but also maintains a certain minimum number of vacancies that assist in promoting the low temperature diffusion required for precipitation within a reasonable time. The rapid quenching rates improve the strength . The degree of distortion that occurs during quenching and the magnitude of residual stress that develops in the products tends to increase with the rate of cooling. In addition, the maximum attainable quench rate decreases as the thickness of the product increases. Because of these effects, much work [18-25] has

been done over the years to understand and predict how quenching conditions and product form influence properties. Water is the most widely used and most effective quenching medium. Cooling rates can be reduced by increasing water temperature.

C. Aging. The purpose of aging is to increase strength and resistance to corrosion by forming GP zones and precipitating second-phase particles from solid solution obtained from quenching. There are two types of aging for 6xxx aluminum alloys: natural aging and artificial aging. Most of the heat treatable alloys exhibit age hardening at room temperature after quenching, called natural aging. Microstructural changes accompanying natural aging are difficult to detect without transmission election microscopy because the hardening effects are attributable solely to the formation of a zone structure within the solid solution. Most of the strengthening at room temperature occurs within a few hours after quenching for most 6xxx aluminum alloys [4,7]. The mechanical properties are usually essentially stable after four days at room temperature. 6xxx alloys stored under refrigeration can retard aging. Fig.2 shows the aging characteristics of 6061 aluminum alloy at ambient and sub-ambient temperature.

The hardening observed at room temperature is attributed to localized concentrations of magnesium and silicon atoms forming Guinier-Preston zones [4,5]. The number of GP zones increases with time, until in the fully aged condition. The electrical and thermal conductivities decrease with the progress of natural aging. Because a reduction of solid solution solute content normally increases electrical and thermal conductivities, the observed decreases are regarded as significant evidence that natural aging is a progress of zone formation, not true precipitation.

By reheating the quenched material to an elevated temperature, the solute content will be precipitated from the solid solution, called artificial aging which greatly affects the mechanical properties of 6xxx aluminum alloys. A characteristic feature of artificial aging effects on tensile properties is that the increase in yield strength is more pronounced than the increase in tensile strength. Also, ductility and toughness decrease [4,5,9] as compared

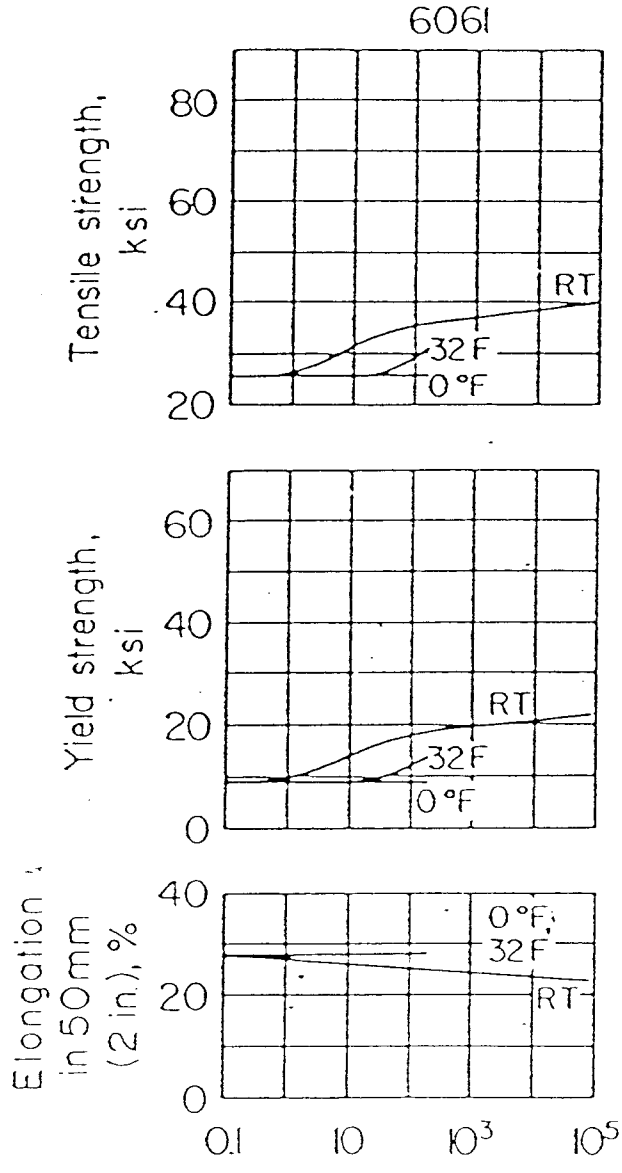

Fig.2 The aging characteristics of aluminum alloys at room temperature, 0°C, and -18°C [5].

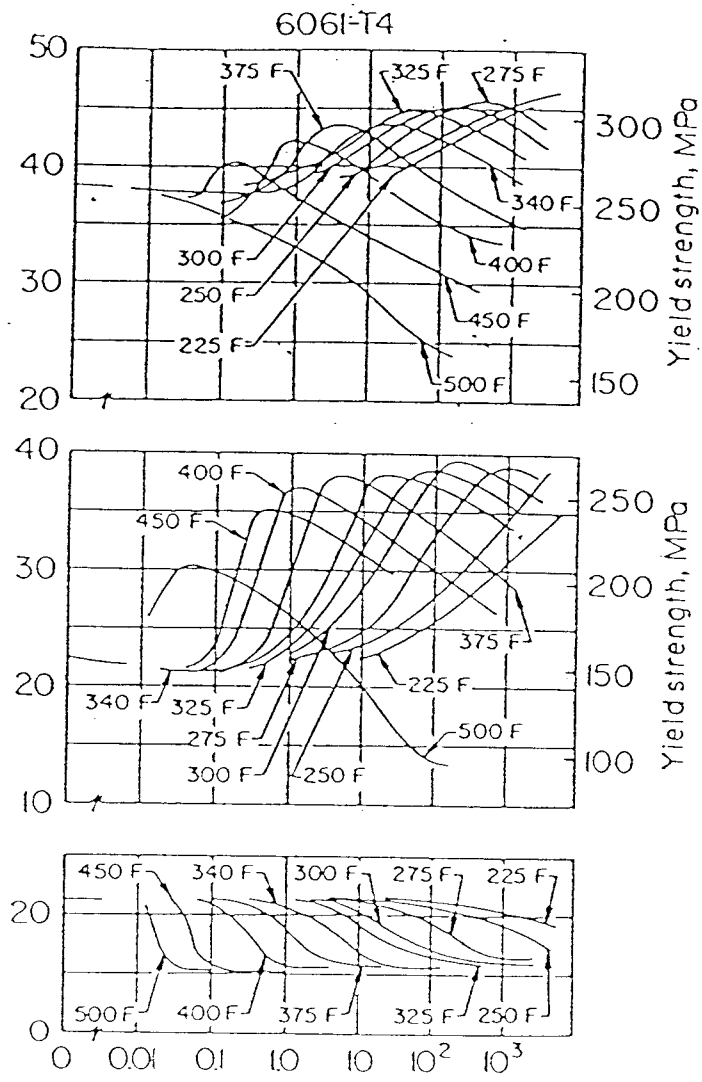

Fig.3 The aging characteristics of two aluminum alloys at elevated temperatures [5].

to saturated solution. Overaging decreases both the tensile and yield strengths, but ductility generally is not recovered in proportion to the reduction in strength, so that the combinations of these properties developed by overaging are considered inferior to those prevalent in the underaged condition. Fig.3 illustrates the aging characteristics of 6061 aluminum alloy at elevated temperatures. Some of the important features illustrated are: a.) hardening can be retarded, or suppressed indefinitely, by lowing the temperature. b.) the rates of hardening and subsequent softening increase with increasing temperature. c.) over the temperature range in which a maximum strength can be observed, the level of the maximum generally decreases with increasing temperature. The mechanisms of artificial aging hardening differ from those of natural aging hardening. For aluminum-magnesium-silicon alloys at temperature up to 200°C for short times, the initial spherical GP zones are converted to needlelike forms. Further aging causes apparent three-dimensional growth of the zones to rod-shaped particles (β') with a structure corresponding to a highly ordered Mg_2Si. At higher temperatures, this transition phase, designated β', undergoes diffusionless transformation to the equilibrium Mg_2Si. No direct evidence of coherency strain is found in either the zone or transition precipitate stages. It has been suggested that the increased resistance to dislocation motion arises from the increased energy required to break magnesium-silicon bonds as dislocations pass through them. The structure sequence may be diagrammed:

$$SS \longrightarrow GP \longrightarrow \beta'(Mg_2Si) \longrightarrow \beta(Mg_2Si)$$

Age hardening mechanisms have been studied over many decades [7, 26-32]. At relatively low temperatures and during initial periods of artificial aging at moderately elevated temperatures, the principal change is the redistribution of solute atoms within the solid-solution lattice to form GP zones. The strengthening effect of the zones results from the additional interference with the motion of dislocations when they cut the GP zones. The progressive strength increase with natural aging time has been attributed to an increase

in the size of the GP zones in some systems and to an increase in their number in others. As aging temperature or time are increased, transition precipitation occurs. The strengthening effects of these transition structures are related to the impedance to dislocation motion provided by the precipitate particles. Strength continues to increase as the size of these precipitates increases as long as the dislocations continue to cut the precipitates. Further progress of the precipitation reaction causes the structure of the precipitate to change from transition to equilibrium form. At this time, strengthening effects are caused by the stress required to cause dislocations to loop around rather than cut the precipitates. Strength progressively decreases with growth of equilibrium phase particles and an increase in interparticle spacing.

The general purpose of this study is to develop an aluminum-magnesium-silicon alloy that may combine strength, extrudability, favorable corrosion resistance with low cost and scrap compatibility. The effects of small composition, heat treatment and mechanical processing changes on the ambient temperature tensile properties of the alloy will be studied. Favorable properties in comparison to 6061 will be emphasized.

The semi-solid metal (SSM) process, a manufacturing method that can be used for forming a wide variety shapes of alloys, is based on a discovery made by researchers at MIT in 1971. Spencer et al. [33] found that Sn-15% Pb alloy in the liquid/solid temperature range exhibited remarkably low shear strength, even at relatively high solid fraction, when the alloy was vigorously agitated. The grain structure obtained in their experiments was spheroidal (nondendritic), and the material behaved in a rheological manner; that is, the more the semi-solid was deformed and became spheroidal, the easier the deformation became. This forming process was named "rheocasting" to signify this distinctive behavior of the material. Many studies have been conducted on the fundamental and engineering aspects of the SSM process. They have shown that SSM applies most engineering alloy families, including aluminum [34], zinc [35], magnesium [36], copper [37], iron [38], titanium [39] and superalloys [40].

Compared to normal casting and forming processes, the SSM process has many advantages. The lower temperature of SSM allows higher speed continuous casting and part forming with lower mold erosion and energy consumption compared to liquid casting. The higher viscosity of the slurry can reduce oxides and gas entrapment. Further, SSM is associated with less casting shrinkage, fewer voids and a finer grain structure in the resulting solid. Lastly, SSM provides for easy creation of composites [41].

Although the SSM process has been researched for about 20 years, there is still much that is not understood about the mechanisms of structure formation or the rheology of semi-solid materials. The following is a summary of the basic studies of the SSM process, especially relevant to study the thermal properties of semi-solids and the mechanical behavior of solidified semi-solids.

The main method for studying the rheological properties of semi-solid materials is based on the process developed and used in the original MIT experiments. This process consists of [33]:

1. Heating the alloy into the liquid region.
2. Cooling the alloy while continuously stirring it.
3. Measuring the force required to maintain the stirring action.

A high temperature Couette viscometer [33] was used to perform the experiments, as shown in Figure 13. The liquid or liquid-solid mixture resides in an annular space between an outer cylinder (cup) and an inner cylinder (bob). Rotating the cup while the bob is held stationary produces shear stresses within the semi-solid which can be measured. These shear stresses, t, as well as the apparent viscosity h , and average shear rate $\dot{\gamma}$ are calculated from [42]:

$$\eta = \frac{M(1-k^2)}{4\pi L\Omega_0 R_0^2 k^2} \qquad (1)$$

$$\dot{\gamma} = \frac{2\Omega_0 k}{1-k^2} \qquad (2)$$

$$\tau = \frac{M}{AR_i} \qquad (3)$$

where M is the torque on the inner cylinder, L is the length of the inner cylinder, k is the ratio of the inner cylinder to that of outer, W_0 is the rotation speed, R_0 is the radius of the outer cylinder, R_i is the radius of the inner cylinder and A is the area of the inner cylinder over which shear occurs. Various rotation speeds, times and temperatures are utilized to study the rheological properties of liquid and semi-solid materials.

Although there is much debate on the details of the process, it is generally accepted that the rheocasting process is based on the thixotropic behavior of metallic slurries. In thixotropic behavior, viscosity decreases as shear stress increases and is explained in terms of the structure build-up and breakdown of particles during stirring. Investigations [41,43-55] indicated that at the onset of the solidification during stirring, small dendrites are the primary nucleation particles. As the temperature drops, these small dendrite nuclei do not grow beyond a certain size (i.e. about 50-100mm for Al-Cu alloys); the fraction of solid, f_S, increases mainly by nucleation, called secondary nucleation, and small grains can be obtained. It is generally accepted that vibration, low pouring temperature and externally induced convection promote grain refinement primarily by a dendrite fragmentation mechanism, but there is not yet agreement the basic mechanism [41].

Vogel [43,54] proposed that the stirring changes the dendritic microstructure into a microstructure of finely dispersed, and almost spherical, solid particles during the initial stage of the rheocasting (stir casting) process. He suggested that the initial formation of grain boundaries in single crystal dendrites occurred by plastic bending of secondary dendrite arms, followed by recrystallization to give a grain boundary. The new polycrystalline dendrite could be fragmented through either liquid phase wetting, if

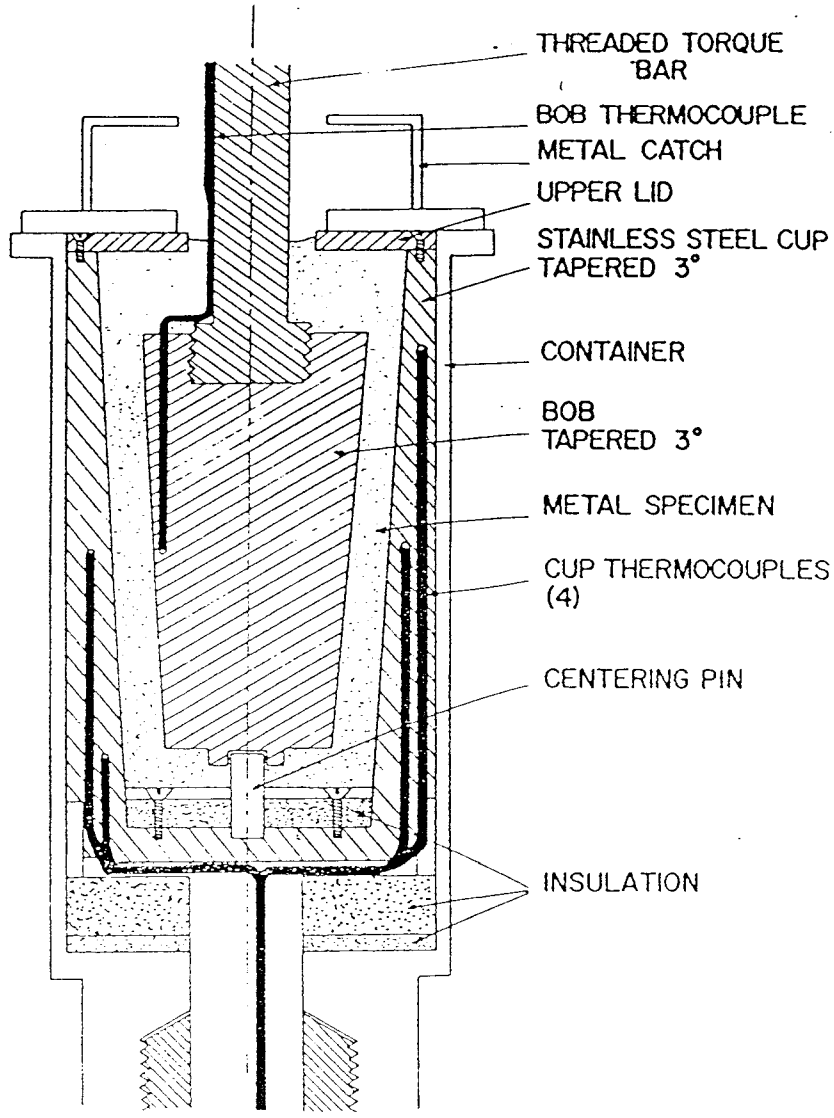

Figure 4. The diagram of High Temperature Couette Viscometer [33].

$s_{gb}>2s_{sl}$, or by grain boundary sliding. Agglomeration of groups of particles could occur by a sintering mechanism where grain boundaries form by contact, if $s_{gb}<2s_{sl}$. This model predicted two types of grain boundaries: one formed by solid state recrystallization; the other by sintering of solid particles. Both types of boundaries have been found in various alloys [43-44]. As the stirring is continued, and the dendritic microstructure is destroyed, the particles become spheriodal in shape and the opportunity for particle deformation, and thus particle fracture, lessens.

Garabedian et al. [53] considered that the refinement is caused by dendrite arm fracture, in which arms shear off as a result of the force on the arm from the fluid flow. Doherty et al. [54,49], like Vogel, considered that the mechanism is the recrystallization of the dendritic arms at their roots, as a result of the stress introduced by the fluid flow, forming new grain boundaries with rapid liquid penetration along the new grain boundary, removing the arm from its "mother grain". Katlamis [55] believed that the mechanism of refinement was the normal ripening of the arm at its root, in which the fluid flow altered or accelerated the solute diffusion and carries the dendrite arm away to where it can grow as a new grain.

In a study of Pb-Sn alloy, Wan et al. [56-57] found that the mechanism described by Vogel is only applicable to the earlier stages of stirring, in which the primary particles are still dendritic. When the particles assumed a spherical shape, the melting of grain boundaries did not appear to be a significant mechanism. "Ostwald ripening" and coalescence due to the collision of primary particles followed by sintering would be the two predominant shape change mechanisms. Ostwald ripening, first described by Ostwald [58] and developed by Lifshitz and Slyozov [59] and Wagner [60], occurs to minimize surface energy. There is a disappearence of the solid phase in regions with an extreme curvature leading to a reduction in the number of small particles and a growth of larger ones. The only mechanism of particle coarsening will be Ostwald ripening if particles never make contact. Coalescence would be described as a process where two or more particles became

interconnected by a solid neck and spheroidized by material transport to the neck region [61]. Theoretical and experimental analysis has shown that Ostwald ripening can be described by the following equation [59-60,62]:

$$(r)^n-(r_o)^n = kt \qquad (4)$$

where r and r_o are the average particle radius during the development and at the onset of coarsening, respectively, n is a coarsening exponent and k is a coarsening rate constant proportional to the shear rate, $\dot{\gamma}^{1/3}$, and the diffusion coefficient, $D^{2/3}$. For the rheocasting (stir cast) process, the coarsening exponent n is equal to 7/3. In the rheocasting of a Pb-37%Sn alloy, the contributions of Ostwald ripening and coalescence are the potential coarsening mechanisms of the solid phase [62]. If the semi-solid is allowed to coarsen without stirring, n has been found to be equal to 3 [63-72], which means that the Ostwald ripening maybe the main coarsening mechanism.

Viscosity, the main rheological property of semi-solid material, is greatly affected by shear stress, shear rate, agitation time, fraction solid and isothermal time. When the viscosity of a semi-solid metal slurry is measured during continuous cooling, it is found to strongly decrease with increasing shear rate. A simple and widely used relation applicable over wide ranges of shear rate is the power law relationship:

$$\eta = c\dot{\gamma}^{m-1} \qquad (5)$$

where h is viscosity, $\dot{\gamma}$ is shear rate, m is the power-law index, and c is the "consistency". For most semi-solid metal slurries, the value of m is smaller than 1. The values of c and m for aluminum alloys are 30 Pa·(s^m) and 0.1, respectively [73].

Viscosity is also strongly dependent on cooling rate in a semi-solid metal slurry, decreasing with decreasing cooling rate. The relationship between viscosity, shear rate, and cooling rate can be understood from structure changes. Many investigations [33,74-88] indicated that both increasing shear rate and decreasing cooling rate resulted in more dense, and spherical particles which moved more easily past one another, resulting in decreasing

viscosity. Further, the ratio of liquid and solid phase can affect the viscosity of semi-solid metal slurry. The viscosity increases as the fraction of solid increases.

Another process for producing the semi-solid has been developed for industrial production, based on reheating an as-cast ingot to the semi-solid temperature which, apparently, allows the resulting solids to be become spheroidal. When the material is reheated to the semi-solid temperature range, the solid phase, in an attempt to reduce surface area, may become large spheroids through Ostwald ripening and/or particle coalescence [89-90]. The typically large diameter solid phase that results from reheating a typical cast structure is, however, not favourable to injection molding requirements [89]. It is therefore necessary to reduce solid phase particle size before forming. Three methods have been used to achieve this in aluminum alloys. First is the strain induced, melt activated (SIMA) type process [34,41], in which the cast material is plastically deformed to a large strain. A very small grain structure results from the recrystallization that occurs upon reheating, resulting in the formation of relatively small spherical solid phase particles in the semi-solid temperature range. The difficulty in using this process is that to achieve the necessary large strain, the resulting semi-solid ingots tend to be of relatively small diameters. Expense is also increased.

The second method is to use grain refiners [34, 91-95]. Typical grain refiners for Al are Ti and Ti with B [92]. However, the quantity of grain refiners typically needed to achieve a small grain size in many aluminum alloys is too large to be commercially feasible. The third method is to rapidly cool the ingot in the liquid/solid temperature range to achieve a refined as-cast structure, which can become fine solid phase particles in the following semi-solid treatment [96]. Direct chill (DC) casting produces a fine grained as-cast ingot that may form a fine spheroidized semi-solid upon reheating. The purpose of this research is to study the development of the microstructure during reheating of direct chill cast aluminum-silicon alloy ingot, and determine the semi-solid formability and mechanical properties of the solid alloy.

Chapter II.

THE NEW ALUMINUM ALLOY AA6069

Part I. The study of DF6C Alloys

EXPERIMENTAL PROCEDURES

A. Chemical Composition and Ingot Size

Six alloy compositions were selected: DF6C2-6. The composition of the alloys are listed in Table I. The alloys were provided in the form of direct chill cast ingot by Northwest Aluminum Company. The ingots sizes used in T6 study were 111 mm in diameter for DF6C2, DF6C4-6, and 105 mm in diameter for DF6C3. Extrusions of DF6C2 were performed on 114 mm ingot while DF6C3-6 on 89 mm ingot.

B. Equipment

Tensile tests were performed on an Instron 4505 screw driven tensile machine with computerized data acquisition. The accuracy of most of the mechanical tests was within $\pm$0.5%. The homogenization treatments were performed in an air velocity controlled furnace with Partlow controller. The temperature were controlled within $\pm$4°C of the set temperature. The solution treatments were performed in a case furnace with an accuracy within $\pm$2°C of the set temperature.

Table 1. Specification for the chemical composition of DF6C2-6 alloys used in this study.

Table 1(a). The chemical composition of DF6C2 used in this study

Limit	Si	Fe	Cu	Mg	Cr					
wt%	.89	.19	.89	1.45	.20					

Table 1(b). The chemical composition of DF6C3 used in this study

Limit	Si	Fe	Cu	Mg	Cr	Ti	V	Ga	Sr	Be
wt%	.92	.20	.83	1.20	.24	.036	.01	.02	.038	.001

Table 1(c). The chemical composition of DF6C4 used in this study

Limit	Si	Fe	Cu	Mg	Cr	Ti	V	Ga	Sr	
wt%	.84	.17	.77	1.47	.20	.015	.02	.02	.019	

Table 1 (Continued)

Table 1(d). The chemical composition of DF6C5 used in this study

Limit	Si	Fe	Cu	Mg	Cr	Ti	V	Ga	Be	
wt%	.92	.17	.78	1.41	.22	.016	.10	.03	.006	

Table 1(e). The chemical composition of DF6C5' (production quantity of DF6C5) used in this study

Limit	Si	Fe	Cu	Mg	Cr	Ti	V	Be		
wt%	.91	.24	.76	1.46	.21	.05	.12	.006		

Table 1(f). The chemical composition of DF6C6 used in this study

Limit	Si	Fe	Cu	Mg	Cr	Ti	V	Ga	Sr	Be
wt%	.86	.18	.75	1.32	.20	.017	.12	.02	.038	.007

C. Mechanical Testing Procedures

The tensile test specimen geometries varied and the typical gage dimensions for ingot characterization and extrusions were 6.35 mm diameter and 25.4 mm length. Some specimens from extrusions had 2.8 mm diameter and 20 mm length or 11.4 mm gage length. Specimens were evaluated from random positions within the ingots and extrusions. It was determined that the mechanical properties were independent of the position. The T6 treatment for DF6C alloys consists of a solution treatment followed by a water quench, 1 hour refrigeration, followed by an artificial age. For solution treatment, a 10 min heat-up was required to achieve the solution temperature, once specimens were inserted into the furnace. Generally, tensile specimens were maintained at temperature for 2 hours.

The ductility was measured as engineering strain to failure (El) equal to $\Delta L/L_0$ where L_0 is the initial length and, also as a reduction in area (RA) equal to $(A_0 - A_f)/A_0$ where A_0 is the initial area and A_f is the final area. The yield and ultimate tensile stress were reported as engineering stresses. The yield stress was based on a 0.002 plastic strain offset. The strain rate was always $0.67 \times 10^{-3} s^{-1}$. Ingot and hot extrusion tests were performed on 89mm to 111 mm diameter ingots. The extrusion was performed by TDA in Oregon by use of Wagstaff "Airslip" tooling. Hot extrusions were typically performed between 849°F (454°C) and 950°F (510°C). Ingot production always used Wagstaff airslip tooling.

RESULTS AND DISCUSSION

A. The effect of homogenization treatment on the T6 properties of DF6C Alloys

Fairly extensive tests were firstly performed on the ingots of DF6C alloys to determine the effects of various homogenization times as well as heating rates (to the homogenization temperature) and various cooling rates to ambient temperature on the T6 properties. The normal selected times heating to the homogenization temperatures were 0, 4, 8, 12 and 16 hours; the duration of the homogenization times was 8 hours; and the time cooling to ambient temperature were 0, 4, 8, 12 and 16 hours for DF6C4-6. The soak times of 4, 8, 12, 16 and 20 hours for DF6C4 alloy were selected to determine the effect of homogenization time on the T6 properties. The homogenization temperature was 1055°F (568°C).

The test results of DF6C4-6 ingots are listed in Table 2-4 and Figure 5. Each value is an average of 3 tests. The results indicates that the T6 properties are not dramatically sensitive to our implemented changes in heating-rate and cool-down time for DF6C alloys. However, it appears that the rapid heat-up times and slower cool-down times may provide the best T6 properties for DF6C4-6 alloys. Basically, T6 properties are independent on the homogenization times for DF6C4 alloy.

B. T6 Study

DF6C3 alloy was selected to find the initial optimum aging for the T6 treatment. DF6C3 ingot was homogenized based on the results of the homogenization study. The homogenization cycle is shown in Figure 6. The homogenization cycle used for DFC3-6 was Cycle #1 and Cycle #2 for DF6C2. Solution temperature and time for the alloy were 1055°F (571°C) and 2 hours, respectively. The artificial aging study of the T6

Table 2

Tensile properties of DF6C4 alloy extracted from 111 mm dia. ingot. (Homogenization temperature was 1055°F (568°C). Solution temperature was 1050°F (565°C) for 1 hour, no solution treatment for water quenched specimens, T6 - 177°C, 20 hours, 4 tests each)

	Heat-up Time (hrs)	Soak Time (hrs)	Cool-Down Time (hrs)	Yield Stress (ksi)	UTS (ksi)	El (%)
1	4	8	0	53.7	59.6	9.69
2	8	8	0	54.4	60.1	11.1
3	12	8	0	53.9	59.6	10.9
4	16	8	0	54.5	60.2	10.8
5	4	8	4	53.3	59.5	13.6
6	8	8	4	53.4	59.7	13.0
7	12	8	4	53.2	59.5	13.2
8	16	8	4	53.5	59.7	13.7
9	4	8	8	53.9	59.9	13.4
10	8	8	8	53.6	60.0	13.4
11	12	8	8	52.9	59.2	13.4
12	16	8	8	53.6	59.2	12.8
13	4	8	12	53.6	59.5	13.0
14	8	8	12	53.6	59.6	13.2
15	12	8	12	53.0	59.0	12.7
16	16	8	12	52.9	58.4	12.4
17	4	8	16	53.7	59.1	13.1
18	8	8	16	53.9	59.3	12.4
19	12	8	16	53.7	59.4	12.6
20	16	8	16	53.7	59.5	13.4

Table 3

Tensile properties of DF6C5 alloy extracted from 111 mm dia. ingot. (Homogenization temperature was 1055°F (568°C). Solution temperature was 1050°F (565°C) for 1 hour, no solution treatment for water quenched specimens, T6 - 177°C, 20 hours, 4 tests each)

	Heat-up Time (hrs)	Soak Time (hrs)	Cool-Down Time (hrs)	Yield Stress (ksi)	UTS (ksi)	El (%)
1	4	8	0	55.9	60.8	8.66
2	8	8	0	56.0	60.7	8.62
3	12	8	0	55.4	60.3	8.43
4	16	8	0	56.0	60.8	8.73
5	4	8	4	54.8	59.9	11.3
6	8	8	4	55.8	60.4	11.3
7	12	8	4	54.3	59.3	11.2
8	16	8	4	54.7	59.6	11.2
9	4	8	8	54.4	59.5	11.6
10	8	8	8	54.1	59.2	11.7
11	12	8	8	54.4	59.5	11.7
12	16	8	8	54.7	60.0	12.1
13	4	8	12	54.6	59.6	12.1
14	8	8	12	54.7	59.7	11.7
15	12	8	12	54.3	59.3	11.9
16	16	8	12	54.8	60.2	12.0
17	4	8	16	55.7	60.4	12.2
18	8	8	16	54.5	59.7	11.8
19	12	8	16	54.5	59.1	11.1
20	16	8	16	54.8	59.7	12.1
21	0	8	0	56.1	61.1	8.82
22	0	8	4	55.5	60.4	11.0
23	0	8	8	55.6	60.1	11.1
24	0	8	12	56.0	60.4	11.7
25	0	8	16	56.0	60.5	11.6

Table 4

Tensile properties of DF6C6 alloy extracted from 111 mm dia. ingot. (Homogenization temperature was 1055°F (568°C). Solution temperature was 1050°F (565°C) for 1 hour, no solution treatment for water quenched specimens, T6 - 177°C, 20 hours, 4 tests each)

	Heat-up Time (hrs)	Soak Time (hrs)	Cool-Down Time (hrs)	Yield Stress (ksi)	UTS (ksi)	El (%)
1	4	8	0	55.6	60.2	7.41
2	8	8	0	55.4	60.0	6.81
3	16	8	0	55.3	60.0	7.53
4	4	8	4	54.2	59.8	10.3
5	8	8	4	53.9	59.9	11.1
6	16	8	4	52.9	59.6	10.8
7	4	8	8	53.8	60.3	11.7
8	8	8	8	53.8	59.8	10.4
9	16	8	8	53.6	59.9	11.1
10	4	8	16	54.0	59.9	10.4
11	8	8	16	53.2	59.5	11.1
12	16	8	16	53.1	59.6	11.1
13	0	8	0	55.6	60.3	6.82
14	0	8	4	54.3	59.7	10.0
15	0	8	8	53.7	59.4	11.5
16	0	8	16	54.2	59.6	10.2

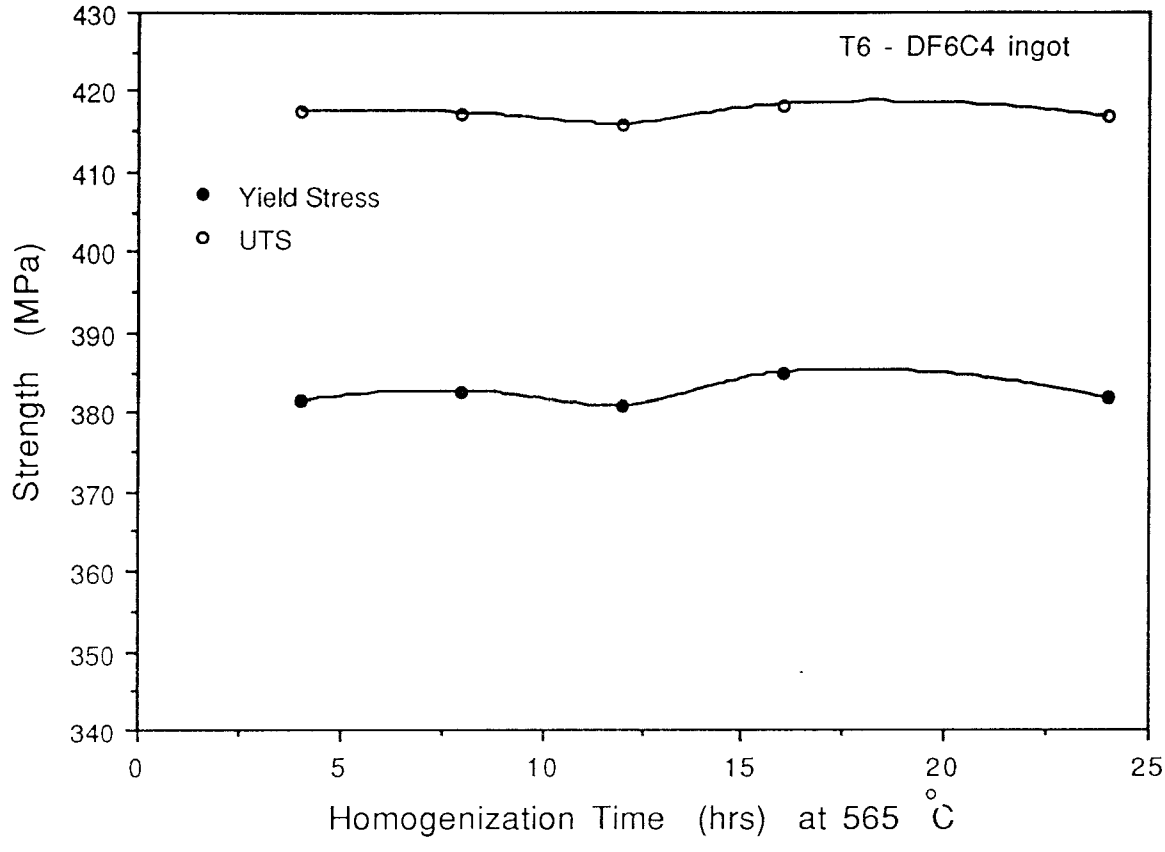

Figure 5 (a). The effect of homogenization times on T6 (177°C, 20 hrs.) properties of DF6C4. Each value represents 5 tests.

Figure 5 (Continued)

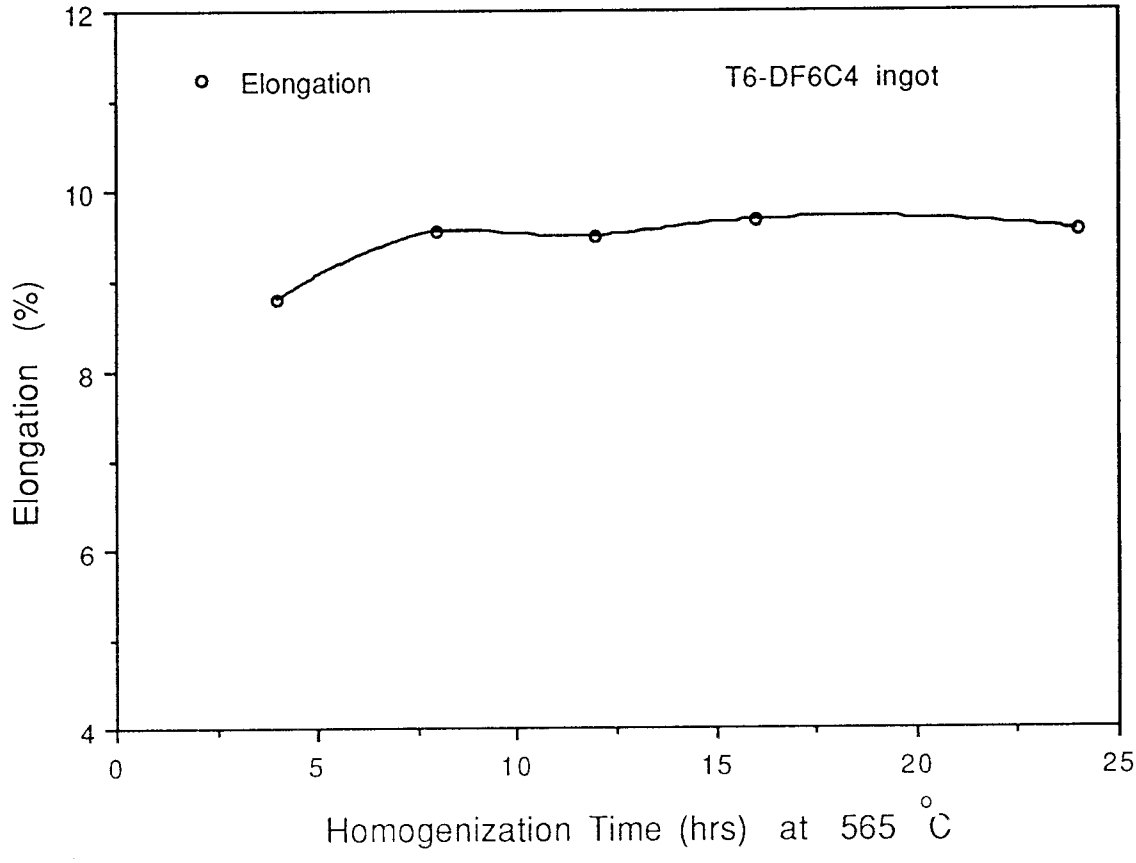

Figure 5 (b). The effect of homogenization times on T6 (177°C, 20 hrs.) properties of DF6C4. Each value represents 5 tests.

Homogenization Cycle 1

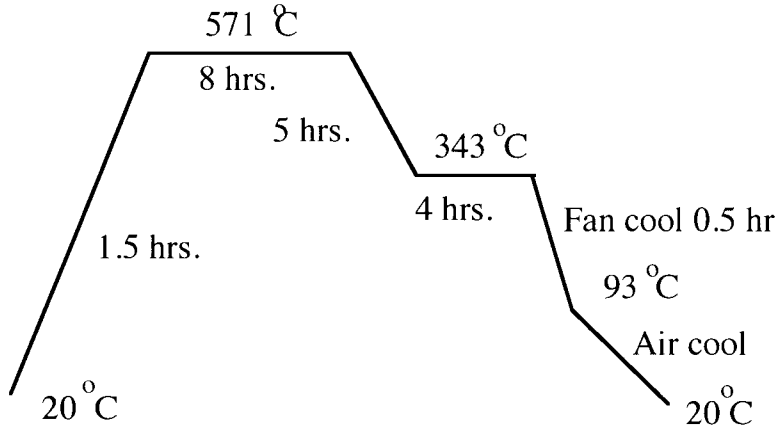

Homogenization Cycle 2

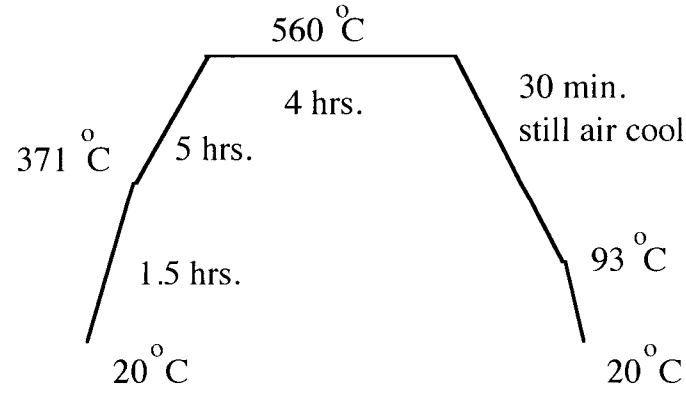

Figure 6. Homogenization cycles for DF6C2 and 3 ingots.

treatment of DF6C3 alloy consisted of three temperatures 330°F, 350°F and 370°F (166°C, 177°C and 188°C) for various times up to 20 hours. The test results are shown in Fig.7. Overall, the best tensile properties occur with a T6 aging of 20 hours at 350°F (177°C). Ductility is somewhat low at 370°F (188°C) and strength is lower at 330°F (166°C). Optimal T6 properties will be shown to be slightly dependent on composition for DF6C ingot alloys.

Once an initial optimum T6 treatment [350°F (177°C) for 20 hours] was determined, the properties of other ingots were established and DF6C3-6 results are listed in Table 5. The values listed are an average of 3-5 tests. The results show that the strength values of DF6C3-6 ingots in the T6 condition are fairly similar. One difference is significantly higher ductility with DF6C4, 5 and 6, with overall best ingot properties with DF6C4 and 5. Typical 6061-T6 wrought strength properties [1] of 275 MPa (40 ksi) yield strength, 310 MPa (45 ksi) UTS, and 12% elongation were exceeded by the DF6C ingots as also shown in the table.

C. Extrusions

The T6 properties of DF6C alloys in the extruded condition were also examined. In particular, three types of configurations were extruded; hollow, relatively thin-wall extrusions with a cross-section illustrated in Fig.8, circular bars (with relatively small dimension gear "teeth" at the surface), and finally, a relatively complex impact extruded air-bag canister with concentric thin walls. Other configurations were later considered once the composition was optimized.

For hollow extrusions, the extrusion process consisted of (105 mm ingots for C2, and 89 mm ingot for C3,4, and 6 prior to extrusion) heating to 849-950°F (454-510°C) . Tensile specimens were extracted parallel to the extrusion axis. The homogenization cycles used for DFC2 was Cycle #2 and Cycle #1 for other DF6C alloys, as illustrated in Fig.

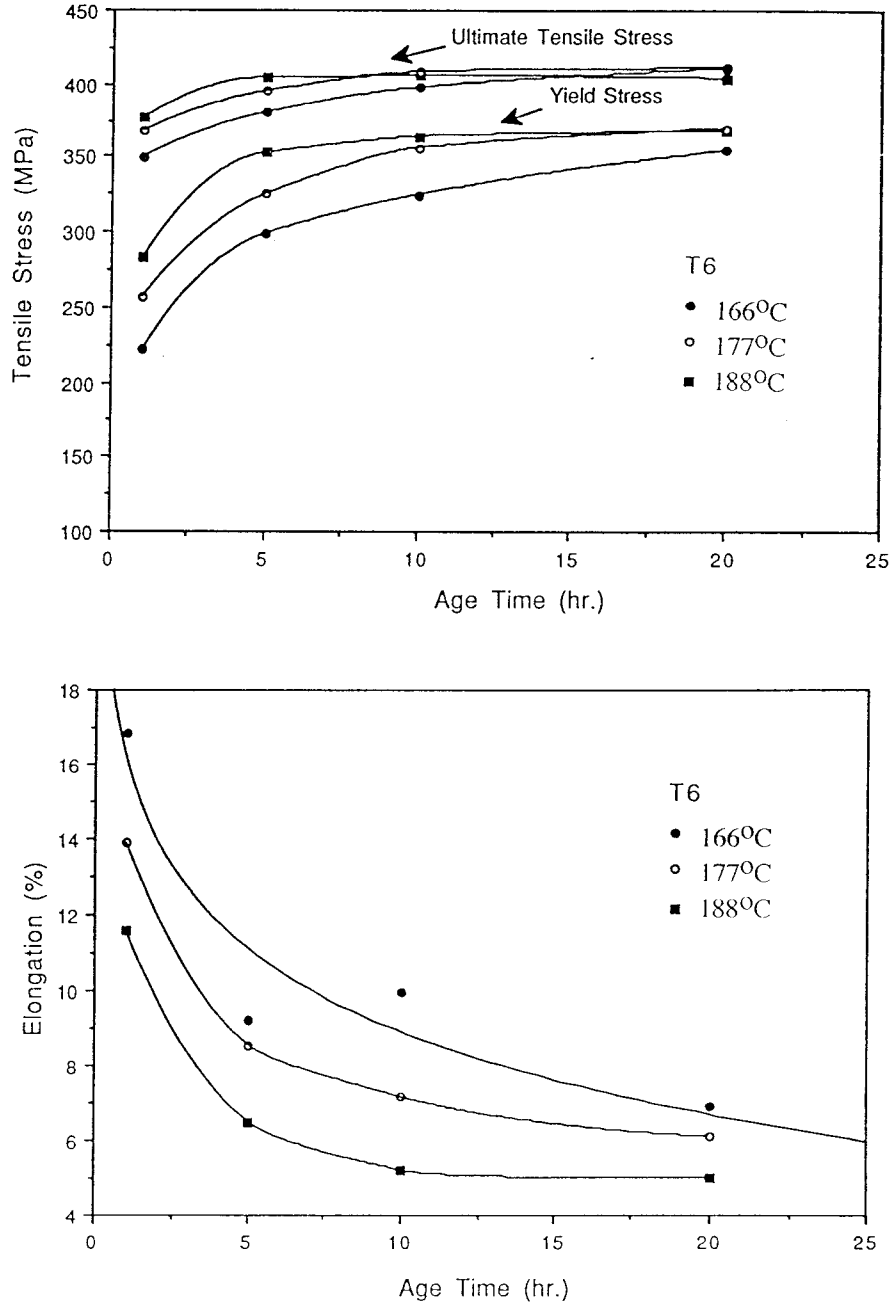

Figure 7. The ambient temperature mechanical properties of DF6C3 ingot with a 568°C solution treatment for 2 hrs. and aged at various temperatures for various times. Each point represents 1-2 tests.

Table 5. T6 properties of DF6C3-6 ingots (4.375 inch dia.)

(3 specimens for each test)

Ingot #	σ_y MPa (ksi)	UTS MPa (ksi)	El (%)
DF6C3	369 (53.5)	410 (59.5)	6.1
DF6C4	370 (53.6)	414 (60.0)	13.4
DF6C5	373 (54.1)	408 (59.2)	11.7
DF6C6	371 (53.8)	412 (59.8)	10.4
6061*	275 (40.0)	310 (45.0)	12.0

T6

Solution anneal for DF6C3 : 1060°F (571°C) for 2 hours.

Solution anneal for DF6C4-6: 1050°F (565°C) for 1 hour.

Aging for all ingots: 350°F (177°C), 20 hours.

*: Ref. 5

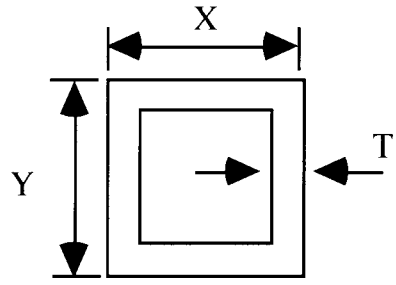

X = 32 mm Y = 32 mm T = 3.18 mm

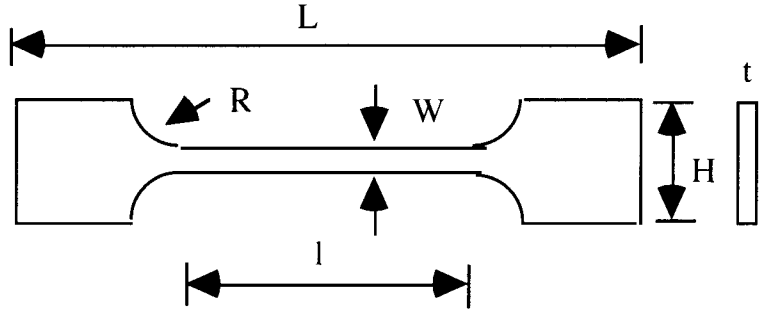

L = 91.4 mm l = 31.2 mm H = 22.9 mm W = 5.84 mm R = 6.35 mm

t (typical) = 2.87 mm

Figure 8. Dimension of DF6C2, 3 and 4 hollow extrusions and extracted tensile specimens.

6. The solution temperature and time were 1060°F (571°C) and 2 hours, respectively. The aging temperature and time were 350°F (177°C) and 20 hours, respectively. The tensile test results are reported in Table 6. Each value reported is an average of 3 tests. The DF6C2, 3, and 4 strength values were lower for these configuration extrusions than ingots of identical composition. It was believed that the decrease in strength of the hollow extrusions was , possibly, partly due to texture softening or changes in the grain size. A 1 to 2.5% stretch was performed on DF6C2 and DF6C3 hollow extruded specimens and also reported in Table 6. The "stretch" increases the density of dislocations that may act as heterogeneous nucleation sites and increase the strength over the undeformed and aged alloy as with 2xxx alloys. For identical thermal treatments, properties are not improved, rather, a 5% increase in yield stresses, 1-2% decrease in UTS, and a factor of 1.15 to 1.30 decrease in elongation is observed. A modification of the solution anneal from 2 to 60 hours was performed with a 2.5% stretch for both alloys. The results are shown in Figure 9. It is observed that solution anneal of 25 hours may result in an increase in yield strength of 8%, UTS increase of 3% and an increase in elongation of a factor of about 1.12, still not an impressive change, considering the inconvenience of the long time of solution anneal. Table 7 shows the scatter of elongation measurements. It should be mentioned that significant scatter of elongation was observed in the C2 tests of extrusions at ±4%. Slightly better elongation is observed in DF6C2 as compared with C3. DF6C4 appears to have similar extruded properties to DF6C2 but less scatter of elongation. DF6C4 and 5 have fair reproducibility, which DFC6 is less impressive. Thus, DF6C4 and 5 compositions were emphasized.

Additionally, one set (of 3) DF6C4 extrusion tensile specimens was ground to 2.54 mm thickness, while a second set (also of 3 specimens) was ground to only 3.00 mm thickness (3.18 mm starting thickness). The yield stress, UTS, and El were identical within testing error, so that the removal of the outermost surface layer does not seem to affect mechanical properties of the extrusion wall.

Table 6. T6 properties of hollow extrusion (parallel to extrusion axis)

(3 specimens for each test)

Ingot #	Stretch %	σ_y MPa (ksi)	UTS MPa (ksi)	El (%)
DF6C2	0	334 (48.4)	374 (54.2)	12.1
	1	354 (51.3)	375 (54.4)	10.6
	2.5	351 (50.9)	336 (53.1)	9.8
DF6C3	0	341 (49.4)	365 (52.9)	9.3
	1	352 (51.0)	362 (52.5)	7.6
	2.5	355 (51.5)	362 (52.5)	6.2
DF6C4	0	338 (49.0)	370 (53.6)	12.0

T6:

Solution anneal : 1060°F (571°C) for 2 hours.

Aging: 350°F (565°C) for 20 hours.

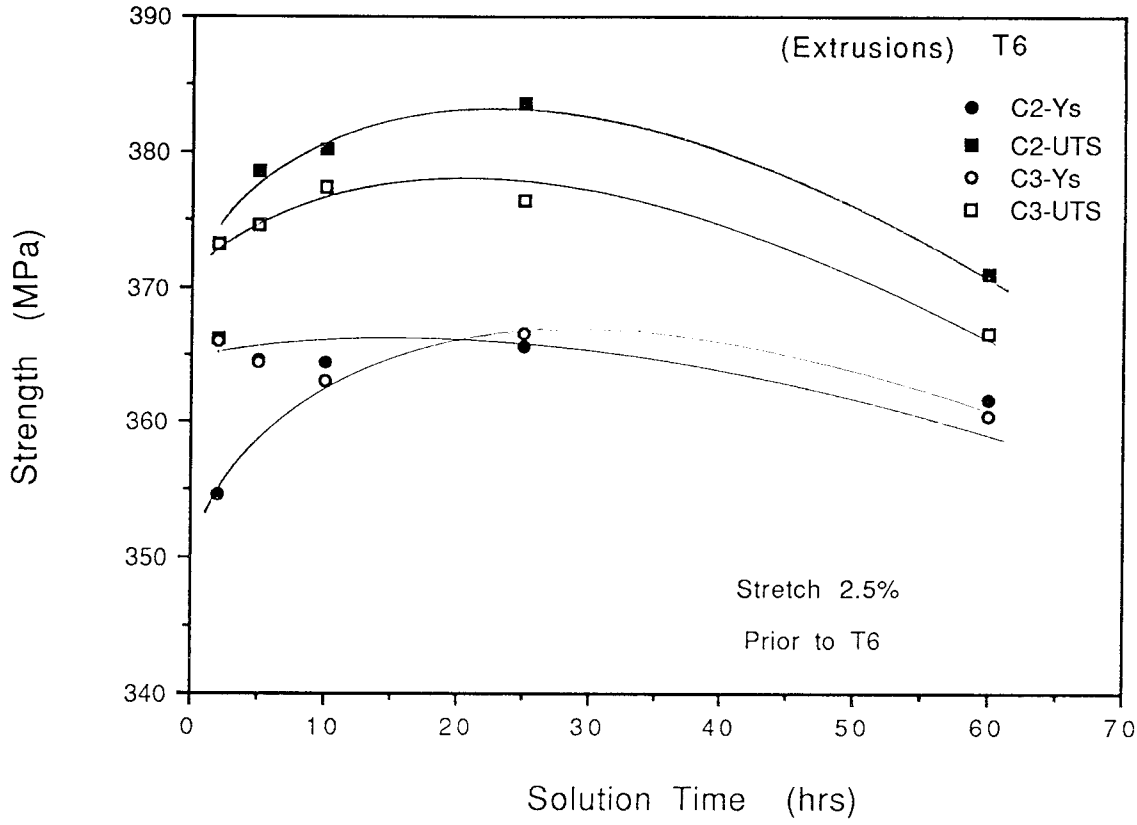

Figure 9 (a). The effect of solution time on DF6C2 and DF6C3 extrusions T6 (177°C , 20 hrs.). Two tests per data point. A 2.5% stretch was performed prior to the T6.

Figure 9 (Continued)

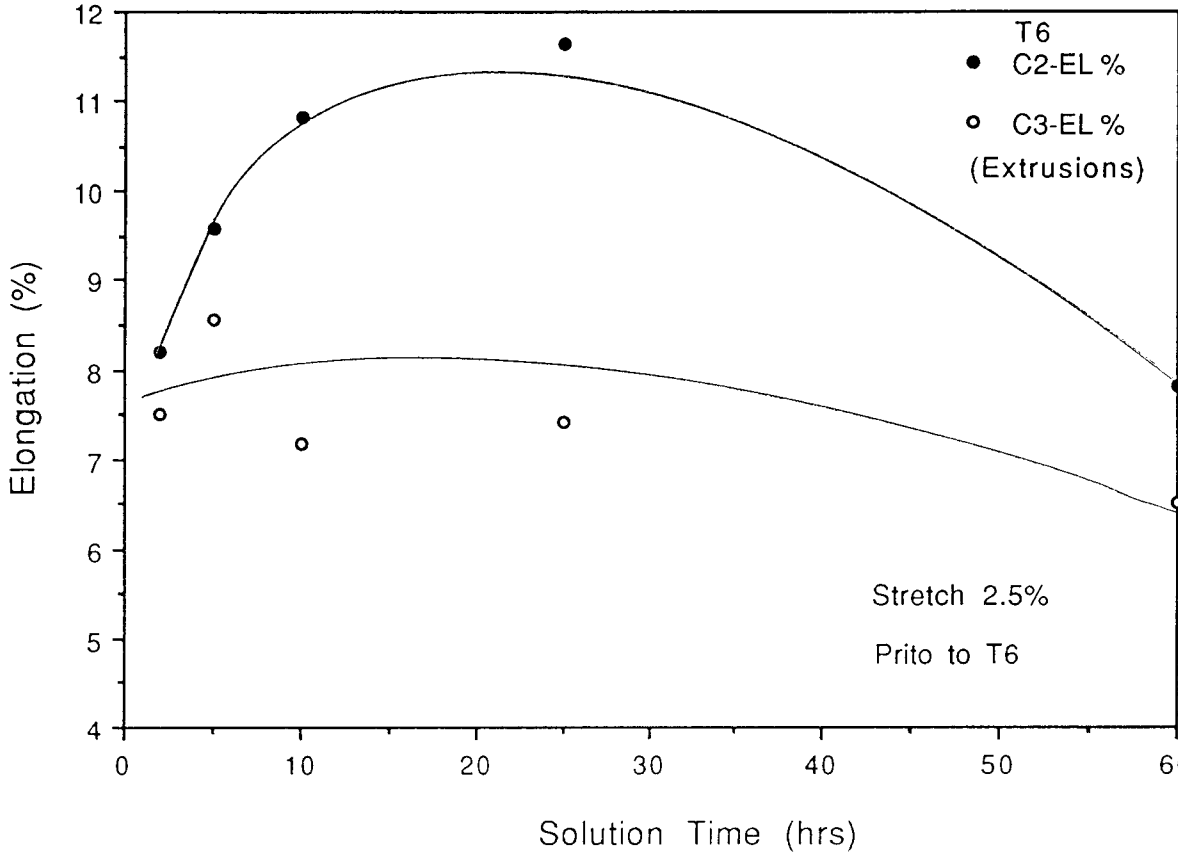

Figure 9 (b). The effect of solution time on DF6C2 and DF6C3 extrusions T6 (177°C, 20 hrs.). Two tests per data point. A 2.5% stretch was performed prior to the T6.

Table 7. Scatter of elongation measurements of DF6C alloys

Type	Average Standard Deviation / Average El
DF6C2 hollow extrusion	0.19
DF6C3 hollow extrusion	0.13
DF6C4 hollow extrusion	0.15
DF6C3 ingot	0.10
DF6C4 ingot	0.06
DF6C5 ingot	0.06
DF6C6 ingot	0.15

The extrusion temperature was the same for circular bars as for hollow extrusions. DF6C4 and DF6C5 specimens were also hot extruded to a solid rod shape approximately 31.8 mm diameter from 89 mm diameter ingot. Tensile specimens were cut parallel to the extruded rod axis, both from the center and about the half-radius position (half-radius and center specimens, both longitudinal, had essentially identical mechanical properties). It was observed that both the parallel and perpendicular directions have substantially higher T6 strength than the thin-wall hollow-square extrusions and ingots (i.e., 25-30% higher than hollow extrusions). The fact that the parallel and perpendicular strength values are similar suggests an absence of a pronounced texture effect. The tensile test results of circular bars of DF6C4 and 5 are reported in Table 8. We observed that the mechanical properties may be somewhat better for DF6C5 and this composition was emphasized.

Hot extrusions were also performed by TDA on 89 mm DF6C5' ingot. The DF6C5' is a production quantity composition based on the test ingot (DF6C5) composition. One set of tensile tests was performed on specimens extracted from flat bar extrusions, 12.7 mm thick and 76.2 mm wide, and another used bars 31.8 mm diameter. The 31.8 mm diameter extrusions were identical in configuration to the circular solid bar of DF6C5 above. These tensile specimens were extracted longitudinal to the extrusion direction and had excellent mechanical properties as reported by Koon-Hall [98] also listed in Table 8.

The results of these extrusion tests emphasize that the mechanical properties of DF6C extruded alloys appear configuration dependent, and not yet fully predictable. Further study of the texture softening will be needed.

Table 8. T6 properties of extrusion bars of DF6C4 and 5 alloys

(3 specimens for each test)

Type	Extrusion direction	σ_y MPa (ksi)	UTS MPa (ksi)	El (%)
DF6C4 Extrusion (bar)	parallel	414 (60.0)	461 (66.8)	13.0
	perp.	385 (55.9)	436 (63.2)	14.4
DF6C5 Extrusion (bar)	parallel	447 (64.8)	478 (69.3)	13.0
	perp.	397 (57.6)	442 (64.1)	14.4
DF6C5' * Extrusion	(flat)	414 (60.0)	448 (65.0)	13-17
	(bar)	462 (67.0)	490 (71.0)	13.0

T6:

Solution anneal : 1055°F (568°C) for 2 hours.

Aging: 350°F for 20 hours.

T6:

* : Solution anneal : 1055°F (568°C) for 1.5 hours.

Aging: 340°F (565°C) for 18 hours.

Part II. The Study of the New Aluminum Alloy of AA6069

The studies of the DF6C experimental alloys revealed that a new 6xxx aluminum alloy with favorable high T6 properties both in ingot and extruded conditions has been developed. These properties are attributable to a combination of proper selection of composition, high solidification rate, controlled homogenization treatment and T6 practice. This new alloy, based on the DF6C5 (and DF6C5') composition, has been designated as AA6069 aluminum alloy. The purpose of this part is to study the mechanical properties of this new 6xxx series alloy. The properties will also be compared with other 6xxx series alloys.

EXPERIMENTAL PROCEDURES

A. Chemical Composition and Ingot Size

All of the alloys used in this study was provided in the form of direct chill cast ingots by Northwest Aluminum Company, The Dallas, Oregon, unless otherwise indicated. Aluminum was provided in the form of direct-chill cast ingots using Wagstaff "air slip" tooling. Ingots in this study (including those used for extrusions) typically varied from 89 mm to 110 mm in diameter. The specification for the chemical composition range of AA6069 aluminum alloy are listed in Table 9. The chemical composition of the 6069, 6061 and 6013 alloys actually used in this study are listed in Table 10, which shows the relatively narrow composition range for several 6069 ingots that were studied.

Table 9. Specification for the chemical composition of new AA6069 alloy

Limit	Si	Fe	Cu	Mn	Mg	Cr	Zn	Ti	V	Sr
Min wt%	0.6	0.0	0.4	0.0	1.2	.05	0.0	0.0	0.1	0.0
Max wt%	1.2	0.4	1.0	0.4	1.6	0.3	0.1	0.1	0.3	0.05

Table 10. The chemical composition of 6069, 6061 and 6013 alloy used in this study.

Alloy Element (wt%)	6069	6061*	6013*
Si	0.87-0.92	0.4-0.8	0.6-1.0
Fe	0.17-0.24	0.7 max	0.5
Cu	0.76-0.78	0.15-0.40	0.6-1.1
Mg	1.41-1.46	0.8-1.2	0.8-1.2
Cr	0.21-0.22	0.15 max	0.1
Ti	0.016-0.032	0.15 max	0.1
V	0.09-0.12	---	---
Mn	---	0.15 max	0.15 max
Ga	0.03 max.	---	---
Be	0.003-0.006	---	---

* : Typical (Ref. [1])

B. Equipment and Experimental Procedures

The equipment and experimental procedures for tensile tests used in this study are the same as those used in the study of DF6C alloys, described in Part I. In addition, constant stress-amplitude fatigue test were removed from random locations within 13 mm diameter 6061 extrusions (Alaska Copper and Brass) and 19 mm thick and 55.6 mm wide 6069 bar extrusions, with the long axis of the specimen parallel with the extrusion direction (longitudinal), as well as 6069 cold-impacted extrusions for high pressure gas cylinders (203 mm ingot diameter). Specimens were machined into circular cross-sections of 6.35 mm gage diameter and 19.1 mm gage length prior to T6 heat treatments, and were polished to minimize surface defects before and after T6. Samples were tested at 1 Hz on a servohydraulic Instron 8521 machine using a collete-ttype gripping system. Alignment was checked using four strain gages.

Corrosion fatigue tests were performed on 6069 and 6061 solid extrusions and ingots, and on 6013 plate. Specimens were machined to 1.0 mm thickness, 178 mm length, and 25.4 mm width. Some specimens were then reduced in width using two 60^0 notches with a notch radius of 1.27 mm, resulting in a minimum cross section of 1 by 17.78 mm and a stress-concentration factor, K_t, of 3. Other specimens were also reduced in width to 9.53 mm using 76.2 mm radius notches or K_t of 1. Specimens were then cleaned with a methanol and acetone wipe and loaded into an Instron 8521 tensile testing machine with a corrosion cell surrounding the specimen. A flow of aerated 3.5 wt% NaCl/water solution was maintained across the specimen at a rate of 0.0105 to 0.0126 liters per second, recycled from either a 14 or 56 liter tank for $K_t = 3$ and $K_t = 1$ tests, respectively. All extrusions and rolled plate used a 56 liter tank. The 56 liter solution was aerated using an air pump with aeration stone; the 14 liter solution used only the aeration supplied by the returning saline solution. The saline solution was generally replaced following every two tests. A constant amplitude fatigue cycle of 103 to 10.3 MPa for $K_t =$

3 specimens and 138 MPa to 13.8 MPa for K_t = 1 specimens, both at a frequency of 0.5 Hz, was applied until specimen failure. T6 treatment was performed after machining.

The 6069 specimens for both corrosion-fatigue and constant-strain-amplitude fatigue tests were solution annealed at 1055°F (568°C) for 2 hours, and aged at 340°F (171°C) for 24 hours. The 6061 specimens were solution annealed at 990°F (532°C) for 2 hours and aged at 350°F (177°C) for 8 hours while 6013 were solution annealed at 1055°F (568°C) for 2 hours and aged at 387°F (197°C) for 4 hours.

RESULTS AND DISCUSSION

A. T6 Study

The aging (T6) treatment was re-optimized over the DF6C study described earlier. Ingot and extruded bar specimens were solution annealed at 1055°F (568°C) for 2 hours and then water quenched. They were aged for various times to 30 hours, at 320, 340, 360, and 380°F (160, 171, 182, and 193°C). Results for 6069 ingot and hot-extruded specimens with 6.35 mm gage diameter and 25.4 mm gage length are shown in Figure 10. A variety of combinations of times between 16 and 24 hours and temperatures between 320°F (160°C) and 340°F (171°C) give favorable properties, some better strength at the expense of ductility. Table 11 lists an average of five 6069 ingot tests for a given T6. Typical strength properties for wrought 6061-T6 [5] and for rolled 6013-T6 [99] were exceeded by the 6069 ingots.

B. Extrusions

The T6 properties of extruded 6069 were also examined. Five configurations were extruded: a) hollow, relatively thin-wall hot extrusions with a 32 mm x 32 mm square cross-section and a 3.18 mm wall thickness; b) solid, hot-extruded, circular, 31.8 mm diameter, bars (with relatively small dimension gear "teeth" at the surface); c) solid, hot-extruded flat (6:1 aspect ratio) bars; d) hot-extruded rectangular (3:1 aspect ratio) bars; and e) relatively complex cold impact-extruded air-bag canisters with concentric thin walls.

Hot Extrusions

Hot Hollow Extrusions

Ingots with a diameter of 89 mm were heated to 900 to 986°F (482 to 530°C) to

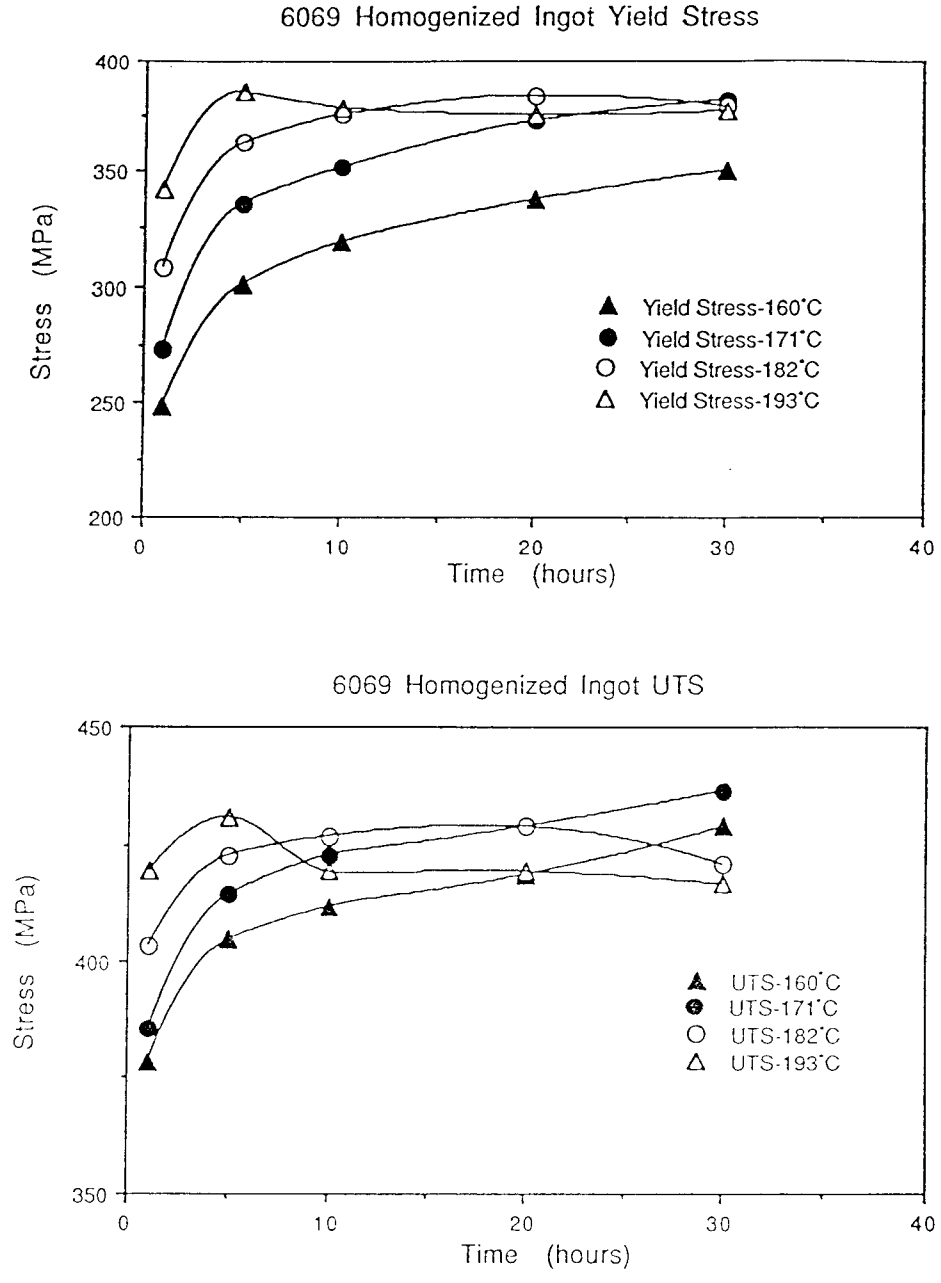

Figure 10(a). The ambient temperature mechanical properties of 6069 ingots with a 1055°F (568°C) solution treatment for 2 hrs. and aged at various temperatures for various times. Each point represents 1-2 tests.

Figure 10 (Continued)

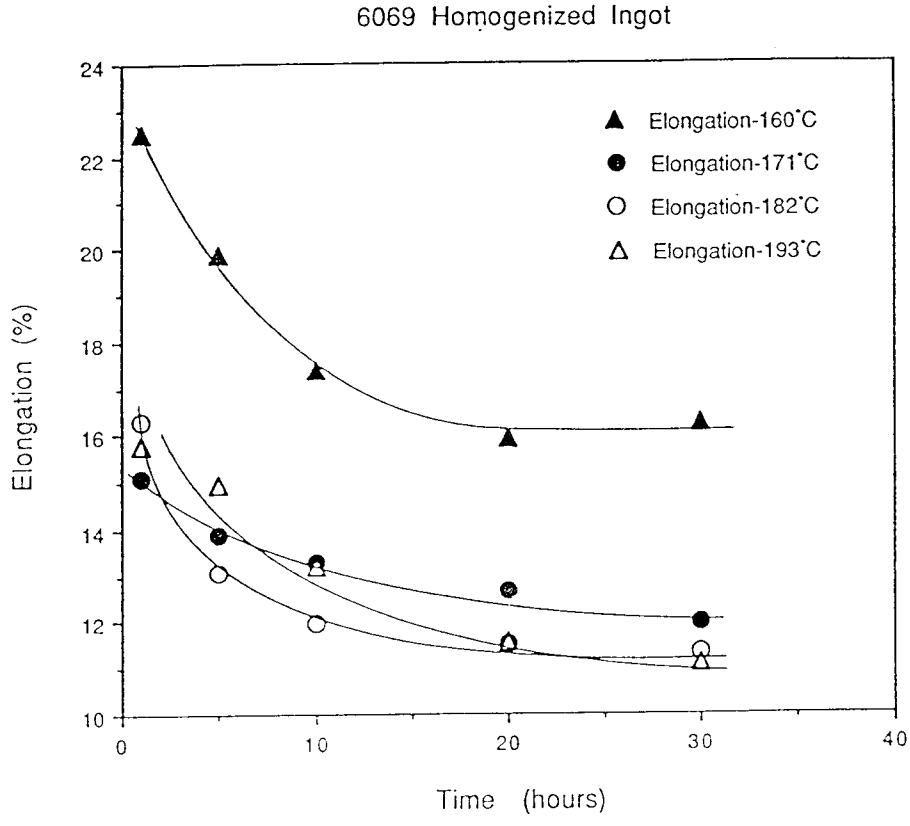

Figure 10(b). The ambient temperature mechanical properties of 6069 ingots with a 1055°F (568°C) solution treatment for 2 hrs. and aged at various temperatures for various times. Each point represents 1-2 tests.

Figure 10 (Continued)

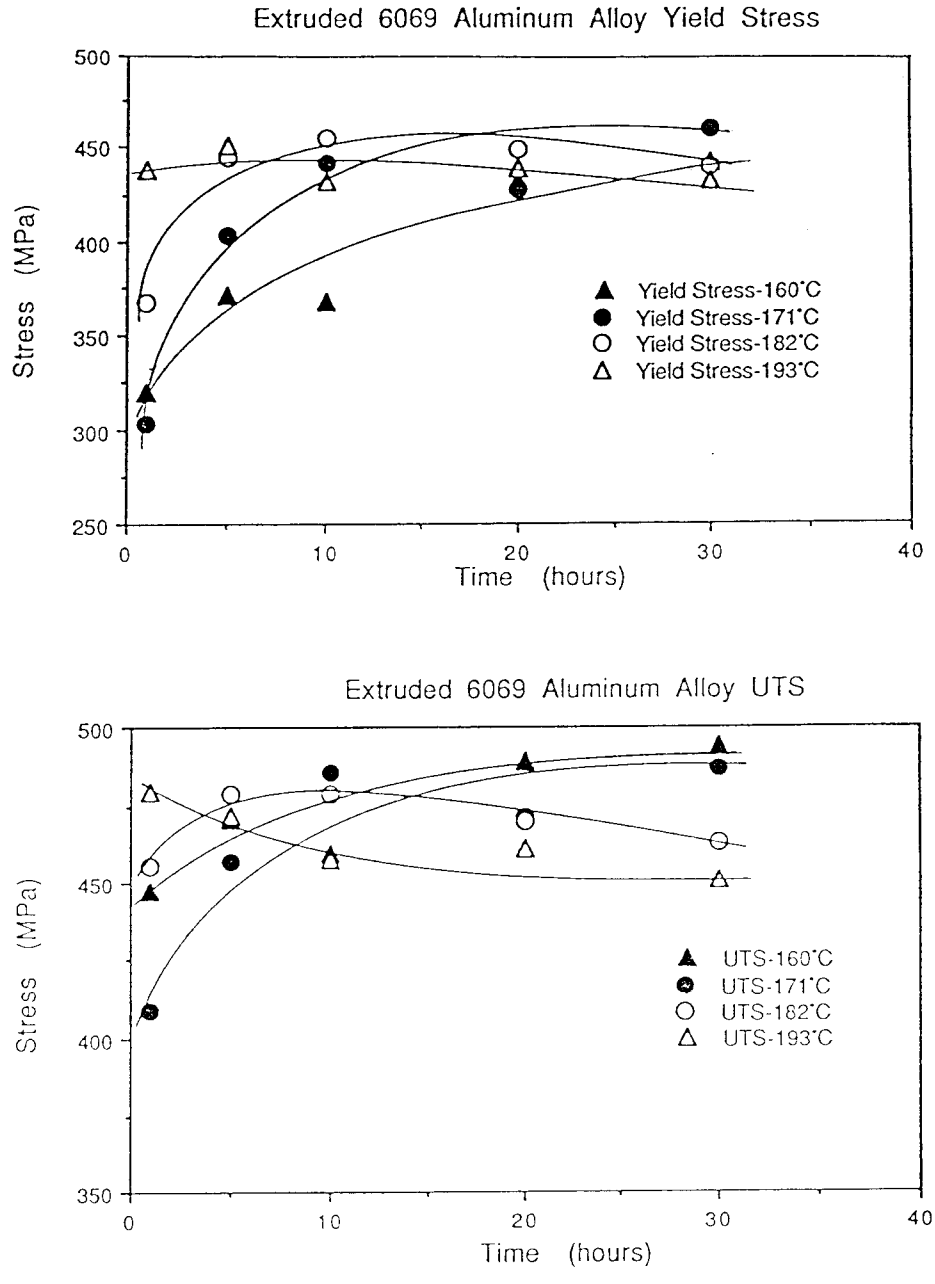

Figure 10(c). The ambient temperature mechanical properties of 6069 hot extrusions with a 1055°F (568°C) solution treatment for 2 hrs. and aged at various temperatures for various times. Each point represents 1-2 tests.

Figure 10 (Continued)

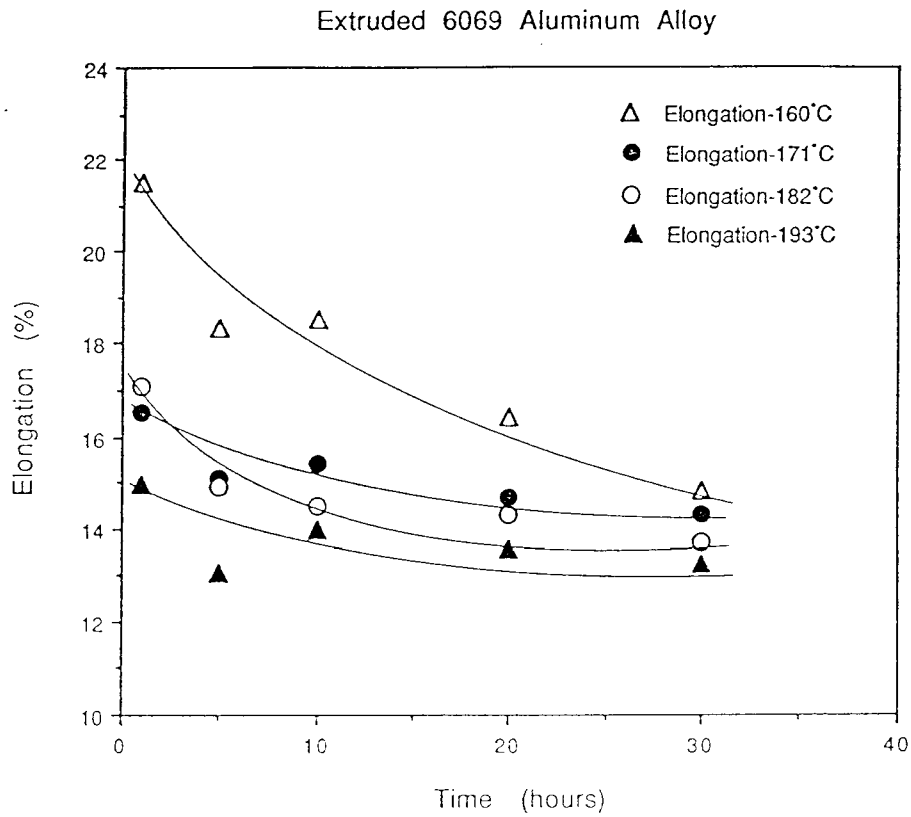

Figure 10(d). The ambient temperature mechanical properties of 6069 hot extrusions with a 1055°F (568°C) solution treatment for 2 hrs. and aged at various temperatures for various times. Each point represents 1-2 tests.

Table 11. T6 properties of 6069 and 6061 ingots used in this study

Ingot #	σ_y MPa (ksi)	UTS MPa (ksi)	El (%)
6069	373 (54.1)	408 (59.2)	11.7
6061 (extruded)	275 (40.0)	310 (45.0)	12.0
6013 (rolled)	324 (47.0)	359 (52.1)	8.0

T6:

Solution anneal for 6069 : 1050°F (565°C) for 1 hours.

Age : 350°F (177°C) for 20 hours.

6061: see Ref. [5].

6013: see Ref. [33].

produce hollow extrusions as discussed in the previous section. Tensile specimens were extruded primarily parallel (longitudinal) but also 45° and perpendicular (transverse) to the extrusion axis. The data for hollow extrusions are reported in Table 12. Each value reported is an average of 5 tests. The strength of hollow "6069" extrusions was lower in longitudinal directions than for ingots. However, the transverse directions always had higher strength than the longitudinal direction and higher strength than the ingot. Specimens extracted 45° to the extrusion direction exhibited an intermediate strength level, but ductility comparable to that of the longitudinal direction. The decrease in strength of the hollow, square extrusions tensile tested in the longitudinal direction was possibly due in part to texture softening. This assumption is supported by the consistent increases in strength in specimens tensile tested in transverse direction.

Hot Solid Circular Bar, Rectangular Bar and Flat-Bar Extrusions

As also discussed earlier in Table 8 with DF6C5', the basis for 6069, specimens of 6069 were hot extruded to a solid, circular rod shape approximately 31.8 mm diameter. Tensile specimens were cut longitudinal, from both the center and about the half-radius position (both types of longitudinal specimens had essentially identical mechanical properties), and transverse to the extruded rod axis. Extruded specimens from both the longitudinal and the transverse directions had substantially higher T6 strength than the ingots. The fact that the parallel and perpendicular strength values are similar also suggests an absence of a pronounced texture. The strengths also are substantially higher than the thin-wall extrusion parallel and 45^0 to the extrusion axis, and overall strength and ductility are somewhat superior to the transverse thin-wall properties. This suggests that lower longitudinal properties in thin-wall extrusions are not entirely due to texture. Tensile values for solid, circular bar specimens are listed in Table 13. Hot extrusions werealso performed by Technical Dynamics Aluminum Corp. on 89 mm 6069 ingot. Other two

Table 12. 6069 hot hollow extrusion properties (T6)

(5 specimens for each tests)

Extrusion direction	σ_y MPa (ksi)	UTS MPa (ksi)	El (%)
longitudinal to extrusion axis	346 (50.1)	396 (57.4)	20.9
transverse to extrusion axis	407 (59.0)	451 (65.4)	9.6
45° to extrusion axis	361 (52.4)	412 (59.7)	21.5

T6:

Solution anneal : 1060°F (571°C) for 2 hours.

Age: 350°F (177°C) for 16 hours.

Table 13. Summary of selected 6069-T6 properties of hot solid circular bar and flat-bar extrusions. (3 specimens for each test)

Type	Extrusion direction	σ_y MPa (ksi)	UTS MPa (ksi)	El (%)
round bar	longitudinal	447 (64.8)	478 (69.3)	14.4
	transverse	397 (57.6)	442 (64.1)	13
6:1 flat bar*	longitudinal	414 (60.0)	448 (65.0)	13-17
3:1 flat bar*	longitudinal	441 (64.0)	469 (68.0)	14.5

T6:

Solution anneal : 1055°F (568°C)for 2 hours.

Age: 350°F (177°C) for 16 hours.

T6:

Solution anneal : 1055°F (568°C)for 2 hours.

*Age : 340°F (171°C) for 24 hours.

sets of tensile tests were performed on specimens extracted from rectangular bar (6:1 aspect ratio) extrusions 12.7 mm thick and 76.2 wide (not listed earlier in Table 8), and flat-bar (3:1 aspect ratio) extrusions 19 mm thick, 55.6 mm wide. These tensile specimens were extracted longitudinal to the extrusion direction and had excellent mechanical properties. The T6 properties of these hot extruded 6069 bars are reported in Table 13. The solution annealing for the three bars was at 1055°F (568°C) for 2 hours. The aging temperature and time were 350° (177°C) and 16 hours for circular bar, 340° (171°C) and 24 hours for rectangular bar and flat-bar, respectively. Both aging treatments produce favorable mechanical properties although a 16 hours age is commercially more allowed.

Cold-Impact Extrusions

T6 properties were determined for driver side automobile air-bag gas canisters that were cold impact extruded from 92 mm 6069 ingot. A canister can be approximately described as three concentric walls of 2.45 to 4.32 mm thickness, parallel to the extrusion direction, attached to a 92.5 mm diameter base, 5.08 mm thick. No machining is performed on canisters. The T6 properties were determined for specimens extracted from the base of the cylinder (transverse to the extrusion direction) and from the outermost thin wall (2.6 mm thick) longitudinal to the extrusion direction. The solution annealing was at 1055°F (568°C) for 2 hours. The aging temperature and time were 340°F (171°C) and 24 hours, respectively. Table 14 shows the tensile test results of the canister. The results reveals favorable T6 properties of 6069 alloy in cold-impact extrusions. Some mild strength and ductility anisotropy were noted.

C. AA6069 Tensile Properties Summary

Extrusion and ingot data for 6069 are compared with data for other aluminum alloys

Table 14. Summary of selected 6069-T6 properties of cold impact canister extrusions. (3 specimens for each test)

Type	Extrusion direction	σ_y MPa (ksi)	UTS MPa (ksi)	El (%)
canister	longitudinal	405 (58.7)	444 (64.4)	18.0
	transverse	386 (56.0)	424 (61.5)	14.0

T6:

Solution anneal : 1055°F (568°C) for 2 hours.

Age: 340°F (171°C) for 24 hours.

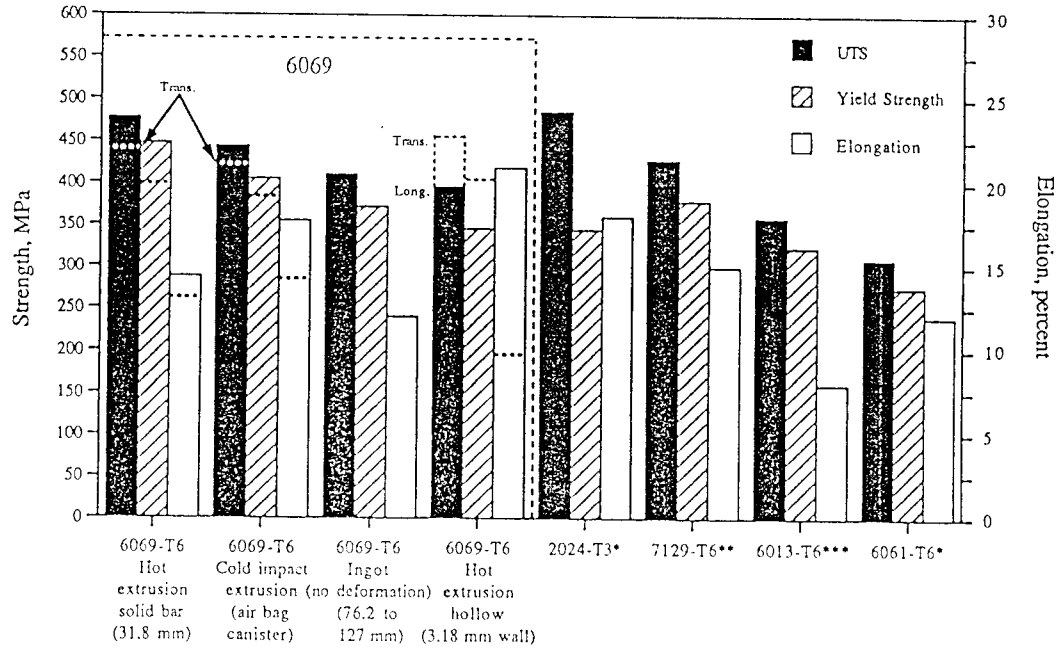

Figure 11. Comparison of the tensile properties of 6069-T6 ingots and various types of extrusions with other aluminum alloys.

in Figure 11 [5, 98, 99]. Overall, 6069-T6 appears to have tensile properties superior to those of 6013-T6 and 6061-T6 and comparable to those of 2024-T3 and 7129-T6. The results of the collective extrusion tests emphasize that the mechanical properties of 6069 extruded alloys appear to be extrusion temperature dependent, and perhaps somewhat configuration dependent. The explanation for this is not always clear, but is the subject of continuing investigation.

D. Fatigue and Corrosion-Fatigue Tests

Figure 12(a) shows the results of the corrosion-fatigue tests on 6069 and 6061-T6 ingots. Very favorable properties are evident in notched ($K_t = 3$) and ($K_t = 1$) specimens tested in aerated 3.5 wt% NaCl solution. The performance of 6069 T6 is comparable or superior to the 6061 T6. The testing procedure is similar to those recently reported in Ref. [97]. Figure 12(b) compares the 6069 T6 flat bar extrusion with 6061 T6 solid circular extrusions and 6013 T6 plate. Again for $K_t = 3$, the 6069 T6 appears superior to 6061 T6 and comparable to 6013 T6. One complication of these tests is the scatter that is evident (as much as a factor of ±3 in cycles to failure).

Constant stress-amplitude fatigue tests were also performed at ambient temperature in air. The 6069 T6 is from solid-flat extrusions as with corrosion fatigue tests and also cold impact high pressure gas cylinder extrusions from 203 mm diameter ingots. The (S-N) results are shown in Figure 13. Properties for both kinds of extrusions are superior to those of 6061 T6 extrusions.

E. Fracture Toughness

Tests on fracture toughness of 6069 T6 from cold-impact high pressure gas cylindies indicates a fracture toughness greater than or equal to 6061-T6 cylinders tested in

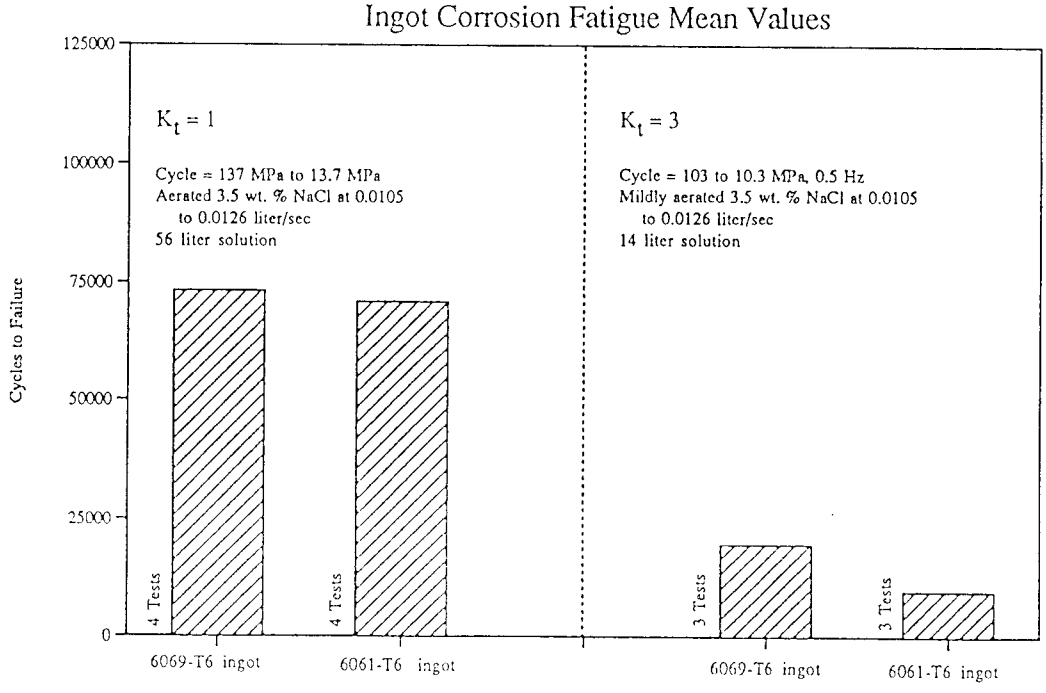

Figure 12(a). Comparison of corrosion fatigue properties of 6069-T6 ingot with 6061-T6 ingot under identical environmental and mechanical conditions with K_t=3 and K_t=1

Figure 12 (Continued)

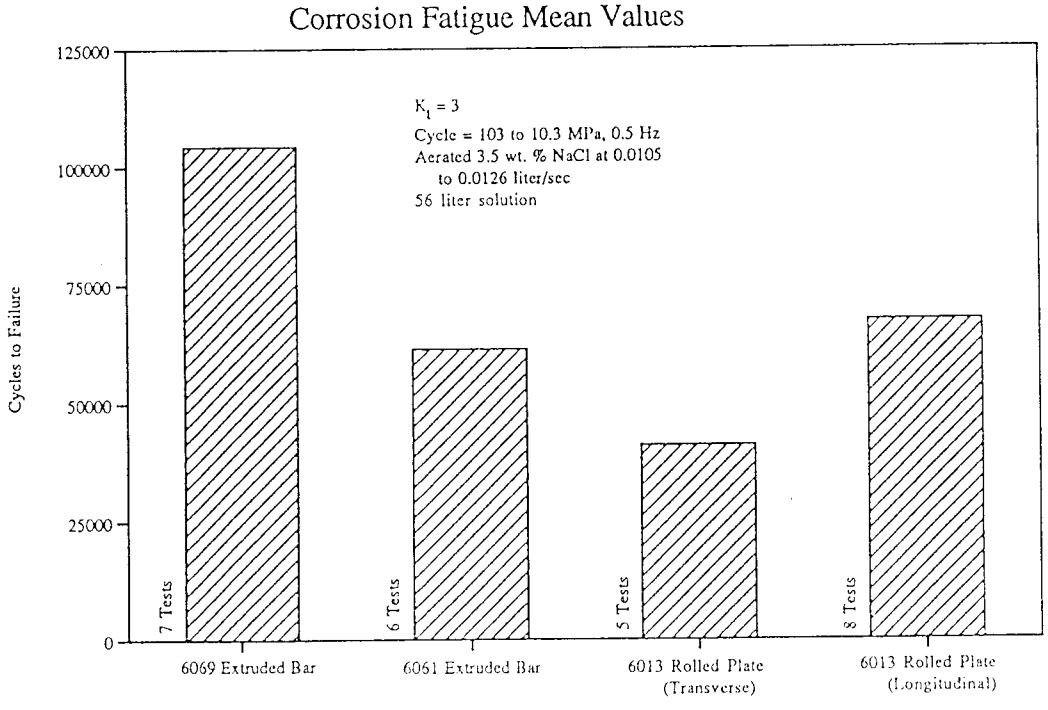

Figure 12(b). Comparison of extruded 6069-T6 with 6013-T6 and 6061-T6 (K_t=3).

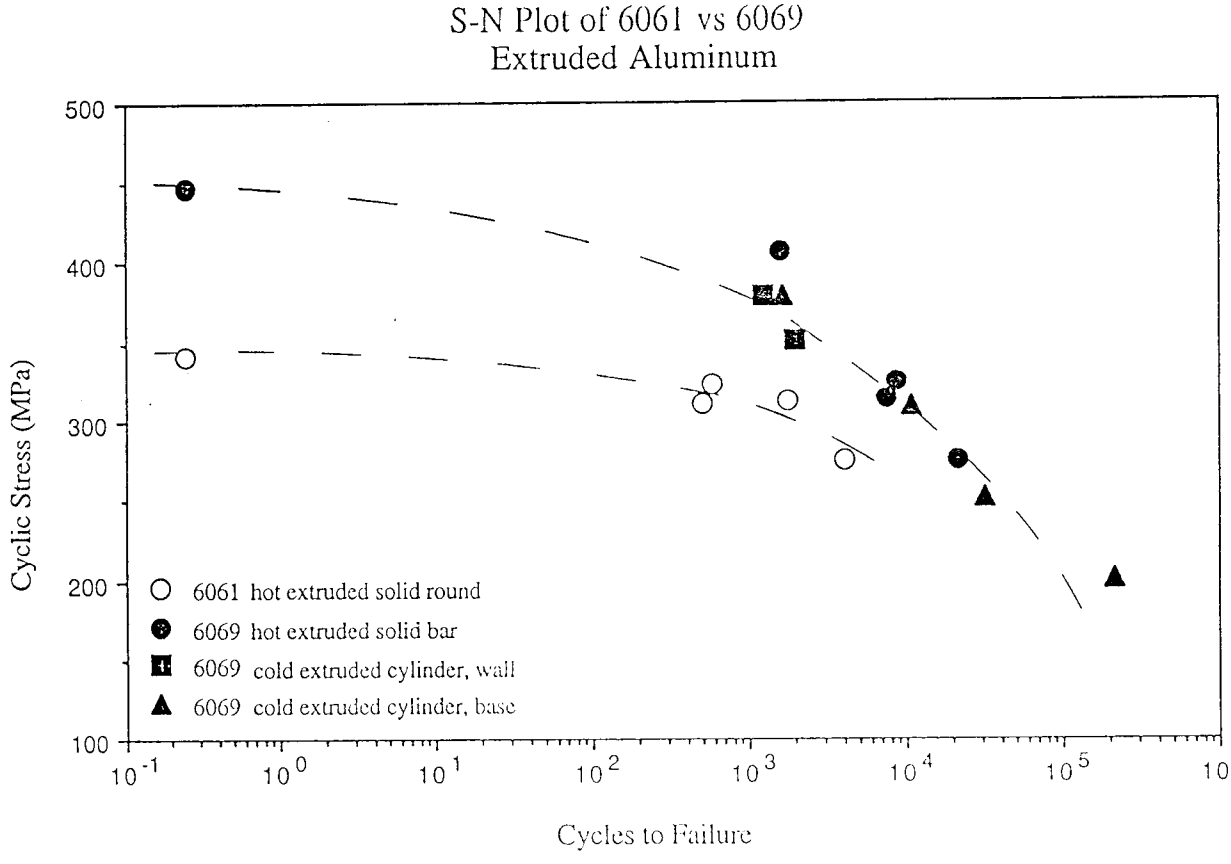

Figure 13. Extruded 6069-T6 and 6061-T6 constant stress amplitude fatigue properties.

the same laboratory at Powertech, Vancouver, Canada [100].

Chapter III.

SEMI-SOLID ALUMINUM SILICON ALLOYS

EXPERIMENTAL PROCEDURES

A. Chemical Composition and Ingot Size

The aluminum alloys that were used in this study, from Northwest Aluminum Company and Wagstaff, were provided in form of direct chill cast ingots typically about 76.2 mm in diameter. Pecheney semi-solid ingot was also studied. The compositions of the ingots are listed in Table 15. Twelve alloy compositions are listed.

B. Equipment

Semi-solid treatment was performed at two locations, Oregon State University (OSU) and The Northwest Aluminum Company, in The Dalles, OR. The semi-solid experiments at OSU were performed in an air velocity controlled furnace with a Partlow controller for ambient atmosphere and a Mellen three-zone vacuum furnace with a Honeywell controller for vacuum treatments. The temperature was held to within 4°C of the set temperature. The solution treatments were performed in a case furnace with an accuracy within 2°C of the set temperature. The liquid to solid phase ratio was evaluated in an Olympus microscope with image analysis software. Hardness tests were performed with a Rockwell hardness testing machine. Tensile tests were performed on an Instron 4505 screw driven tensile machine with computerized data acquisition. Northwest Aluminum Company utilized an inducting heating device using an ABB controller.

Table 15. Specification for the chemical composition for aluminum alloys used in this study.

Table 15-1. Specification for the chemical composition of Alloy #1 (NWA A356-2A 3.25" ingot) used in this study.

A356	Si	Mg	Fe	Ti	Zn	Cu	Ga
wt%	6.93	0.36	0.12	0.12	0.04	0.02	0.01

Table 15-2. Specification for the chemical composition of Alloy #2 (NWA A356-2 S105) used in this study.

A356	Si	Mg	Fe	Ti	Zn	Cu	B	Ca	Ga
wt%	7.04	0.36	0.12	.125	0.03	0.01	.007	.001	0.01

Table 15-3. Specification for the chemical composition of Alloy #3 (Wagstaff A357-1A 3" ingot) used in this study.

A357	Si	Mg	Fe	Ti	Sr	Cu	Be
wt%	6.89	0.45	0.12	0.16	0.05	0.03	0.04

Table 15-4. Specification for the chemical composition of Alloy #4 (Wagstaff 357N #100793-2A 3" ingot) used in this study.

A356	Si	Mg	Fe	Ti	Zn	Cu	B	Ca	Ga
wt%	6.99	0.56	0.10	.122	.012	.028	.002	.004	.013

Table 15 (Continued)

Table 15-5. Specification for the chemical composition of Alloy #5 (Wagstaff A357 #100793-3A 3" ingot) used in this study.

A357	Si	Mg	Fe	Ti	Zn	Cu	B	V	Ga	Sr
wt%	7.07	0.53	0.11	.164	.012	.028	.013	0.01	0.14	.048

Table 15-6. Specification for the chemical composition of Alloy #6 (NWA A357 G002-2 3.9" ingot) used in this study.

A357	Si	Mg	Fe	Ti	Zn	Be	Ga	Sr
wt%	6.77	0.53	0.13	0.18	0.03	.002	0.02	.025

Table 15-7. Specification for the chemical composition of Alloy #7 (NWA A357 6001-3 2.9" ingot) used in this study.

A357	Si	Mg	Fe	Ti	Zn	Be	Ga	Sr
wt%	6.74	0.49	0.13	0.14	0.03	.003	0.02	.016

Table 15-8. Specification for the chemical composition of Alloy #8 (Pechiney 357) used in this study.

A357	Si	Mg	Fe	Zn	Ca	Sr
wt%	7.35	0.54	0.15	.012	.011	.043

Table 15 (Continued)

Table 15-9. Specification for the chemical composition of Alloy #9 (Wagstaff DF 92-1A 3.23" ingot) used in this study.

	Si	Mg	Fe	Ti	Cr	Cu	B	V	Be	Ga	Mn
wt%	1.92	1.35	0.24	.043	0.21	0.72	.002	0.11	.005	0.02	0.01

Table 15-10. Specification for the chemical composition of Alloy #10 (Wagstaff DF 93 #2 3.23" ingot) used in this study.

	Si	Mg	Fe	Ti	Cr	Cu	Ca	V	Be	Ga	Mn
wt%	2.92	1.37	0.26	.036	0.22	0.76	0.01	0.10	.005	0.02	0.01

Table 15-11. Specification for the chemical composition of Alloy #11 (Wagstaff DF 94-1A 3.23" ingot) used in this study.

	Si	Mg	Fe	Ti	Cr	Cu	V	Be	Ga	Mn
wt%	3.79	1.33	0.24	.044	0.22	0.72	0.11	.004	0.02	0.01

Table 15-12. Specification for the chemical composition of Alloy #12 (Wagstaff DF 95-1B 3.23" ingot) used in this study.

	Si	Mg	Fe	Ti	Cr	Cu	V	Be	Ga	Mn
wt%	4.73	1.32	0.24	.046	0.22	0.72	0.11	.005	0.02	0.01

Table 15 (Continued)

Table 15-13. Specification for the chemical composition of Alloy #13 (NWA A357.1 L110-1 log1 2.9" ingot) used in this study.

	Si	Mg	Fe	Ti	Cu	B	V	Ga	Sr
wt%	6.76	0.53	0.12	0.17	0.02	.006	0.01	0.01	0.02

Table 15-14. Specification for the chemical composition of Alloy #14 (NWA A357.1 L110-2 log 1 2.9" ingot) used in this study.

	Si	Mg	Fe	Ti	Cu	B	V	Ga	Sr	Ni
wt%	6.86	0.49	0.12	0.17	0.02	.004	0.01	0.01	0.02	0.03

Table 15-15. Specification for the chemical composition of Alloy #15 (NWA A357.1 L100-2 2.9" ingot) used in this study.

	Si	Mg	Fe	Ti	Cu	B	Ga	Sr
wt%	6.72	0.53	0.13	0.13	0.01	.005	0.02	.029

Table 15-16. Specification for the chemical composition of Alloy #16 (NWA A357.1 L109-2 3.9" ingot) used in this study.

	Si	Mg	Fe	Ti	Be	B	V	Ga	Sr
wt%	6.76	0.53	0.11	0.16	.002	.004	0.01	0.02	.021

Table 15 (Continued)

Table 15-17. Specification for the chemical composition of Alloy #17 (NWA A357.1 L108-2 3.9" ingot) used in this study.

	Si	Mg	Fe	Ti	B	Ga	Sr
wt%	6.82	0.52	0.13	0.15	.004	0.02	0.02

Table 15-18. Specification for the chemical composition of Alloy #18 (NWA A357.1 L109-1 3.9" ingot) used in this study.

	Si	Mg	Fe	Ti	V	B	Ga	Be	Sr
wt%	6.75	0.54	0.11	0.16	.004	.004	0.02	.002	.026

Table 15-19. Specification for the chemical composition of Alloy #19 (NWA A357.2 G002-1 0601-13 3.9" ingot) used in this study.

	Si	Mg	Fe	Ti	B	Ga	Sr
wt%	6.73	0.54	0.13	0.17	.005	0.01	.022

Table 15-20. Specification for the chemical composition of Alloy #20 (NWA DF93 3F100 drop 1 2.9" ingot) used in this study.

	Si	Mg	Fe	Ti	Pb	Cu	Zn	V	Be	Ga	Sr
wt%	3.09	1.47	0.23	.072	0.01	0.80	0.02	0.01	.004	0.02	.039

Table 15 (Continued)

Table 15-21. Specification for the chemical composition of Alloy #21 (NWA DF94 4F001 Prod. 96 2.9" ingot) used in this study.

	Si	Mg	Fe	Ti	Pb	Cu	Zn	V	Be	Ga	Sr
wt%	3.82	1.40	0.27	.082	0.01	0.80	0.02	0.01	.003	0.02	.024

Table 15-22. Specification for the chemical composition of Alloy #22 (Wagstaff 390 040996-1A-2 3.0" ingot) used in this study.

	Si	Mg	Fe	Ti	Cu	Ga
wt%	16.64	0.66	0.38	0.06	4.40	0.02

Table 15-23. Specification for the chemical composition of Alloy #23 (Wagstaff 390 040996-2A-2 3.0" ingot) used in this study.

	Si	Mg	Fe	Ti	Cu	Ga	B	Zn
wt%	15.40	0.63	0.38	0.07	4.41	0.02	0.01	0.01

C. Experimental Procedures

Several studies, listed below, were performed to determine several properties of the A356, A357 and modified Al-Si-Mg aluminum alloys. Several semi-solid heat treatment cycles were selected in order to determine the effect of heating rate, cooling rate, soak time, soak temperature, atmosphere, and composition on the microstructure and T6 properties of semi-solid alloys. A T6 treatment usually consisted of a solution treatment, water quench, 1 hour refrigeration, followed by an artificial age. For the solution treatment of A356 and A357, a 10 minute heat-up to the solution temperature of 538°C (1000°F) was followed by a 3 hour soak at that temperature followed by a water quench. The artificial age was performed at 154°C (310°F) for 16 hours. Modifications to these were occasionally performed and are specified in the results section. The dimensions for tensile test specimens of semi-solid materials varied and are also specified in the results section. The ductility was measured as engineering strain to failure (El) equal to $\Delta L/L_o$, where L_o is the initial length and a reduction in area (RA) equal to $\Delta A/A_o$ where A_o is the initial area. The yield and ultimate tensile stresses are reported as engineering stresses. The yield stress was based on a 0.002 plastic strain offset. The strain rate used was typically $6.67 \times 10^{-4} s^{-1}$.

1. A357 semi-solid microstructure formation in conventional furnaces at OSU

To examine the semi-solid microstructure evolution in the 357 (Alloy #3) as-cast aluminum alloy, an ingot was cut into cubic samples with dimension of 11.4 mm x11.4 mm x11.4 mm. Three heat-up cycles with different heat-up rates were utilized, Cycles "1", "2" and "3", shown in Figures 14, 15 and 16, respectively, were utilized to determine the effect of heat-up time (especially before eutectic reaction) on the semi-solid microstructure. One thermocouple was located inside the center of each sample. The samples were held at temperature for 0, 3, 10 and 30 minutes after they reached the eutectic

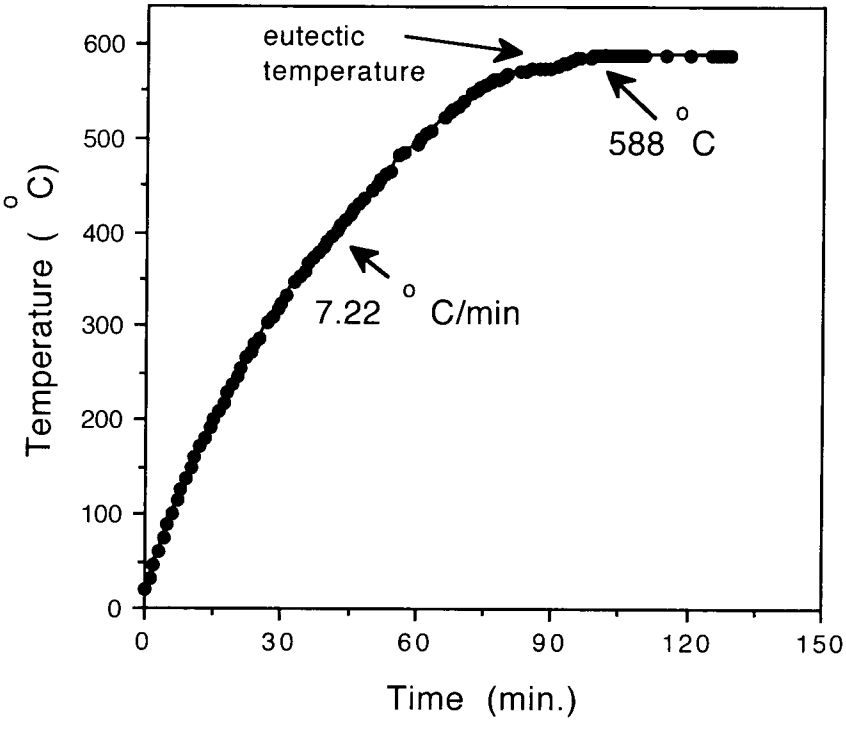

Figure 14. Semi-solid treatment Cycle 1. Air Furnace. One thermocouple in the center of each sample. Final temperature of the sample is 588°C (1090°F). Set temperature is 591°C (1095°F).

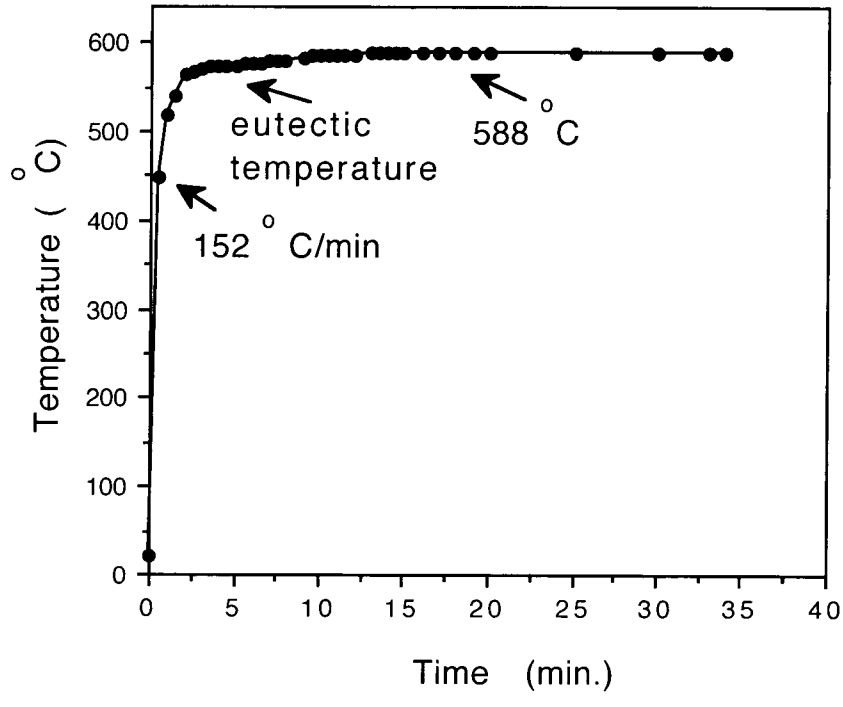

Figure 15. Semi-solid treatment Cycle 2. Air Furnace. One thermocouple in the center of each sample. Final temperature of the sample is 588°C (1090°F). Set temperature is 591°C (1095°F).

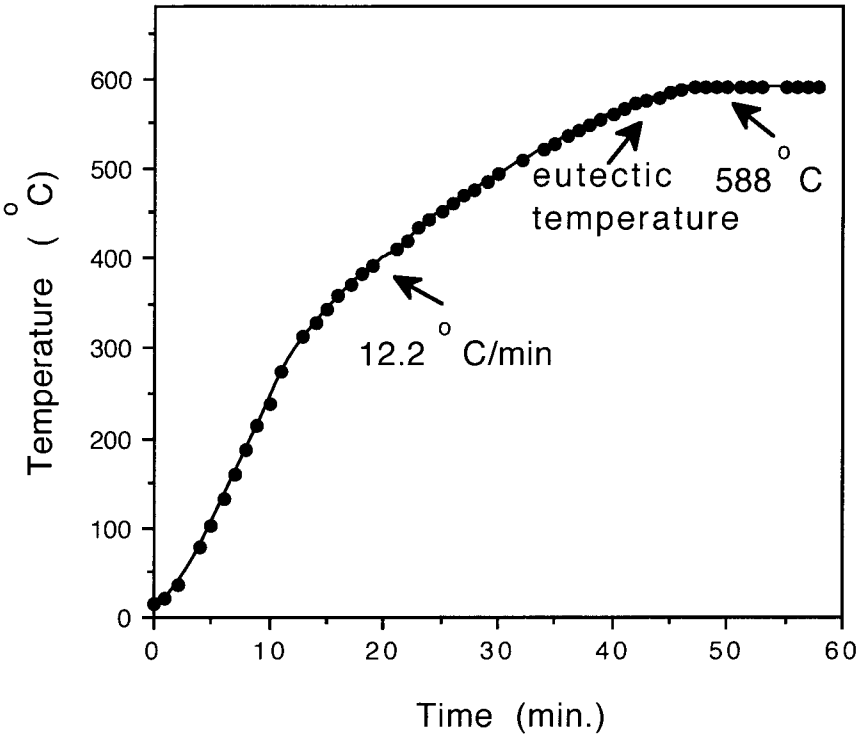

Figure 16. Semi-solid treatment Cycle 3. Air Furnace. One thermocouple in the center of each sample. Final temperature of the sample is 588°C (1090°F). Set temperature is 591°C (1095°F).

temperature of 578°C (1063°F), and then fan cooled or water quenched. The microstructures were analyzed in the microscope after etching for 45 seconds (1ml HF and 200ml H_2O).

2. Isothermal grain growth of solid phase

In this part of the study, cubic samples of A357 (Alloy #3) aluminum alloy with dimension of 11.4 mm x11.4 mm x11.4 mm were heated to 579°C (1075°F) using heat-up "Cycle 4", shown in Figure 17, and to 588°C (1090°F) using heat-up "Cycle 5", shown in Figure 18. The thermocouples were located inside the center of samples. The samples were kept at either 579°C (1075°F) or 588°C (1090°F) for 10, 20, 30, 45 and 60 minutes and then water quenched.

3. Heat up cycle analysis

The purpose of this study was to determine the heat-up time from ambient temperature to various semi-solid temperatures, especially the time in eutectic reaction. The experiments were performed in a Blue M Oven (Model CW5512). The sample size of the A356 aluminum alloy was 20.3 mm x20.3 mm x38.1 mm. Two thermocouples were used, one in the sample center and one wired to the sample surface. The data was collected by computer using a Fluke data acquisition system. The samples were placed into the furnace at set temperatures of 578°C (1073°F), 581°C (1078°F), 584°C (1083°F), 589°C (1092°F) and 594°C (1102°F). Figures 19 through 23 show Cycles 6-10, indicating the relationship between heat-up time and temperature. Temperature range from 538°C (1000°F) to the given furnace set temperature were chosen to illustrate the shapes of these cycles.

4. A356 and A357 mechanical properties

Five semi-solid treatments and heat-up rates (Cycles 1, 2, 3, 11 and 12 as shown in Figures 14, 15, 16, 24 and 25) were used in determining the mechanical properties of the

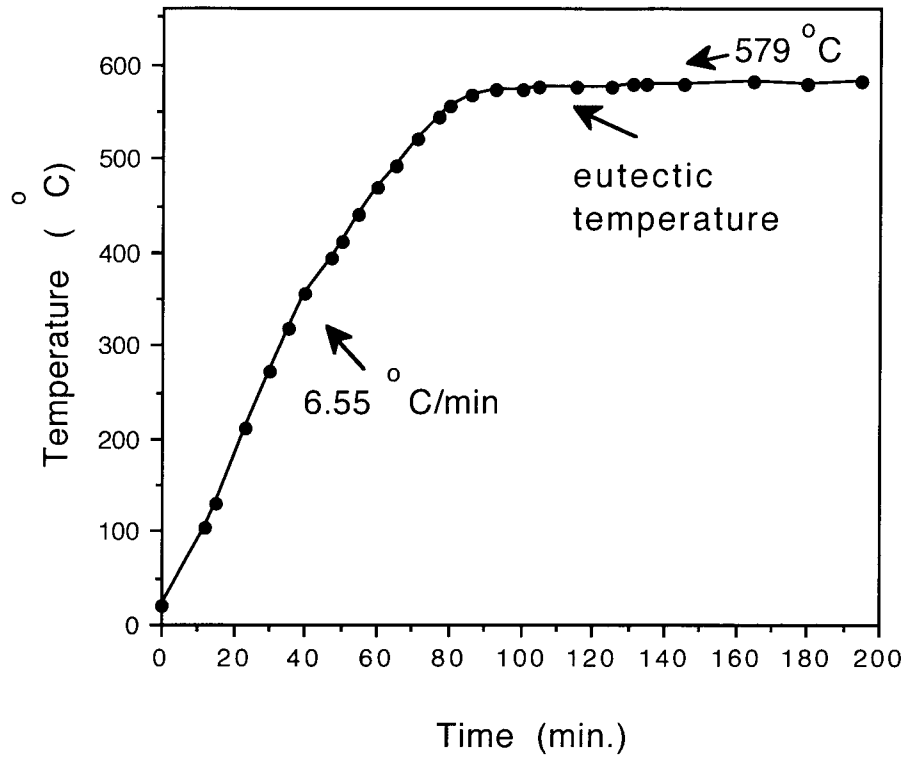

Figure 17. Semi-solid treatment Cycle 4. Air Furnace. One thermocouple in the center of each sample. Final temperature of the sample is 579°C (1075°F). Set temperature is 582°C (1079°F).

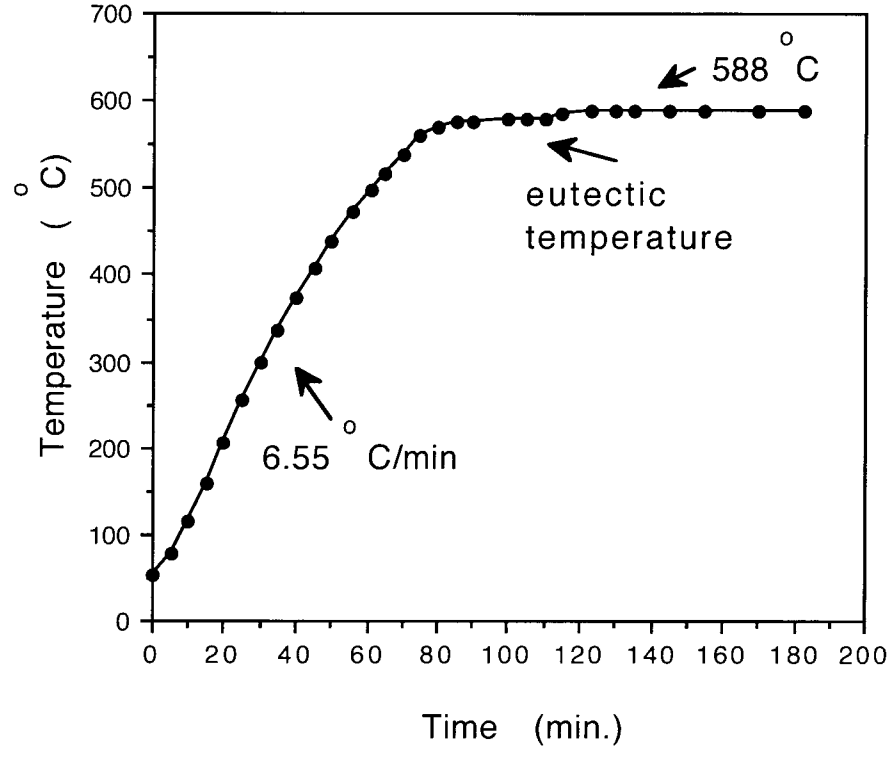

Figure 18. Semi-solid treatment Cycle 5. Air Furnace. One thermocouple in the center of each sample. Final temperature of the sample is 588°C (1090°F). Set temperature is 591°C (1095°F).

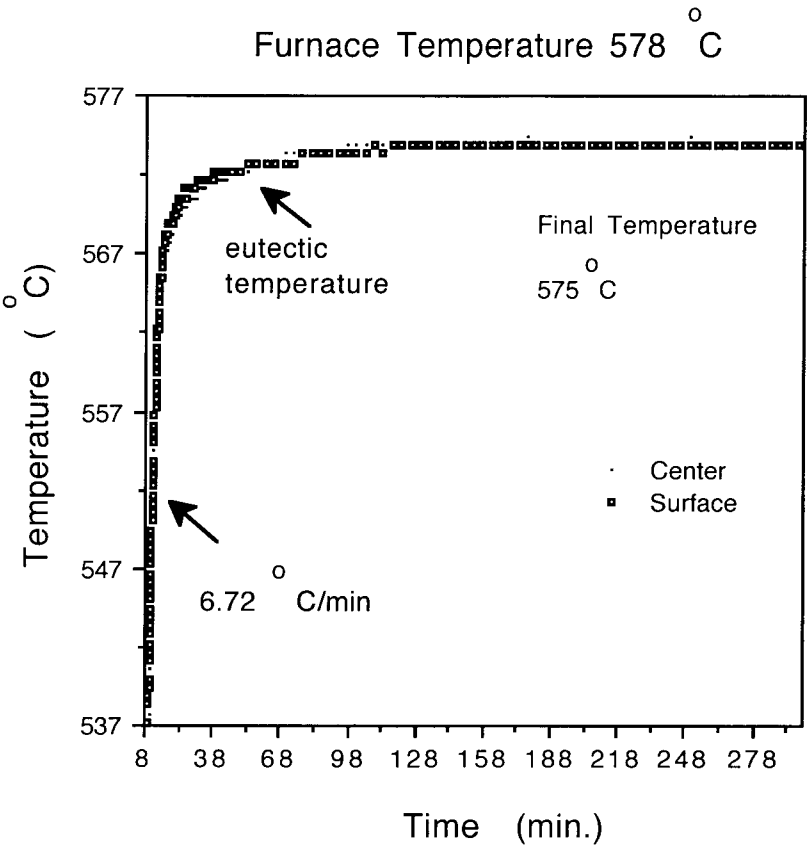

Figure 19. Semi-solid treatment Cycle 6 for Alloy #1. One thermocouple is located in the center and another at the surface.

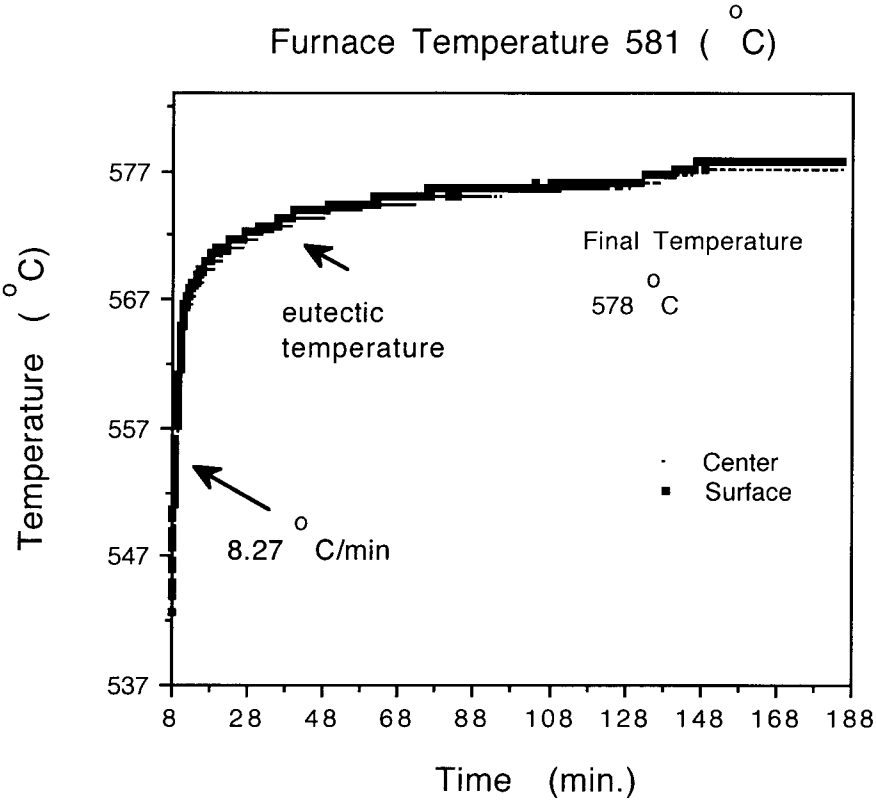

Figure 20. Semi-solid treatment Cycle 7 for Alloy #1. One thermocouple is located in the center and another at the surface.

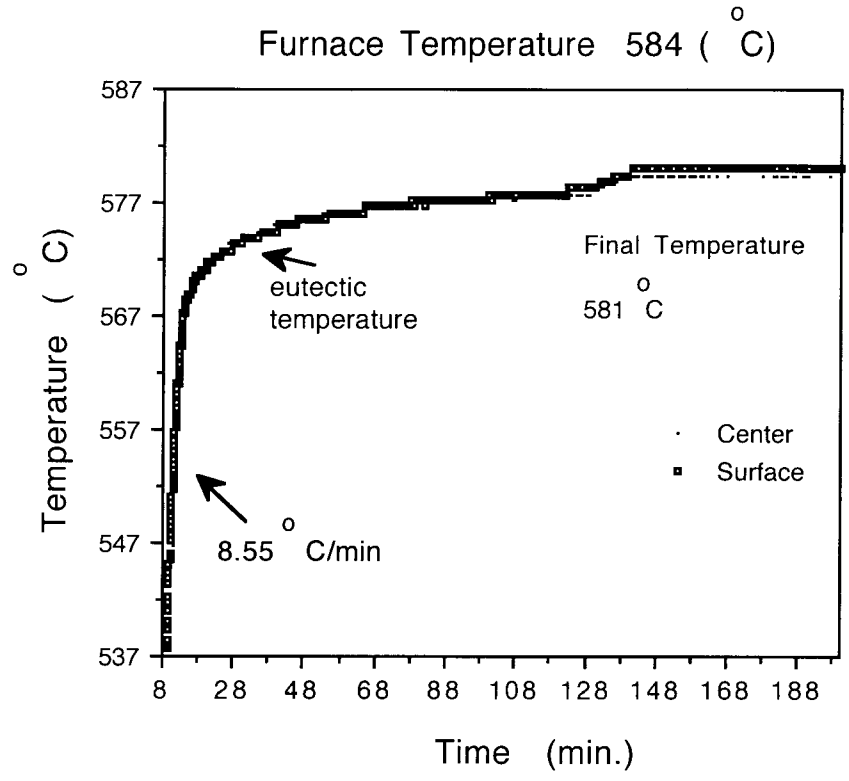

Figure 21. Semi-solid treatment Cycle 8 for Alloy #1. One thermocouple is located in the center and another at the surface.

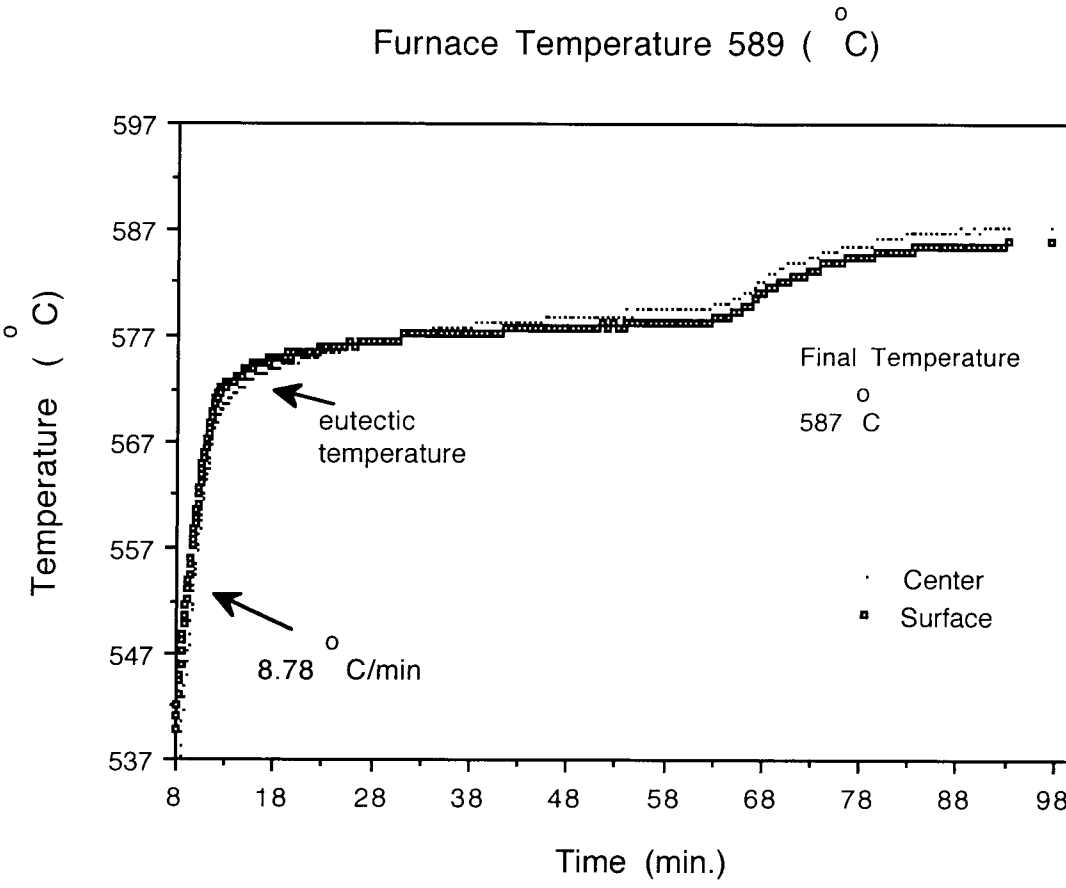

Figure 22. Semi-solid treatment Cycle 9 for Alloy #1. One thermocouple is located in the center and another at the surface.

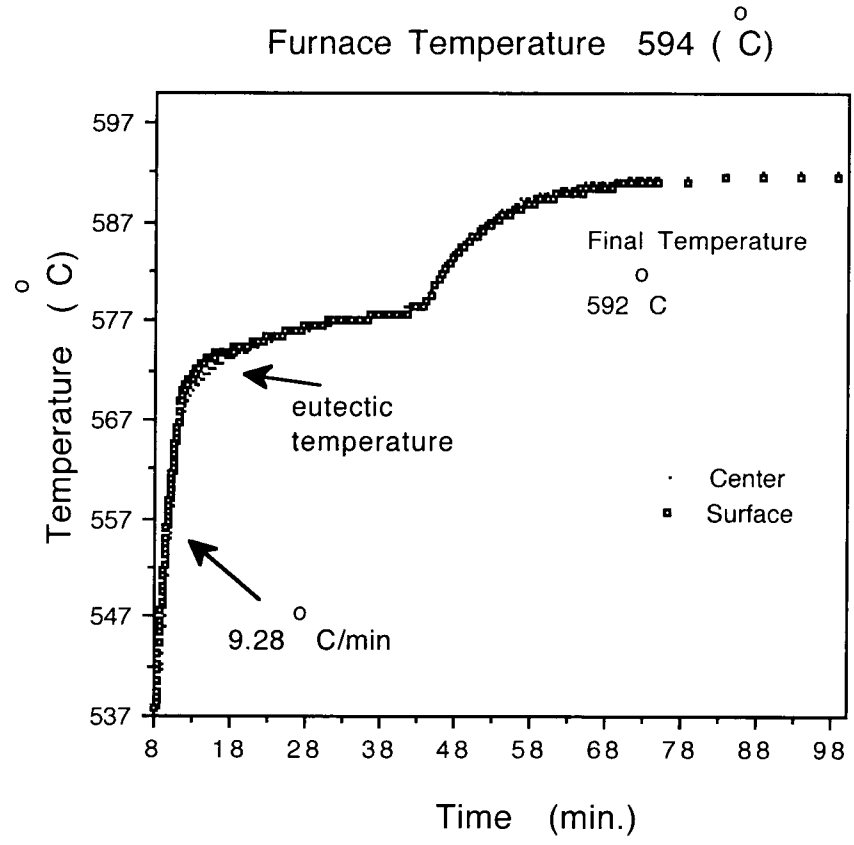

Figure 23. Semi-solid treatment Cycle 10 for Alloy #1. One thermocouple is located in the center and another at the surface.

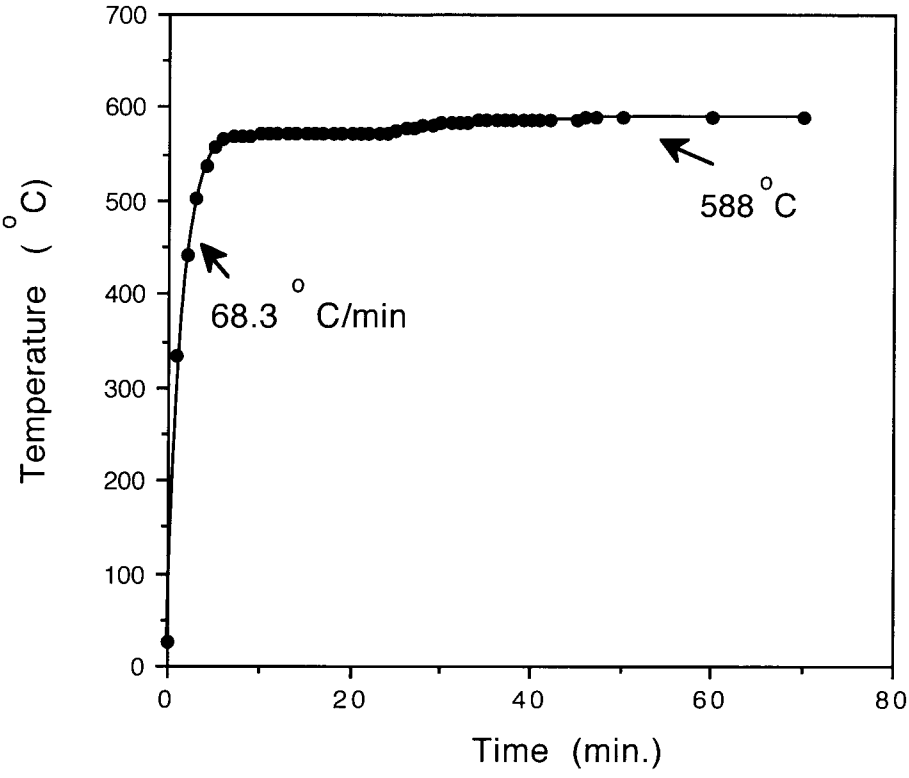

Figure 24. Semi-solid treatment Cycle 11 for Alloy #1. Air Furnace. One thermocouple is located on the surface of each sample. Initial set temperature: 598°C (1109°F) for 30 min. Final set temperature: 591°C (1095°F) for 30 min. followed by water quench. Samples were placed into the furnace at 598°C (1109°F).

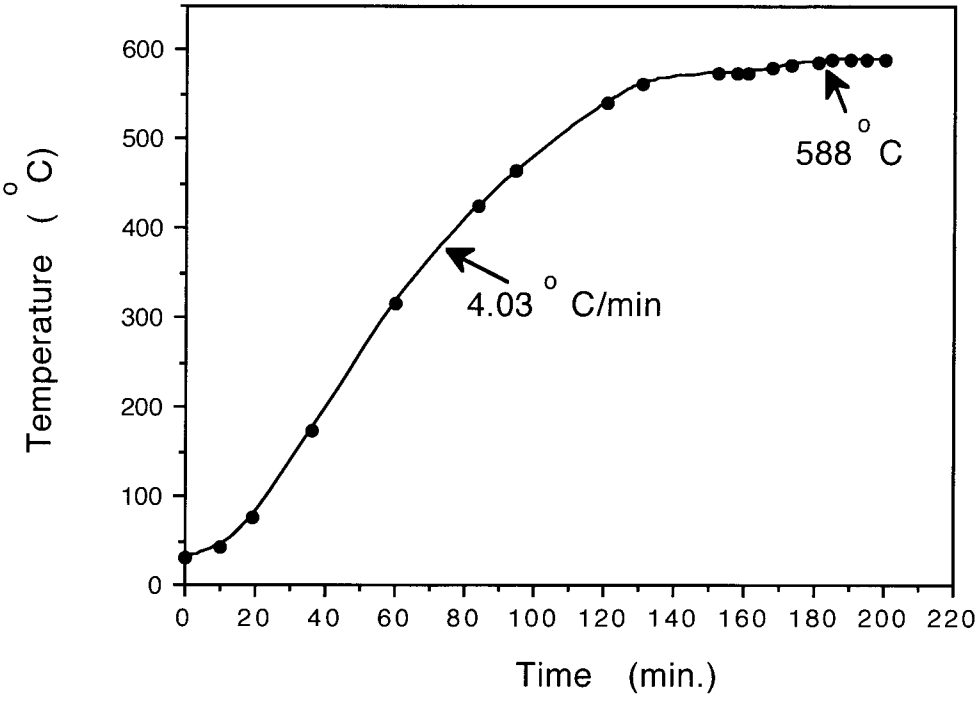

Figure 25. Semi-solid treatment Cycle 12 for Alloy #1. Vacuum Furnace. One thermocouple is located on the surface of each sample. Set temperature: 588°C (1090°F) until water quench. Samples were placed into the furnace at 20°C (68°F).

A356 (Alloy #1) and A357 (Alloy #3) alloys. Two initial sample sizes were used, 15.2 mm x15.2 mm x38.1 mm and 20.3 mm x20.3 mm x38.1 mm, to determine the T6 properties. The effect of holding the sample for various times (from 0 to 50 minutes) after reaching the eutectic temperature of 573°C (1063°F) on the T6 mechanical properties was studied. The effect of the cooling rate (air cool, oven cool, water quenching and liquid nitrogen quenching) on the T6 properties was also studied. In order to determine the effect of the environment on the mechanical properties, semi-solid treatments were performed in open air, vacuum furnace (200 millitorr) and in argon. The hardness and liquid/solid ratio of some A357 samples were also determined. Two groups of specimens were used to determine the mechanical properties of semi-solid treatments of A356 aluminum alloy. In one case, the specimens did not have a homogenization treatment before semi-solid treatment. In the other, the specimens had a homogenization treatment (see Fig.26 for heat-up to 566°C (1050°F) in 1.5 hours, kept at 566°C (1050°F) for 2.5 hours and cool down to room temperature in 4 hours) before semi-solid treatment.

5. Void studies

After semi-solid treatment, a small section was cut from each semi-solid specimen and the remainder machined into specimens for tensile testing. Voiding was evaluated from the removed portions and as well as the cross sections of fractured tensile specimens (gage section) using optical microscopy.

6. Press forging study

The semi-solid treatment and press forgings in this portion of the study were performed at the Northwest Aluminum Company (NWA) and HMM in Arkansas. At NWA, aluminum ingot specimens (often cubes of 25.4 mm x25.4 mmx25.4 mm) were heated in an induction furnace to the semi-solid state and were then low pressure compressed under approximately 0.7MPa (0.1 ksi) pressure or forklift pressing (55MPa or

8 ksi) after removal from the furnace. Water quenching was generally performed after forming. The press forge time was about 5-7 seconds and roughly 30 seconds for forklift pressing. The specimens were T6 treated and tensile tested after compression and cooling. Some semi-solid A356 aluminum alloy ingots produced by NWA also were press formed at HMM. The initial ingot size was 82 mm diameter and 127 mm long. The size of ingot before press forming was reduced to 76 mm diameter and 90 mm long by machining. The semi-solid treatment cycle at NWA prior to shipping to HMM is shown in Figure 27. HMM induction heated, formed and quenched the parts. The press forming parameters were unknown for HMM induction heated, formed and quenched parts. Two sections of a part (0313.2H and 0313.2EX1) were selected for void analysis. The areas for analysis positions are illustrated in Figure 27. The void analysis of polished and etched samples (etchant: 1 ml 48% HF and 200 ml water) was performed using an Olympus microscope. The magnifications were 50X and 200X. The number of voids was counted at 50X. The T5 and T6 properties of press formed parts 0313.H and 0313.EX1 were performed by Koon-Hall Testing Corp. in Portland, OR. The solution temperature and time were 538°C (1000°F) and 5 hours, respectively. The age temperature and time were 154°C (310°F) and 16 hours, respectively. The T5 treatment consisted of quenching from the die and aging at the T6 temperature.

7. Homogenization treatment

The 83 mm diameter ingot of A356 (Alloy #1) aluminum alloy was cut into 20.3 mm x20.3 mmx76.2 mm samples before homogenization treatment. Three homogenization treatments, before semi-solid treatment, were used to determine the effect of homogenization on the mechanical properties. The cycles are illustrated in Figure 28. The semi-solid treatment cycle is that in Figure 12. The "soak" times at 588°C (1090°F) were 0, 5 and 20 minutes. The microstructure analysis of samples before and after semi-solid treatment were performed in an Olympus microscope. The samples were polished and

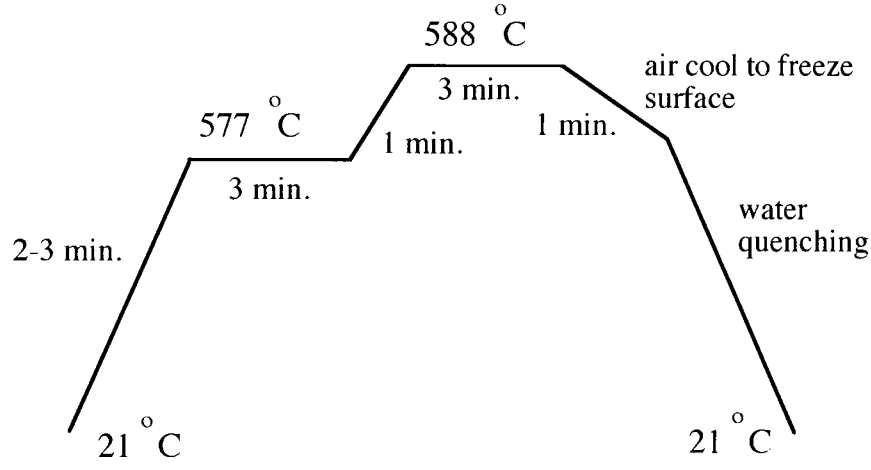

Figure 26. The semi-solid treatment of A356 aluminum alloy at NWA prior to forming at HMM to Fig. 27 configuration.

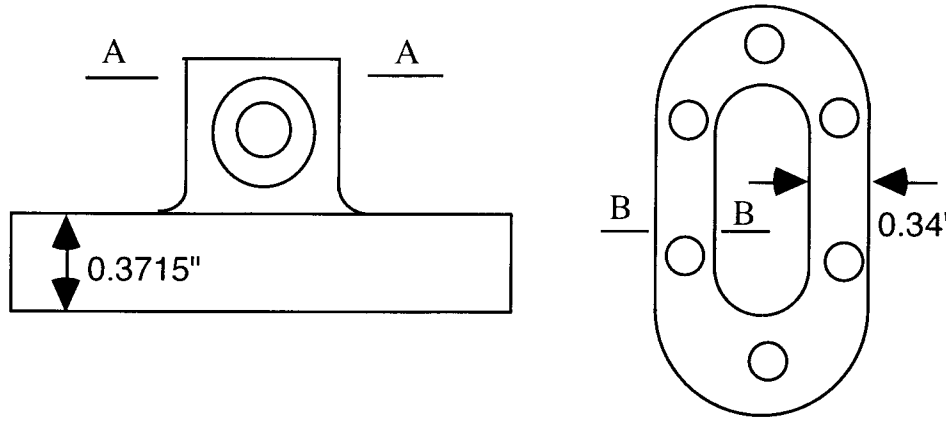

Side View

Bottom View

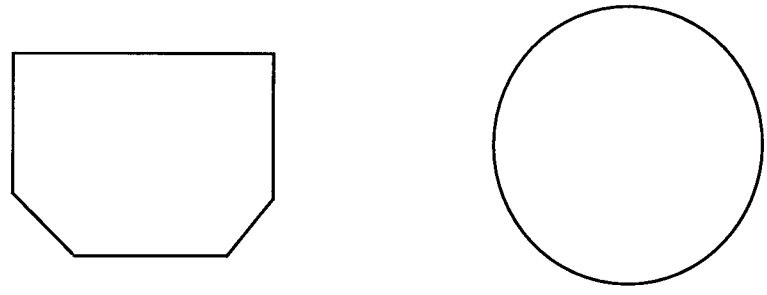

0313.2H

B-B

0313.2EX1

A-A

Figure 27. The shape of cross section of press formed samples 0313.2H and 0313.2EX1 of A356 aluminum alloy for void analysis.

etched (etchant: 1 ml 48% HF and 200 ml water) before analysis. The magnifications were 100X and 400X. The T6 properties were determined using a 4505 Instron testing machine, and three specimens were tested for each homogenization treatment.

8. Formability Studies

Formability test were performed at Northwest Aluminum Company on many of the alloys listed in Table 15. Formability was assessed for various thermal treatments. Variability consisted of different heating rates in an Asea Brown Boveri induction furnace. The heating rates were controlled by different power settings, measured in kilowatts. As the aluminum alloys are heated, they will ususlly experience an endothermic reaction at the eutectic temperature for Al-Si, decreasing the relatively rapid heating rate and, followed by an acceleration in heating rate. The time in the vicinity of the invariant temperature was varied as well as the final temperature and time at the final temperature.

Pressing consisted of removing an induction heated cube (approx. 25.4 mm x25.4 mmx25.4 mm) onto a cylinder block using Fiberfax insulating sheets. The semi-solid cube was then pressed at 0.3-0.7 MPa and quenched. Favorable formability was measured by the reduction in height of the semi-solid and an absence of visual tearing. Metallography was occasionally performed on the quenched semi-solid, particularly to determine void concentration, solid phase size and distribution.

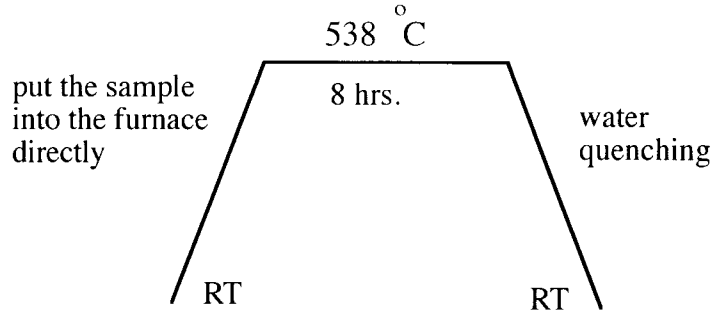

a.) Homogenization Cycle 1

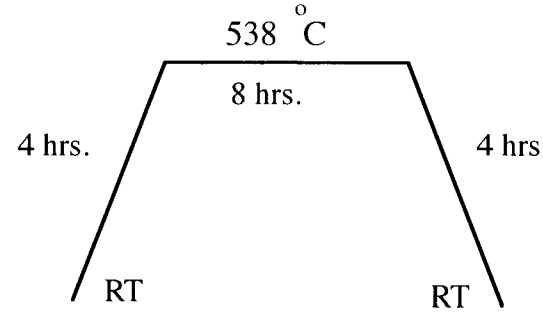

b.) Homogenization Cycle 2

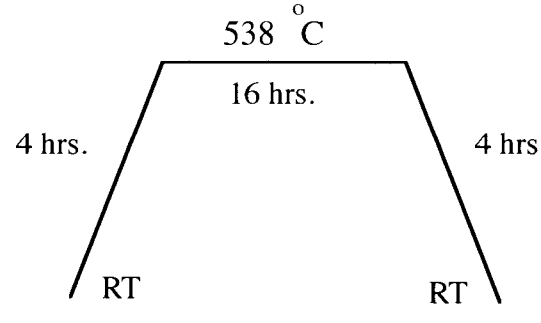

c.) Homogenization Cycle 3

Figure 28. Three homogenization cycles before semi-solid treatment for Alloy #1.

RESULTS AND DISCUSSION

A. The Study of Formation of Semi-solid Microstructure of A357 Aluminum Alloys

Unlike continuous stirring casting in which the semi-solid is formed from cooling molten metal, the spheroidal semi-solid microstructure in this study was formed by directly heating an as cast material into the semi-solid temperature range. The as-cast structure (Alloy #3) appears in Figure 29. The microstructural changes during the three heat-up cycles (Figure 14-18) are shown in Figure 30-37.

From Fig. 30 and Fig. 31, we notice that the as-cast structure disappears just after 573°C (1063°F) (eutectic) is reached for both Cycle 1 and Cycle 2. Also, Si exists at the grain boundaries as well as within the grains. The grain size is similar in the two figures. The as-cast structure disappeared relatively quickly, even in Cycle 2 which has a very high heating rate. This implies that the disappearance of as-cast structure is more sensitive to temperature than heating rate.

Figure 32 shows the microstructure in a specimen 3 minutes after it reached eutectic temperature of 573°C (1063°F), heated using Cycle 2. The final temperature, before water quenching, was 577°C (1070°F). It was observed that melting initiates at the grain boundary, implying that the grain size before melting may affect the solid phase size in the semi-solid state. The eutectic reaction also occurs inside the grain where Si particles exist. The dissolving of Si particles inside the grains may leave a large quantity of entrapped liquid inside the solid phase particles.

Figures 33 and 34 show two specimens that have undergone heating Cycle 1 and 2, respectively, 10 minutes after they reached 573°C (1063°F) and then water quenched. The final temperature reached by the samples was 584°C (1083°F). There is little difference in the heat up rate for the two cycles once 573°C (1063°F) is reached. There is little apparent difference in cycle microstructures resulting from the two cycles; again, implying that the

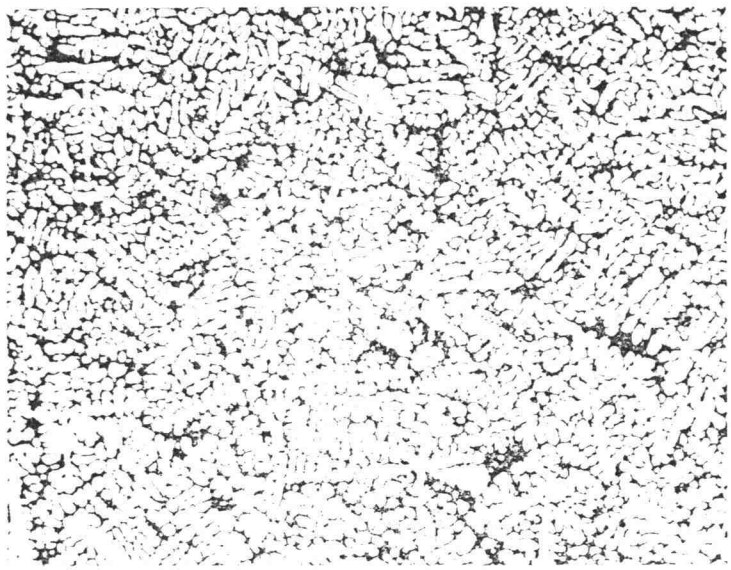

Fig. 29 As-cast for Alloy #3. 100X

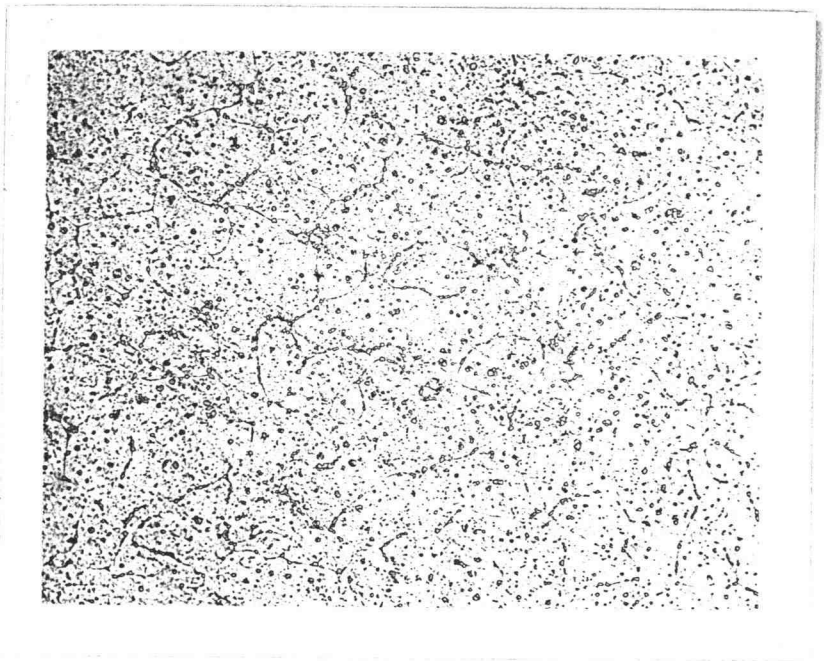

Fig. 30 10 sec. after the temperature reaches 573°C (1063 °F) followed by cold water quench. 100X. Alloy #3 Cycle 1

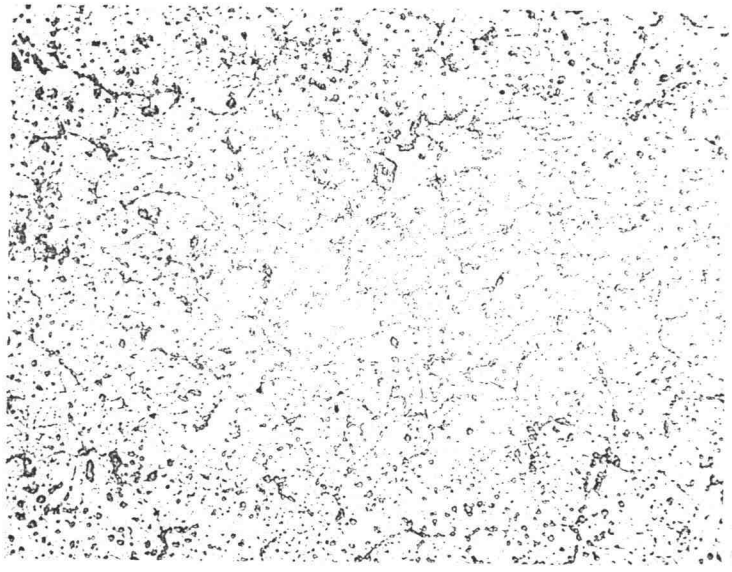

Fig. 31 10 sec. after the temperature reaches 573°C (1063 °F) followed by cold water quench. 100X. Alloy #3 Cycle 2

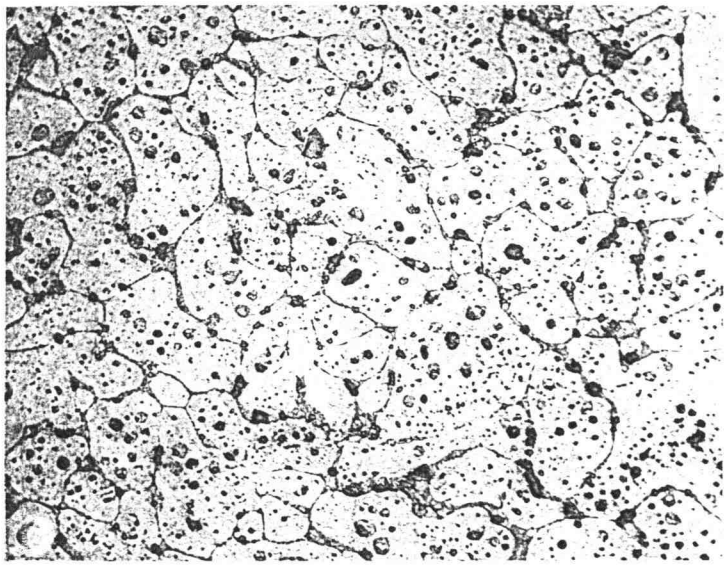

Fig. 32 3 min. after the temperature reaches 573°C (1063 °F) followed by cold water quench. 100X. Alloy #3 Cycle 2

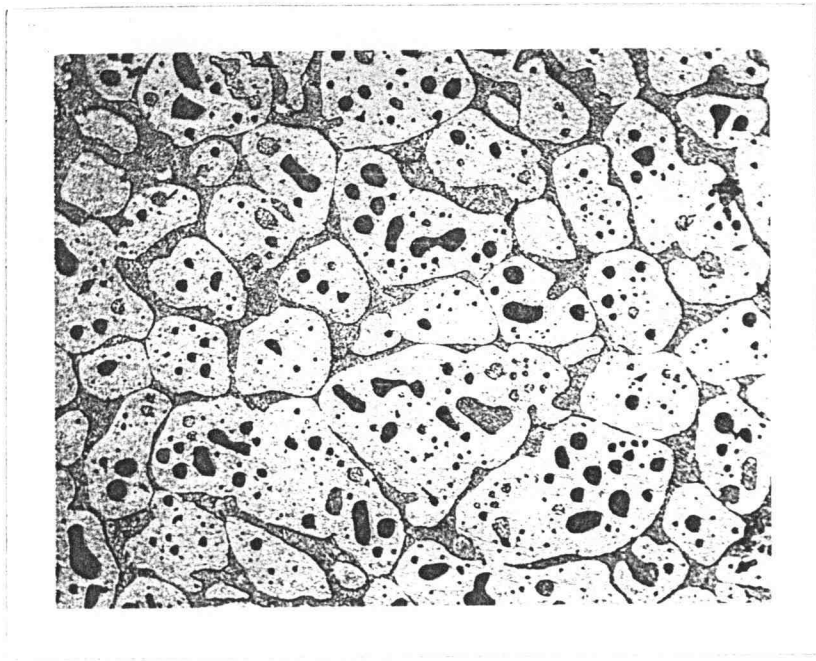

Fig. 33 10 min. after the temperature reaches 573°C (1063 °F) followed by cold water quench. 100X. Alloy #3 Cycle 1

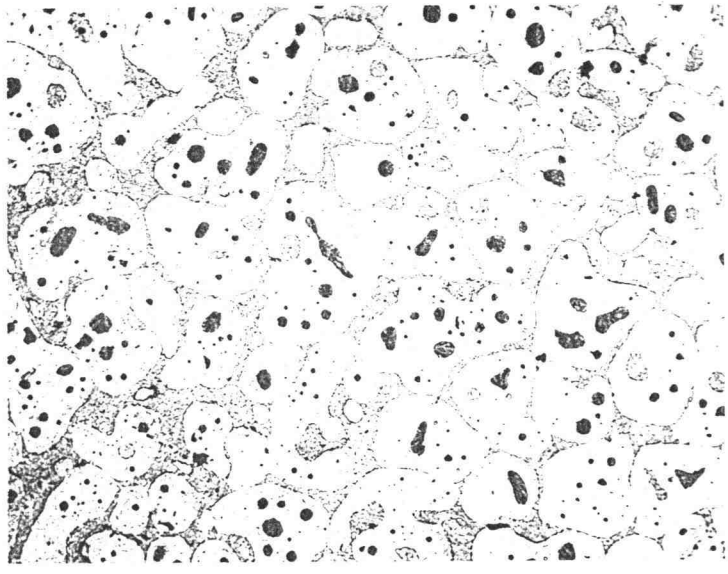

Fig. 34 10 min. after the temperature reaches 573°C (1063 °F) followed by cold water quench. 100X. Alloy #3 Cycle 2

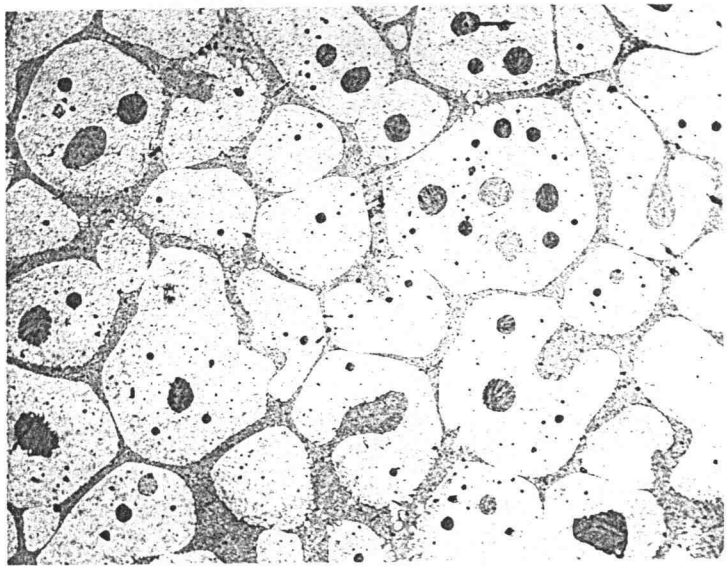

Fig. 35 588°C (1090 °F) 30 min. Cold water quenched. 100X
Alloy #3 Cycle 1

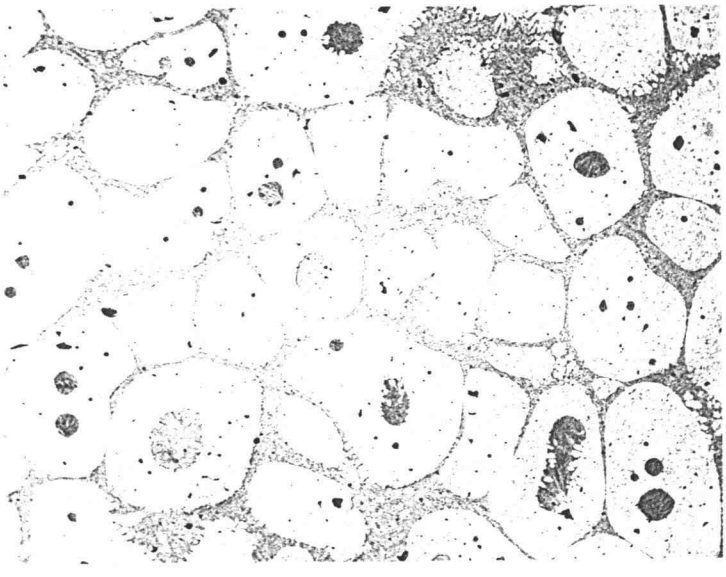

Fig. 36 588°C (1090 °F) 30 min. Cold water quenched. 100X
Alloy #3 Cycle 2

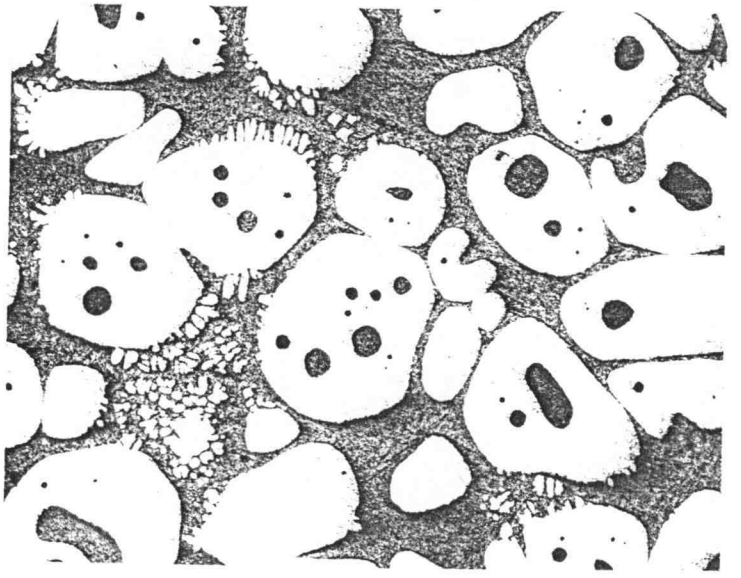

Fig. 37 588°C (1090 °F) 30 min. Cold water quenched. 100X
Alloy #3 Cycle 3

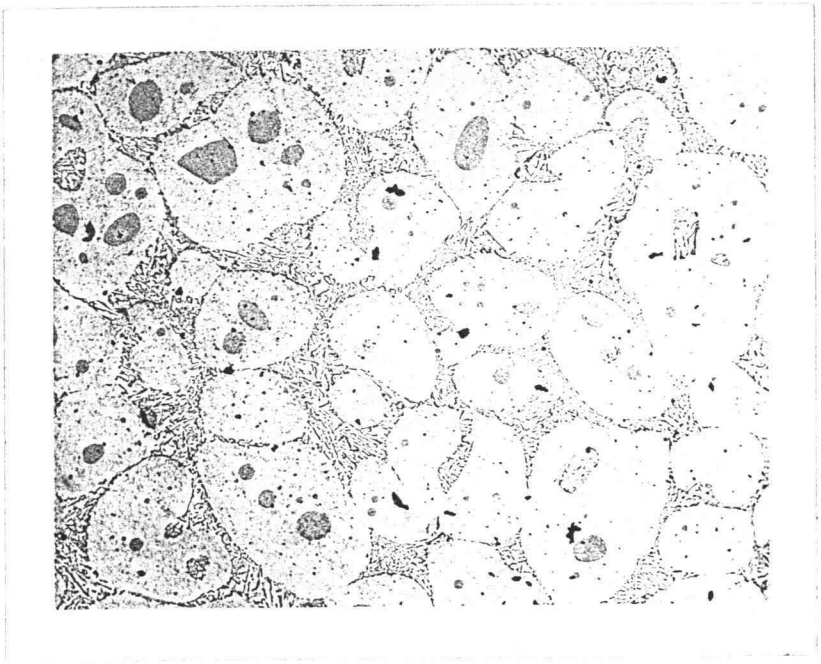

Fig. 38 588°C (1090 °F) 30 min. Fan cool. 100X
Alloy #3 Cycle 1

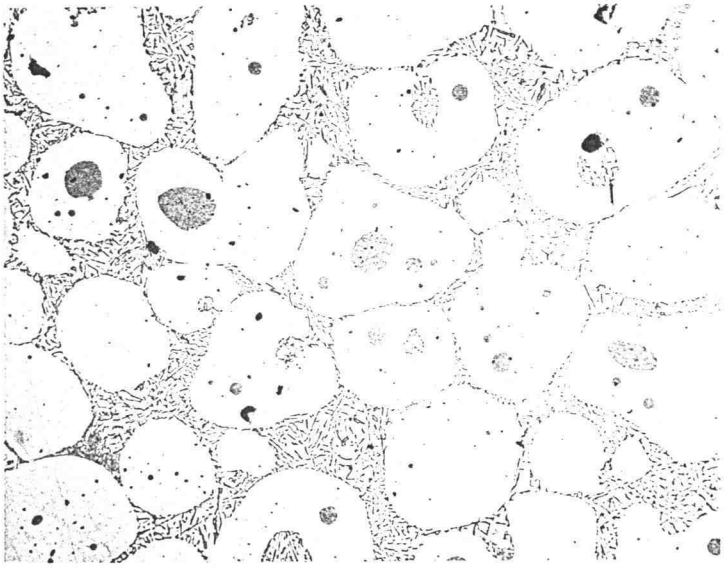

Fig. 39 588°C (1090 °F) 30 min. Fan cool. 100X
Alloy #3 Cycle 2

microstructure is relatively independent of heat up rates, at least within the range examined.

Figures 35, 36, and 37 show the semi-solid microstructure 30 minutes after the specimens had reached 588°C (1090°F), for Cycle 1, Cycle 2, and Cycle 3, respectively. The three samples were water quenched. The size and shape of the solid phase are observed to be similar for these cycles. The sizes of the solid phases are larger than those shown in Figure 33 and 34, implying that higher temperature and longer soak time may be associated with growth of the solid spherical phase. Note that the specimen in Figure 37, which underwent the Cycle 3 heating cycle shows some dendritic-like microstructure in the liquid phase. The reason for this, perhaps, is an inadvertent cooling slightly slower than normal, allowing the liquid to begin a eutectic decomposition. These will be referred as "toes".

Figures 38 and 39 show two specimens that underwent the Cycle 1 and Cycle 2 heating procedure, respectively, to 588°C (1090°F). They remained at that temperature for 30 minutes and were then fan cooled. As expected, the size and shape of the semi-solid phase is similar to the samples that spent an equal time at 588°C (1090°F) but were water quenched (Figure 35, 36, and 37). In these two slower cooled cases, though, the Si precipitates in the liquid phase are more obvious.

The nondendritic and spheroidal semi-solid microstructures formed through heating of the as-cast ingot to the semi-solid temperature are similar to the semi-solid microstructures of other aluminum alloys (A356 [101], Al-6.5% Si [41] and Al-15% Cu [49]) formed through continuous stirring. This indicates that the method used in this research to obtain semi-solid is comparable to the continuous stirring casting method from a microstructural vantage.

B. The Study of Isothermal Grain Growth of Solid Phase Particles for A357 Aluminum Alloy

The grain size and shape of the solid particles in the semi-solid material is an important factor that affects mechanical properties and hot workability. As mentioned in the introduction, the mechanism of coarsening of solid particles for continuous stirring casting are Ostwald ripening and/or coalescence. Figures 40 through 44 show the microstructure of the samples at 579°C (1075°F) and Figures 45 through 49 show the microstructure of the samples for the temperature at 588°C (1090°F), both from 10 to 60 minutes at each temperature.

It can be observed from Figures 40 through 44 that the grain size of solid phase grows as the time increases at a semi-solid temperature of 579°C (1075°F). The significant spheroidal growth appears from 10 minutes to 20 minutes. From 30 to 60 minutes, there is little change in microstructure. The same results are observed for the semi-solid temperature of 588°C (1090°F) (Figs. 45-49); the significant spheroidal growth is most pronounced before 20 minutes. The results indicate that spheroidal growth rate is time-dependent.

Comparison of the microstructures at the temperatures of 579°C (1075°F) and 588°C (1090°F) at 10 minutes (Figures 40 and 45) indicates that there is no significant difference in grain size although, of course, more liquid phase exists at 588°C (1090°F). It is also observed that the grain sizes are similar for both temperatures after about 30 minutes (Figure. 42 through 44 and 47 through 49). This indicates that the grain size changes depend mainly on the time at temperatuure rather than temperature, at least over the range investigated. Also, it is found that some grains are connected at both temperatures at all times (see Figure 40 through 49), which may imply that the mechanism of solid phase grain growth in the semi-solid process is, in part, coalescence.

The tendency of coarsening under isothermal conditions of the solid particles in this study is consistent with results of coarsening of solid particles in continuous stirring [41].

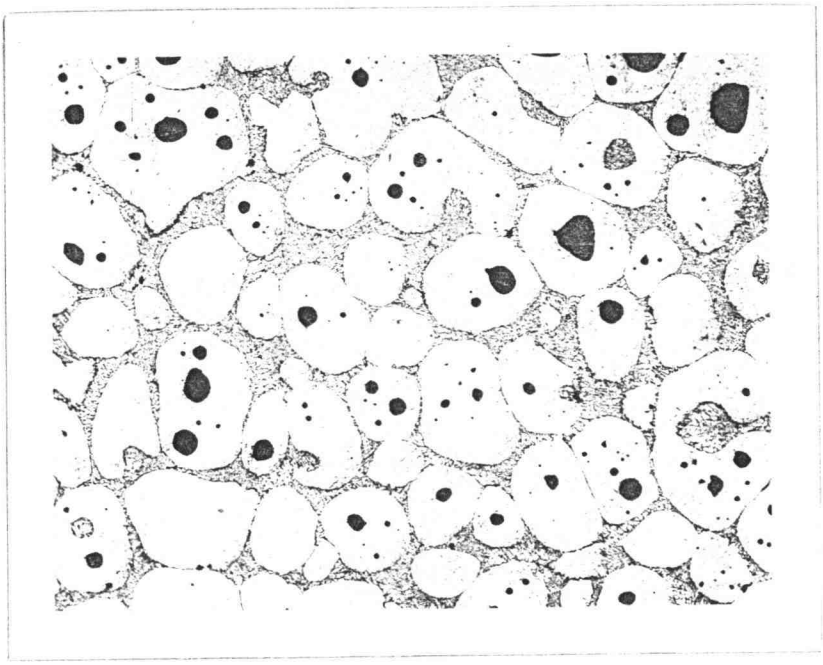

Fig. 40 579°C (1075 °F) 10 min. 100X

Alloy #3 Cycle 4

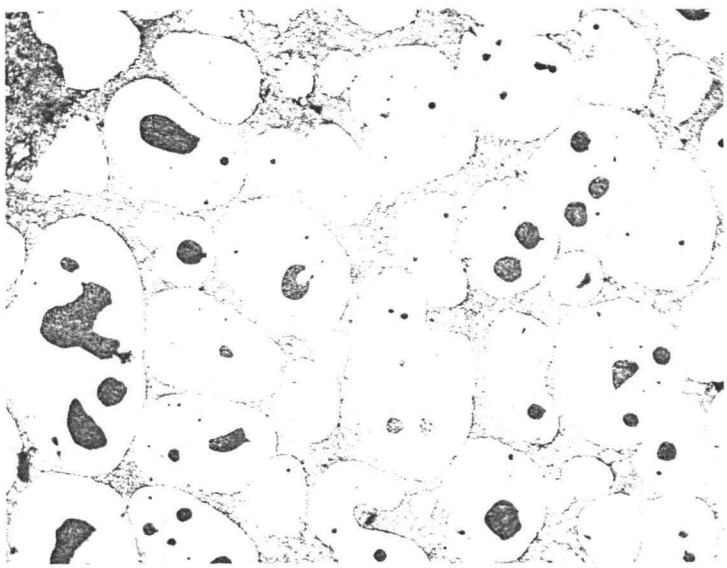

Fig. 41 579°C (1075 °F) 20 min. 100X

Alloy #3 Cycle 4

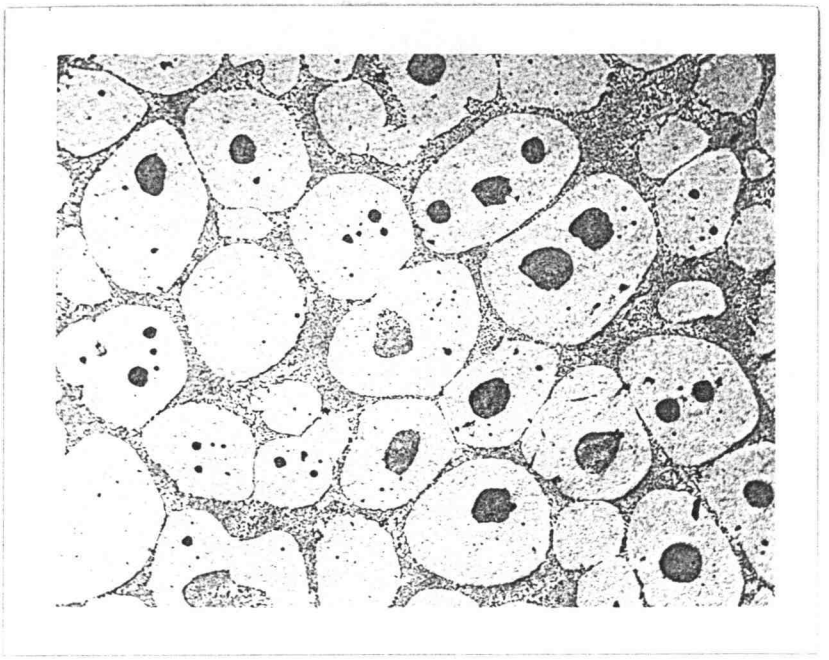

Fig. 42 579°C (1075 °F) 30 min. 100X

Alloy #3 Cycle 4

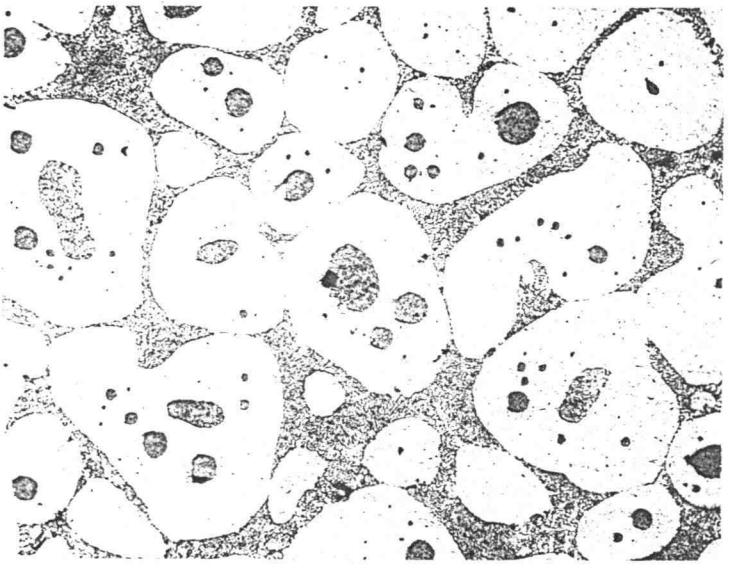

Fig. 43 579°C (1075 °F) 45 min. 100X

Alloy #3 Cycle 4

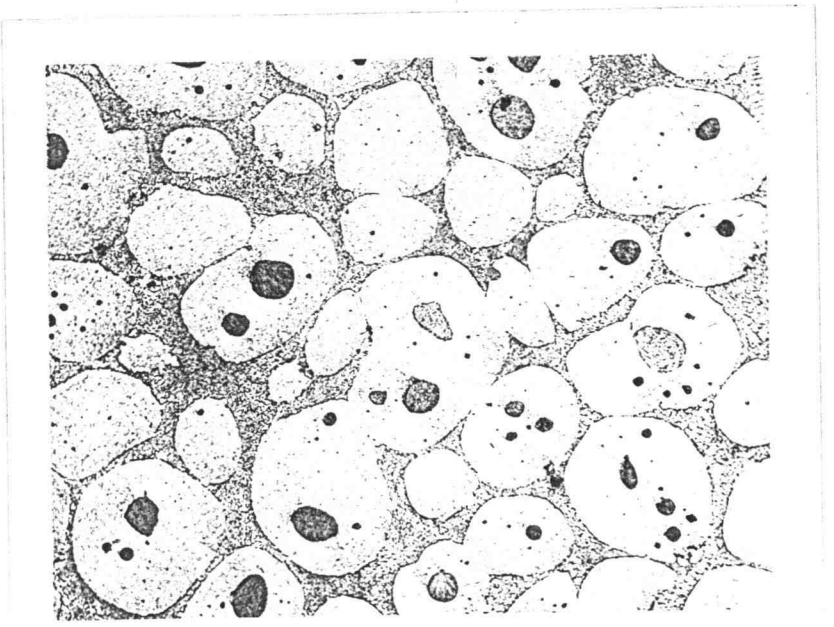

Fig. 44 579°C (1075 °F) 60 min. 100X

Alloy #3 Cycle 4

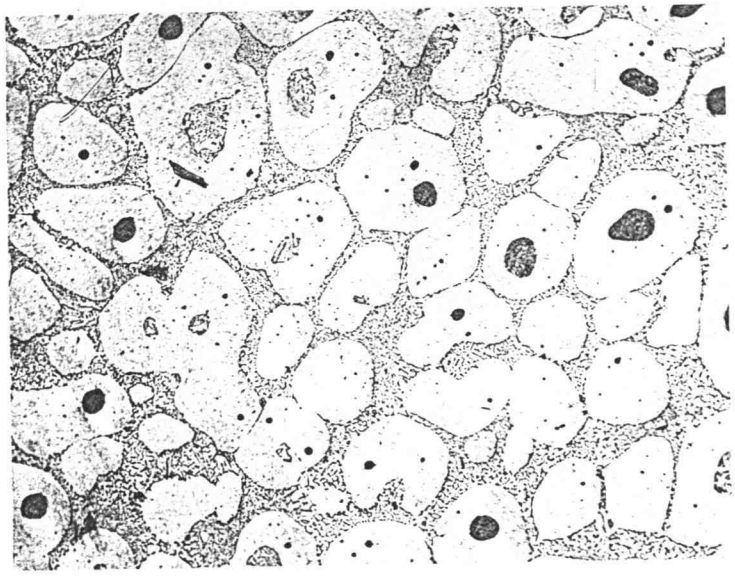

Fig. 45 588°C (1090 °F) 10 min. 100X

Alloy #3 Cycle 5

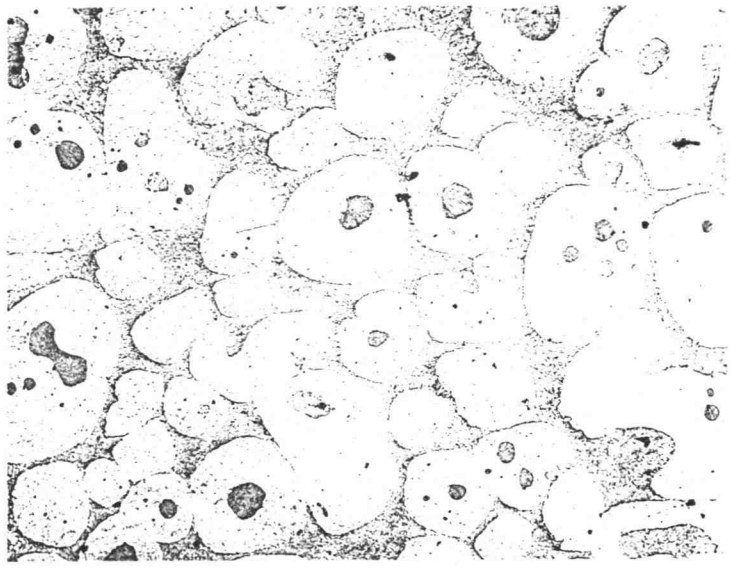

Fig. 46 588°C (1090 °F) 20 min. 100X

Alloy #3 Cycle 5

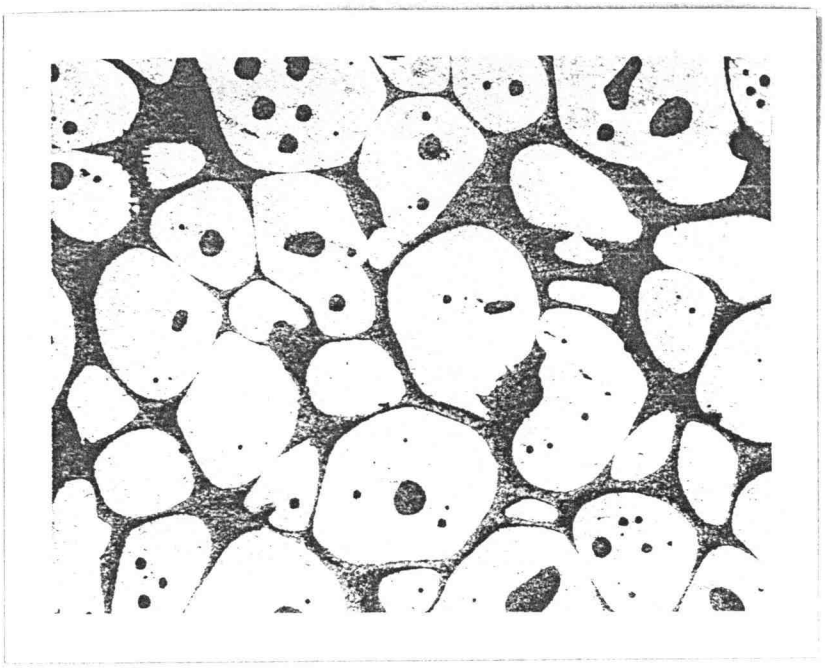

Fig. 47 588°C (1090 °F) 30 min. 100X

Alloy #3 Cycle 5

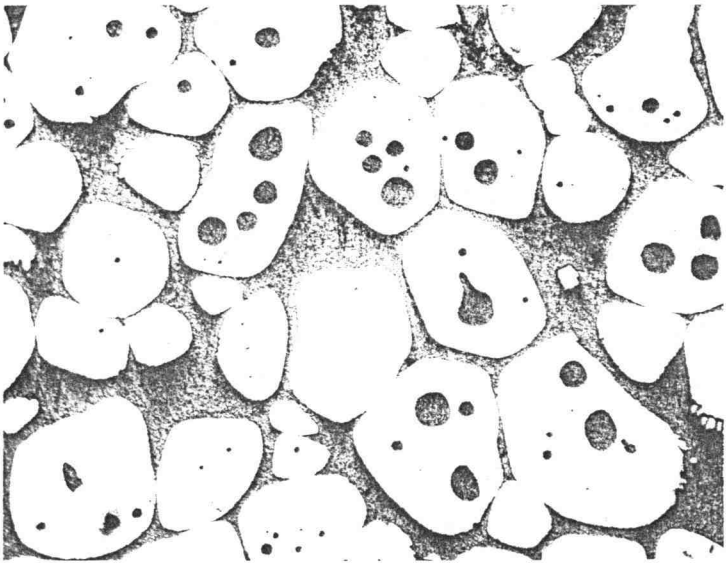

Fig. 48 588°C (1090 °F) 45 min. 100X

Alloy #3 Cycle 5

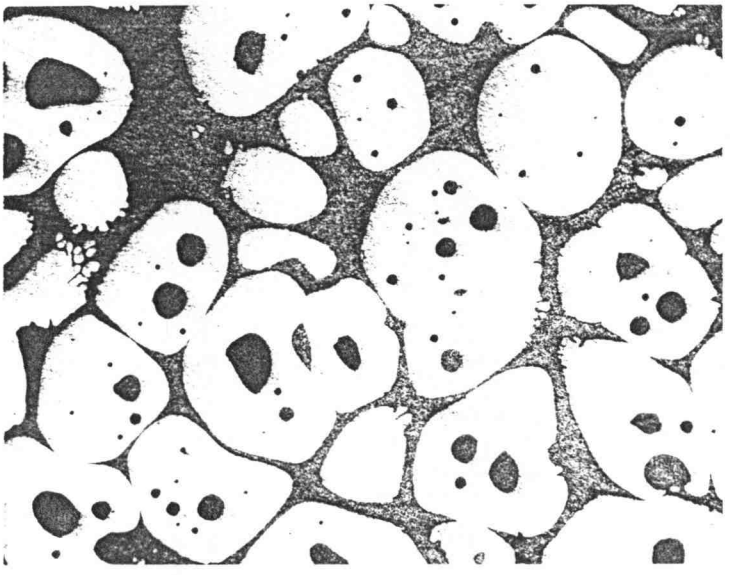

Fig.49 588°C (1090 °F) 60 min. 100X

Alloy #3 Cycle 5

Many studies of continuous stirring casting have indicated that both the solid grain size and spheroidicity of the solid phase increase as the isothermal "rest" time following stirring increases. Further research is needed for a better understanding of the coarsening mechanism.

C. The Study of Heat-up Cycle in the Semi-solid Treatment of A356 Aluminum Alloy

Reduction of the total time of the semi-solid treatment cycle is another objective of this study. The important phase transition reaction in semi-solid treatment of A356 and A357 aluminum alloys is the eutectic reaction. It is observed that the heat-up cycle can be divided into three stages for the furnace set temperature greater than 581°C (1078°F) (see Figures 20 through 23). In stage I (from RT to eutectic temperature), the temperature increases greatly with time. There is not much difference in the relationship between time and temperature in stage I for different given furnace set temperatures. In stage II, as the eutectic temperature is reached, the temperature increases very slowly and the total heat-up time, of course increases. The higher the furnace temperature, the shorter stage II. It is observed that the end temperature of stage II is around 577°C (1071°F) regardless of the furnace temperatures. The temperature increases rapidly in stage III, after the eutectic. For the furnace set temperature of 578°C (1073°F), only stage I and stage II are observed in the heat-up cycle.

Microstructural changes in the semi-solid material are associated with the heat-up stages. In stage I (from ambient temperature to near the eutectic temperature), the material is solid. Figure 50 and 51 show the as-cast structure before heating and the microstructure just at the eutectic temperature of 573°C (1063°F) for the A356. It is observed that the results are similar to that of A357 aluminum alloy. The disappearance of the as-cast structure is the main characteristic at the end of Stage I.

Figure 52 shows the microstructure of A356 (Alloy #1) at 576°C (1068°F). It can

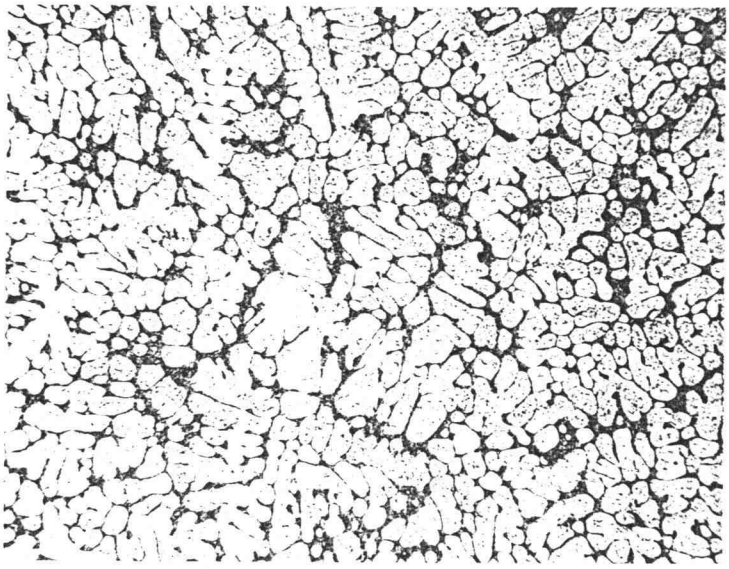

Fig. 50 As-cast of A356 (Alloy #1) 200X

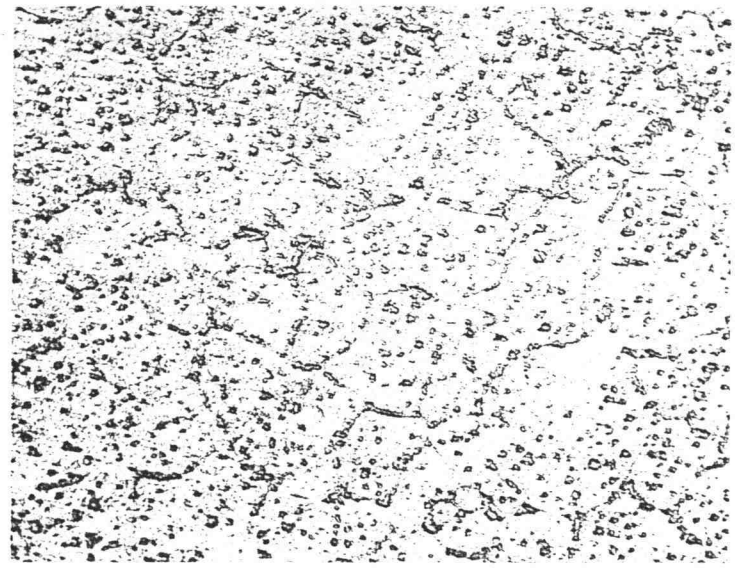

Fig. 51 Just after the temperature reaches 573°C (1063°F) and then water quenched for A356 (Alloy #1) 100 X
Semi-solid Cycle 9

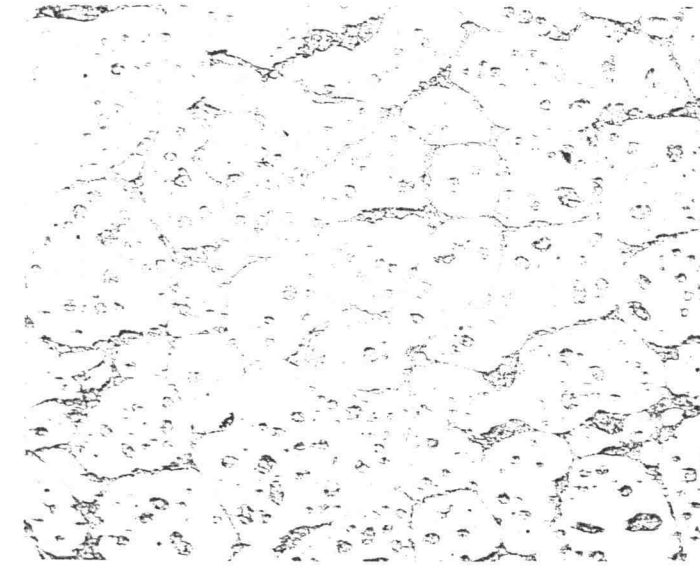

Fig. 52 Just after the temperature reaches 576°C (1068°F) and then water quenched for A356 (Alloy #1) 100 X
Semi-solid Cycle 9

be observed that, just as with the A357 alloy, the eutectic reaction of the A356 alloy starts in the grain boundariesand the Si particles inside the grain. Many small entrapped liquid regions are observed inside the solid particles. Figures 53 and 54 show the microstructure of specimens at 578°C (1072°F) which is the end of stage II. It is observed that most of the Si particles have been dissolved in the liquid. The dissolving of Si increases the time of stage II because it involves the diffusion of Si from the solid phase to the liquid phase. The final temperature of stage II for A356 aluminum alloy in this study, is about 577°C (1071°F).

Figures 55 and 56 show the microstructure of A356 alloy samples at 582°C (1080°F) and 587°C (1088°F), respectively. It was observed that the solid particles become larger, indicating that the solid particles grow in stage III. It was also observed that the number of entrapped liquid regions at 587°C (1088°F) is less than that at 582°C (1080°F), which implies that the number of entrapped liquid phase regions can be decreased in Stage III. Figure 57 shows the microstructure of the A356 alloy at 587°C (1088°F) for 30 minutes. It is observed that the solid particles have become more spheroidal over time. The growth and increased spheroidicity of the solid phase which is consistent with other research results [65] and the decrease in the number of entrapped liquid phase regions are the main microstructural changes in stage III.

Stage II appears to be the dominant stage which requires the longest time of the three heat-up stages of the semi-solid treatment. The relationship between heat-up time (from 538°C (1000°F) to the final temperature of stage II) and furnace temperature is shown in Figure 58. It is observed that the higher the furnace set temperature, the less the time of stage II. This is because the heat exchange rate in stage II is higher with higher furnace set temperatures than that with lower set temperatures.

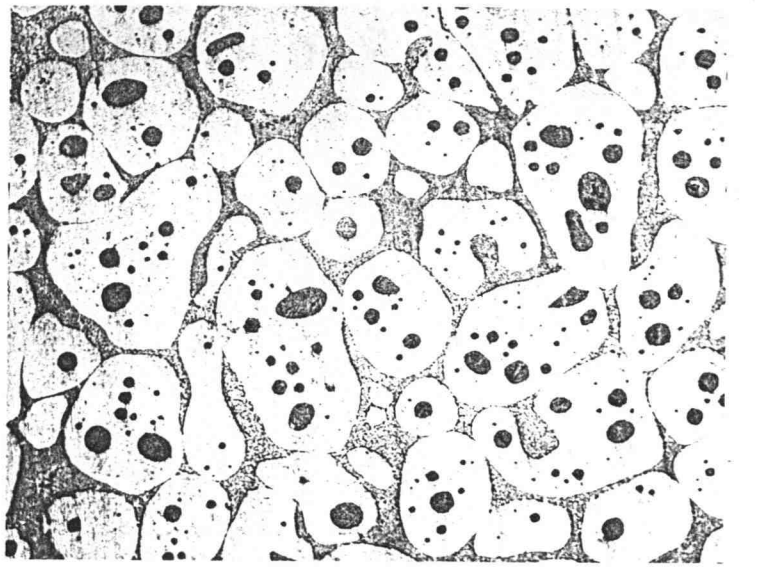

Fig. 53 Just after the temperature reaches 578°C (1072°F) and then water quenched for A356 (Alloy #1) 100 X
Semi-solid Cycle 9

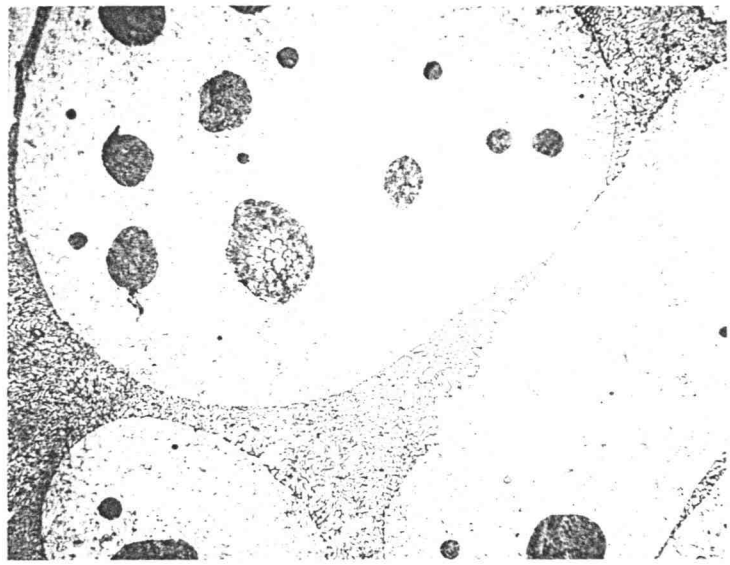

Fig. 54 Just after the temperature reaches 578°C (1072°F) and then water quenched for A356 (Alloy #1) 400 X
Semi-solid Cycle 9

Fig. 55 Just after the temperature reaches 582°C (1080°F) and then water quenched for A356 (Alloy #1) 100 X
Semi-solid Cycle 9

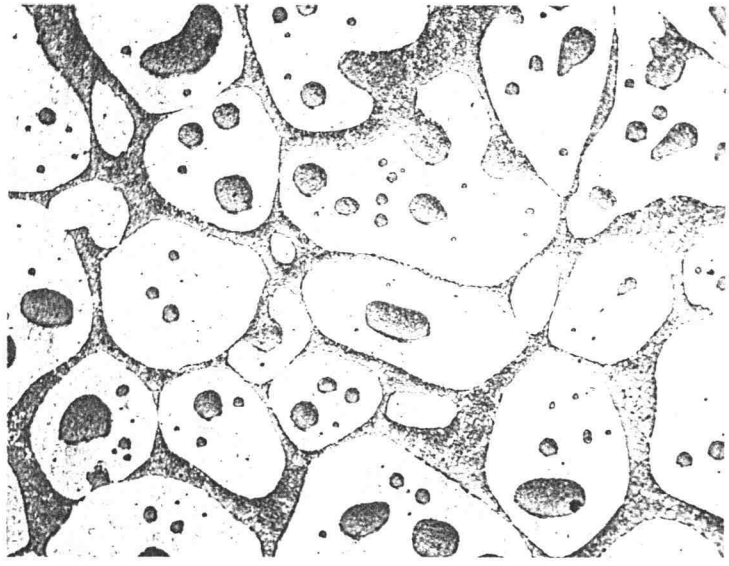

Fig. 56 Just after the temperature reaches 587°C (1088°F) and then water quenched for A356 (Alloy #1) 100 X
Semi-solid Cycle 9

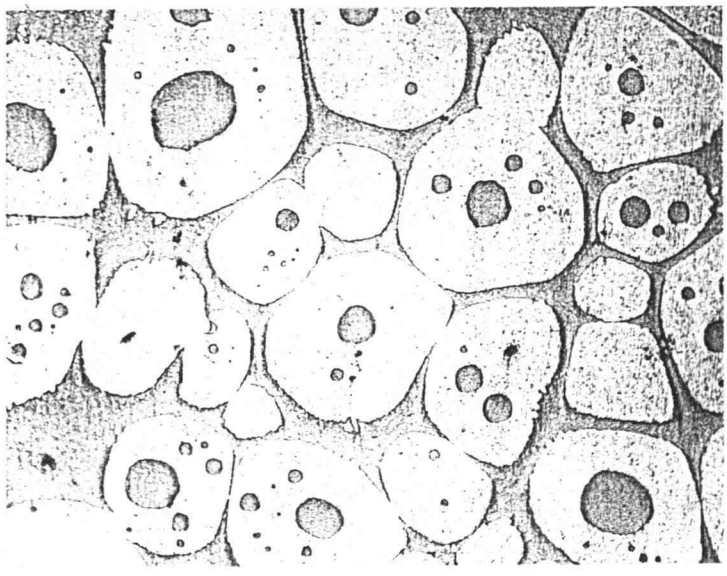

Fig. 57 At 587°C (1088°F) for 30 min and then water quenched for A356 (Alloy #1). 100 X Semi-solid Cycle 9

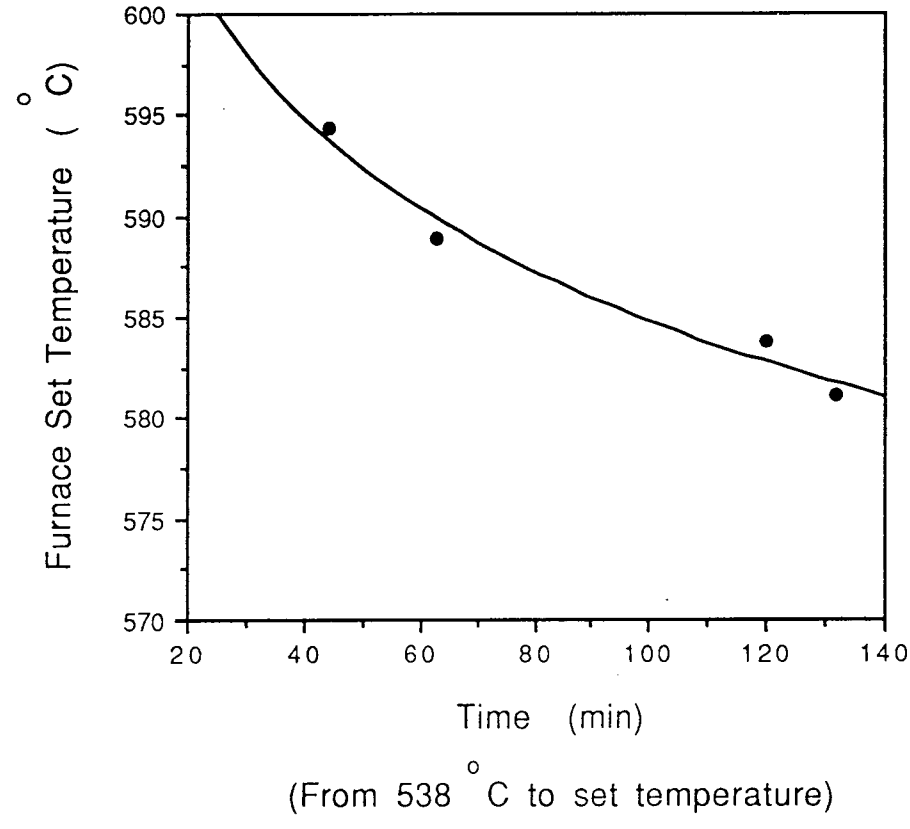

Figure 58. The relationship between heat-up time in the temperature range from 538°C (1000°F) to the final temperature of the samples and the furnace set temperature for Alloy #1.

D. The Study of Mechanical Properties of Semi-solid A356 and A357 Aluminum Alloys

The purpose of this part of the study is to determine the hardness, liquid/solid ratio and T6 properties of the A356 and A357 aluminum alloys (Alloy #1,3). The hardness and liquid/solid ratio and T6 properties of semi-solid A357 aluminum alloys are listed in Table 16. We observe that the amount of liquid phase is similar (about 35%) at 588°C (1090°F) for Cycle 1, 2 and 3. The time at 588°C (1090°F) did not affect the liquid/solid ratio. This indicates that the liquid/solid ratio mainly depends on the semi-solid temperature. It is also found from Table 16 that the hardness was similar for all water quenched samples (about RHB 61) and for all fan cooled samples (about RHB 56) regardless of the semi-solid cycle used. The hardness increased as cooling rate increased. The T6 properties were tested in sample SS-1, 4 and 7. The semi-solid A357 appeared to be brittle with little ductility. UTS was 227, 190 and 202 MPa (32.9, 27.5 and 29.3 ksi) for Cycle 1, 2 and 3, respectively. The reduction at area was very small (about 1%) for all three cycles. This will be partly shown to be due to relatively high hydrogen in Wagstaff alloy leading to, perhaps, porosity.

In order to compare the T6 mechanical properties of A356 aluminum alloy before and after semi-solid treatment, it was necessary to determine the T6 properties of the as-cast ingot. Table 17 lists the results of the T6 properties of A356 as cast ingot. It is noticed from Table 17 that there is not significant difference in two groups. Group 1 was not homogenized before T6. The results imply that the T6 tensile properties of as-cast ingot may not be sensitive to the homogenization treatment although only one homogenization cycle was used in this study.

The semi-solid treatment cycle of A356 aluminum alloy in an atmosphere of air was Cycle 11, is shown in Fig. 24. Three cooling rates (water quenching, liquid nitrogen quenching and air cool) were used. After the temperature reached 573°C (1063°F), the specimens were kept for 10, 20, 25 and 30 minutes before cooling, and the T6 properties were tested.

Table 16. The mechanical properties of semi-solid A357 (Wagstaff Alloy #3) Aluminum alloy in this study.

Sample #	Atmosphere	Semisolid Treatment Cycle	Time after 573°C (min)	Final tempt. (°C)	Time at 588°C (min)	Cool down	Yield Stress (MPa)	UTS (MPa)	Elongation (%)	Reduction at Area (%)	Hardness (RHB)	Liquid (%)
SS-1	Air	1	36	588	30	Water	---	227	0	0.72	62.4	34.4
SS-2	Air	1	36	588	30	Fan Cool	---	---	---	---	56.2	35.1
SS-3	Air	1	9	588	3	Water	---	---	---	---	60.9	35.4
SS-4	Air	2	34	588	30	Water	---	190	0	0.56	61.2	34.8
SS-5	Air	2	34	588	30	Fan Cool	---	---	---	---	55.7	35.5
SS-6	Air	2	10	588	6	Water	---	---	---	---	61.4	36.4
SS-7	Air	3	36	588	30	Water	---	202	0	1.02	64.7	34.1

One sample for each test.
Initial sample size: 15.2 mm x 15.2 mm x 76.2 mm

Table 17. T6 properties of as cast Alloy #1 specimens from 76.2 mm diameter ingot.

Group No.	Homogenization Cycle (Homogenization temp. 1050°F)			Yield Stress (MPa)	UTS (MPa)	El (%)
	Heat-up Time (hrs)	Soak Time (hrs)	Cool-down Time (hrs)			
1	--	--	--	274	336	17.1
2	1.5	2	4	275	332	15.9

Three samples for each test.
T6: Solution temperature and time were 538°C (1000°F) and 3 hours, respectively. Aging treatment and time were 154°C (310°F) and 16 hours, respectively.

Table 18 shows the T6 properties of semi-solid A356 aluminum alloy with a sample size of 15.2 mm x 15.2 mm x 76.2 mm. The diameter of final tensile specimen is 6.35 mm. It is observed that the maximum and minimum value of elongation were 4.08% and 0% in semi-solid Cycle 11. In general, the results showed that semi-solid A356 appeared to be similar to the semi-solid A357 in Table 16, although somewhat better ductility (and strength) perhaps partly due to decreased hydrogen. UTS varied from 163 to 304 MPa (23.6 to 44.1 ksi). It is observed from Table 18 that the stress and ductility are better in the specimens kept for 0 min. or for more than 5 min. at 588°C (1090°F) regardless of the cooling method. This indicated that the time kept in semi-solid state may vary the mechanical properties of the material.

In the study of effect of atmosphere on the T6 properties of semi-solid A356 aluminum alloy, the semisolid treatment of samples SS-20, 21 and 22 were performed in a vacuum furnace and sample SS-23 in Argon. Semi-solid Cycle 12 was showed in Figure 25. The cooling method for sample SS-22 and 23 was oven cool. The time kept at 588°C (1090°F) is 30 minutes. The results of T6 properties are also shown in Table 18. It can be seen that the T6 properties were not improved in vacuum or Argon specimens, despite relatively lengthy soak time.

The effect of additional times after temperature reached 588°C (1090°F) on the T6 properties for vacuum semi-solid treatment was also determined for the sample size of 15.2 mm x 15.2 mm x 76.2 mm. The results are shown in Table 19. It is observed that the stress and ductility are better of the specimens kept for 0.1 and 5 minutes at 588°C (1090°F) than those kept for 0 and 10 minutes regardless of the cooling method used in contrast to the Table 18 work. Sample SS-26 had very good mechanical properties with yield stress of 261 MPa (37.9 ksi), UTS of 321 MPa (46.6 ksi), and elongation of 13.8%, which is close to the as-cast samples. It appears that water quenching has the best T6 properties. The explaination for this is unclear.

Table 20 showed the T6 properties in Cycle 13 for the increased initial sample size

Table 18. The T6 properties of semi-solid A356 (Alloy #1) Aluminum alloy in this study.

Sample #	Atmosphere	Semisolid Treatment Cycle	Time after 573°C (min)	Final tempt. (°C)	Time at 588°C (min)	Cool down	Yield Stress (MPa)	UTS (MPa)	Elongation (%)	Reduction at Area (%)
SS-8	Air	11	10	583	0	Water	---	211	0	0.25
SS-9	Air	11	20	588	0.1	Water	256	304	4.08	7.75
SS-10	Air	11	25	588	5	Water	259	295	2.55	7.47
SS-11	Air	11	30	588	10	Water	---	204	0	0.32
SS-12	Air	11	10	583	0	Liquid Ni	248	263	0.68	2.03
SS-13	Air	11	20	588	0.1	Liquid Ni	240	274	2.31	5.12
SS-14	Air	11	25	588	5	Liquid Ni	233	261	1.87	3.92
SS-15	Air	11	30	588	10	Liquid Ni	236	258	1.02	2.42
SS-16	Air	11	10	583	0	Air	---	163	0	0.01
SS-17	Air	11	20	588	0.1	Air	242	270	1.43	2.96
SS-18	Air	11	25	588	5	Air	250	285	3.21	6.67
SS-19	Air	11	30	588	10	Air	236	259	1.11	2.71
SS-20	Vacuum	12	60	588	30	Liquid Ni	247	272	1.76	4.13
SS-21	Vacuum	12	60	588	30	Water	---	254	0	0.24
SS-22	Vacuum	12	60	588	30	Oven Cool	---	167	0	0.16
SS-23	Argon	12	60	588	30	Oven Cool	232	242	0.56	2.72

One sample for each test.
Initial sample size: 15.2 mm x 15.2 mm x 76.2 mm

Table 19. The T6 properties of semi-solid A356 (Alloy #1) Aluminum alloy in this study.

Sample #	Atmosphere	Semisolid Treatment Cycle	Time after 572°C (min)	Final tempt. (°C)	Time at 588°C (min)	Cool down	Yield Stress (MPa)	UTS (MPa)	Elongation (%)	Reduction at Area (%)	Distance of voids from mini-ingot edge (mm)	# voids ave. in tensile specimen ($1/mm^2$)
SS-24	Vacuum	12	20	582	0	Water	-----	169	0	0.56	8.4	0.35
SS-25	Vacuum	12	30	588	0.1	Water	260	317	9.93	15.34	5.9	0.03
SS-26	Vacuum	12	35	588	5	Water	261	321	13.79	20.36	5.2	0
SS-27	Vacuum	12	40	588	10	Water	-----	233	0	0.96	3.1	0.54
SS-28	Vacuum	12	20	588	0	Liquid Ni	211	219	0.49	2.67	8.3	0.69
SS-29	Vacuum	12	30	588	0.1	Liquid Ni	231	237	0.72	3.34	7.8	0.88
SS-30	Vacuum	12	35	588	5	Liquid Ni	230	259	1.27	4.12	3.2	0.57
SS-31	Vacuum	12	40	588	10	Liquid Ni	195	197	0.18	1.96	8.0	0.60
SS-32	Vacuum	12	20	582	0	Air	-----	146	0	0.89	8.2	1.45
SS-33	Vacuum	12	30	588	0.1	Air	221	228	0.54	2.65	7.9	0.57
SS-34	Vacuum	12	35	588	5	Air	228	237	0.47	2.32	8.1	0.41
SS-35	Vacuum	12	40	588	10	Air	-----	205	0	1.22	7.7	1.23

One sample for each test.
Initial sample size: 15.2 mm x 15.2 mm x 76.2 mm

Table 20. The T6 properties of semi-solid A356 (Alloy #1)Aluminum alloy in this study.

Sample #	Atmosphere	Semisolid Treatment Cycle	Time after 573°C (min)	Final tempt. (°C)	Time at 588°C (min)	Cool down	Yield Stress (MPa)	UTS (MPa)	Elongation (%)	Reduction at Area (%)	Distance of voids from mini-ingot edge (mm)	# voids ave. in tensile specimen ($1/mm^2$)
SS-36	Vacuum	12	40	588	10	Water	262	321	11.21	15.01	2.3	0
SS-37	Vacuum	12	45	588	15	Water	265	325	10.34	12.74	5.1	0
SS-38	Vacuum	12	50	588	20	Water	263	320	14.06	22.20	4.7	0
SS-39	Vacuum	12	60	588	30	Water	-----	231	0	1.02	3.2	1.04
SS-40	Air	12	15	588	0	Water	259	299	2.42	6.13	5.2	0.63
SS-41	Air	12	20	588	0	Water	264	325	9.97	12.86	5.9	0.17
SS-42	Air	12	30	588	0.1	Water	248	266	1.12	4.08	4.4	0.89
SS-43	Air	12	35	588	5	Water	250	278	1.57	4.95	6.3	0.77
SS-44	Air	12	40	588	10	Water	264	322	12.22	18.32	3.9	0
SS-45	Air	12	45	588	15	Water	265	326	11.46	16.36	4.2	0
SS-46	Air	12	60	588	30	Water	260	320	13.36	20.03	2.7	0
SS-47	Air	12	40	588	10	Liquid Ni	----	255	0	0.88	8.1	1.12

One sample for each test.
Initial sample size: 20.3 mm x 20.3 mm x 76.2 mm

of 20.3 mm x 20.3 mm x 76.2 mm. That the mechanical properties of the samples with initial sample size of 20.3 mm x 20.3 mm x 76.2 appear better than those with initial sample size of 15.2 mm x 15.2 mm x 76.2 mm for the same thermal treatment. The T6 properties of samples with initial sample size of 20.3 mm x 20.3 mm x 76.2 mm are close to those of as-cast samples after the temperature reaches 588°C (1090°F) for more than 10 minutes. It is observed from the results of SS-40 to SS-46 that the T6 properties are not changed greatly with time at the temperature of 588°C (1090°F) from 10 minutes to 30 minutes. This implies that the T6 properties of A356 Al alloy may not be sensitive to the soak time at given temperature. This is also in contradiction to Table 20 which shows a decrease in ductility from 25 to 30 minutes. The semi-solid treatment of samples SS-40 to SS-46 was in air. It is observed that the T6 properties were not changed compared to those in vacuum condition. These results indicate that the atmosphere of semi-solid treatment does not greatly affect the T6 properties of semi-solid A356. The effect of cooling rate of the initial sample size of 20.3 mm x 20.3 mm x 76.2 on the T6 properties has the same trends as those of 15.2 mm x 15.2 mm x 76.2 in Table 19, but not in Table 18. For unclear reasons, it appears that the T6 properties decrease as cooling rate decreases.

E. The Analysis of Voids after Semi-solid Treatment for Semi-solid A356 Aluminum Alloy

The most important defect in A356 aluminum alloy after semi-solid treatment appears to be voids. The analysis of voids may help to understand the relationship between microstructure and mechanical properties of the alloy. The results of void concentration calculations are listed in Table 19, 20 and 21. It is observed from examining the microstructure of samples of A356 that three types of voids exist in the samples after semi-solid treatment. Type I voids are found on the surface or subsurface (only) in water quenched samples. Fig. 59 shows the surface voids of sample SS-27. Fig. 60 shows that the void existed 2 mm below the surface. The size of voids are relatively large (up to several mm), and the resulting in poor surface quality. These may be associated with large

Table 21. The T6 properties of semi-solid A356 (Alloy #1) Aluminum alloy in this study.

Sample #	Atmosphere	Semisolid Treatment Cycle	Time after 573°C (min)	Final tempt (°C)	Time at 588°C (min)	Cool down	Yield Stress (MPa)	UTS (MPa)	Elongation (%)	Reduction at Area (%)	Distance of voids from mini-ingot edge (mm)	# voids ave in tensile specimen (1/mm²)
SS-48	Air	11	10	583	0	Water	221	225	0.04	0.56	8.1	1.07
SS-49	Air	11	20	588	0.1	Water	203	205	0.02	0.98	4.2	0.37
SS-50	Air	11	25	588	5	Water	252	301	3.24	6.37		
SS-51	Air	11	30	588	10	Water	261	325	9.97	18.30		
SS-52	Air	11	50	588	30	Water	260	320	13.36	23.03		
SS-53	Air	11	30	588	10	Boiled Water	252	302	4.07	7.73	5.6	0.28
ROD203#1	Air	---	1.75	588	1.33	Water	141	190	0.62	1.81	-----	0.60
ROD205#1	Air	---	3.0	588	1.50	Water	129	204	0.74	1.47	-----	1.07
ROD205#3	Air	---	2.66	588	1.66	Air Cool	218	245	1.88	3.87	-----	1.77

One sample for each test.
Initial sample size: 20.3 mm x 20.3 mm x 76.2 mm

ROD203 and 205 Samples (Alloy #1):
Ingot size : 83.8 mm
Three samples for each test.

Fig. 59 Type I void of sample SS-27 (water quench) 37.5 X

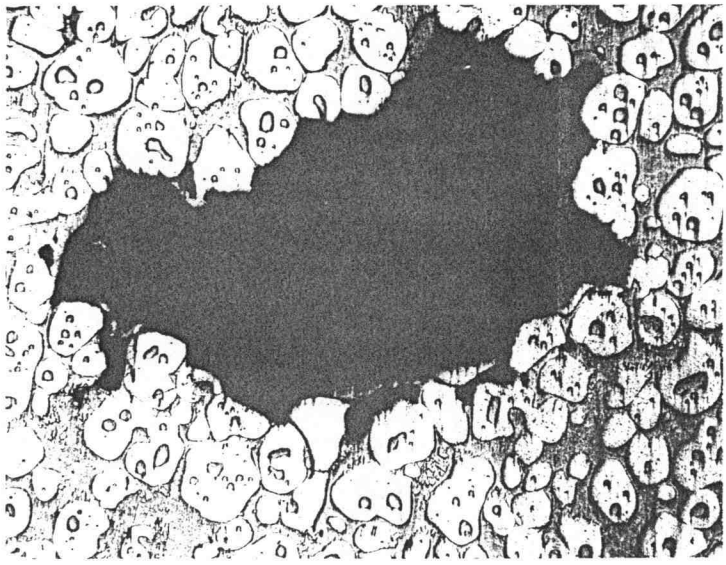

Fig. 60 Type I void of sample SS-27 (water quench) 37.5 X

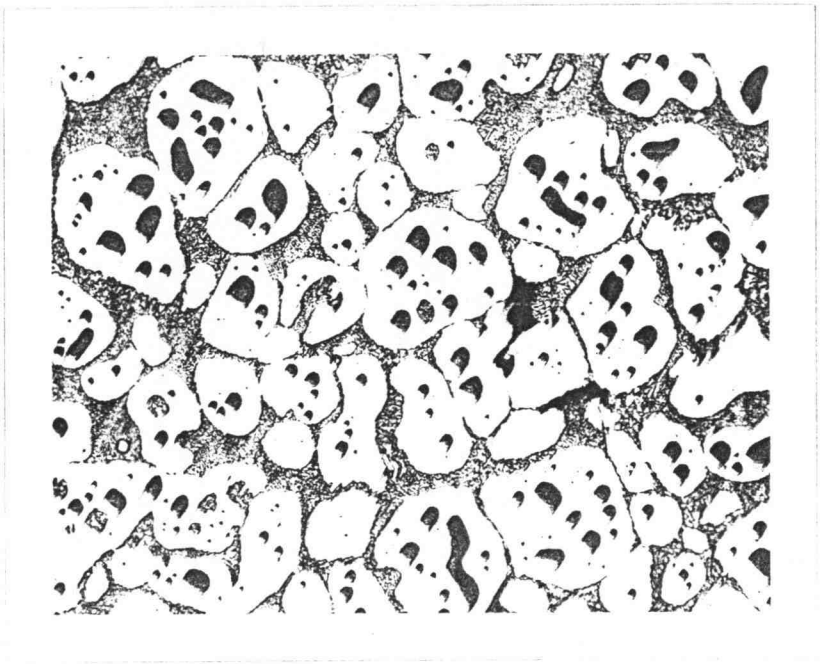

Fig. 61 Type II void in sample SS-35 (air cool)
50 X

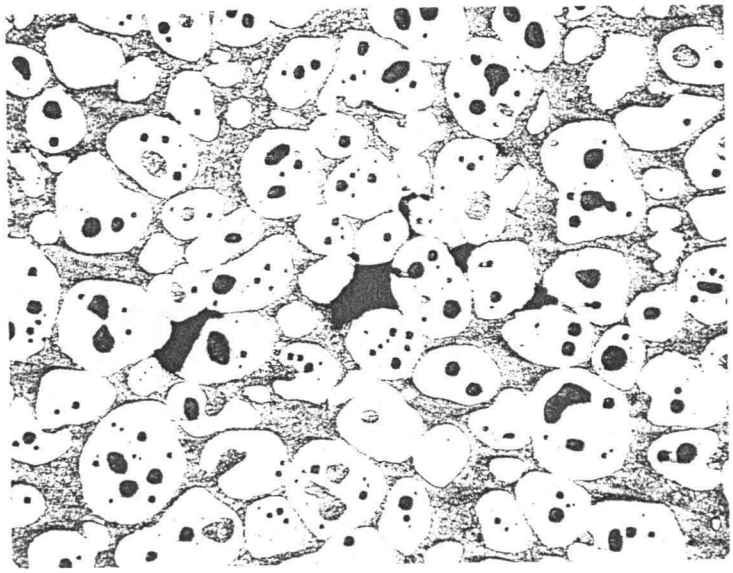

Fig. 62 Type II void in sample SS-31 (liquid Ni cool)
50 X

thermal stress on the semi-solid due to relatively fast cooling rate. Since the strength of semi-solid material at semi-solid state is very low [2,9], the thermal stress may be large enough to tear the material on the surface during water quenching. Type II voids are mainly found in air cooled or liquid nitrogen quenched samples. Fig. 61 and 62 show the voids in the samples SS-35 and SS-31, respectively. It is observed that the size of voids is smaller than that of surface (Type I) voids. Unlike surface voids, Type II voids may exist everywhere in the samples. It is also observed from examining the microstructure of semi-solid A356 alloy, that Type II voids appear in the liquid phase, which implies that the voids form in the liquid during cooling/solidification. Kenney et. al [2] suggested that shrinkage porosity be prevented by adjusting forming parameters such as die temperature, feeding sections, time and pressure during dwell after forging. Type III voids may be found in the samples in different cooling rates, such as samples SS-27, 31 and 35 as shown in Fig 63, 64, and 65. It is observed that the voids mainly exist in the entrapped liquid phase within spheriodal particles and the size is relatively small. Therefore, decreasing the number of entrapped liquid phase may decrease the concentration of Type III voids.

The voids may affect the T6 properties of A356 aluminum alloy. It is observed from Table 19, 20 and 21 that the T6 mechanical properties of specimens from a sample size of 20.3 mm x 20.3 mm x 76.2 have better and more consistent properties than those from 15.2 mm x 15.2 mm x 76.2 sizes. This indicates that Type I voids may affect T6 properties of A356 aluminum alloy, if the sample size is small and the surface voids are not completely removed from the tensile specimens. As mentioned above, the evaluation of voids in the ingot and the cross section of tensile specimens was performed in a microscope at 50X. The results of void evaluation in Table 19-21 are principally determined Type I and II voids for small ingot samples and mainly Type II voids for tensile specimens (tensile specimens have less "surface voids"). The results indicate that the Type II voids in the samples associated with relatively poor T6 mechanical properties. Relatively voids are observed in the tensile specimens with good T6 properties, such as water quenched

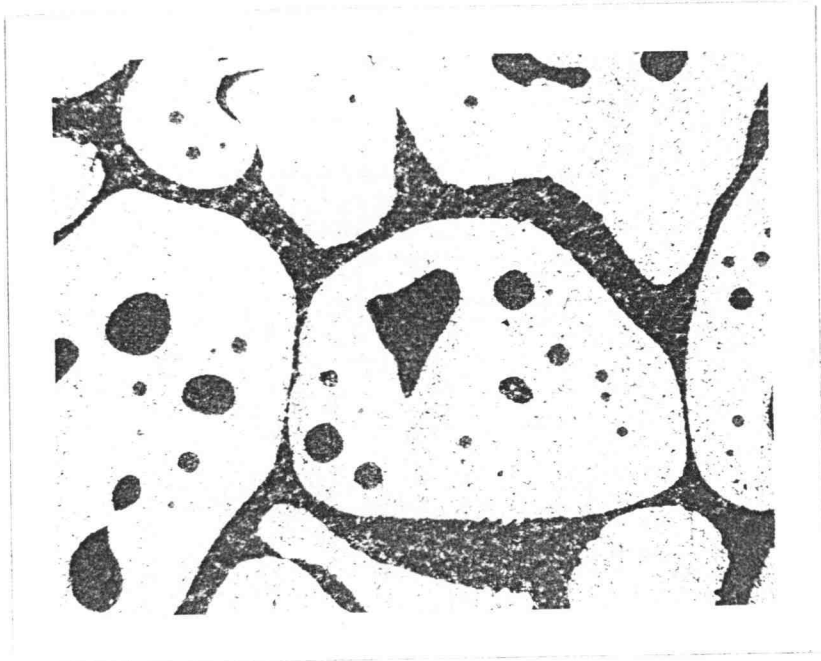

Fig. 63 Type III void in sample SS-27 (water quench)
200 X

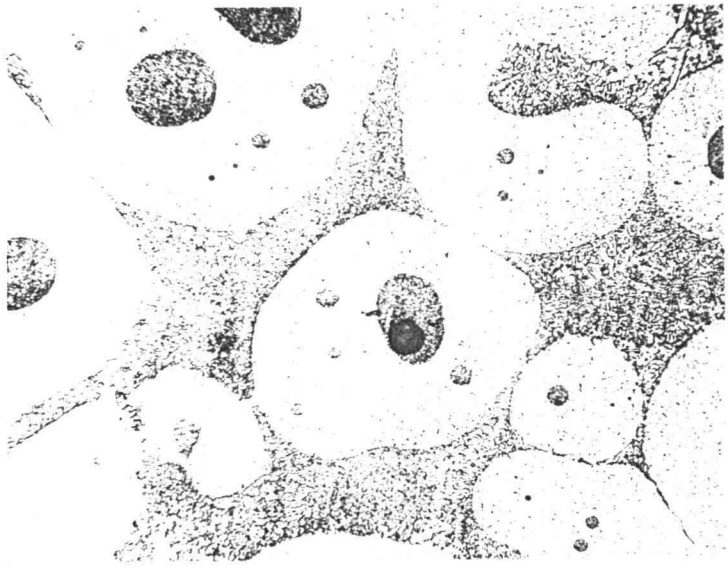

Fig. 64 Type III void in sample SS-31 (liquid Ni cool)
200 X

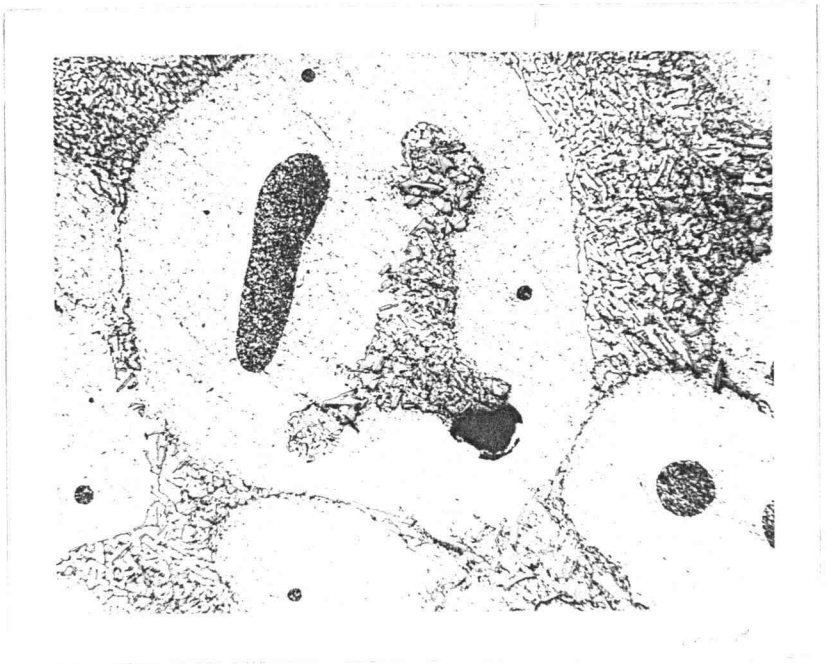

Fig. 65 Type III void in sample SS-35 (air cool)
200 X

samples SS-36 to SS-38 and SS-44 to SS-46. Some voids were found on the surface of the quenched specimens but are machined away during specimen preparation. The mechanical properties deteriorate (e.g. air cooled and liquid nitrogen quenched samples), when the average number of voids in the cross section of tensile specimens is greater than $0.3/mm^2$. Type III voids are relatively small and isolated in the entrapped liquid phase, and the effect on the T6 properties of A356 aluminum alloy is small. Cooling rate would greatly affect the distribution of voids. The results indicate that the elimination of voids (mainly Type II voids) can improve the T6 properties significantly.

F. The Mechanical Properties of Semi-solid A356 Aluminum Alloy after Press Forming

As mentioned above, one advantage of semi-solid process is the ability to easily shape the alloy. The mechanical properties of semi-solid material after forming are vital. The three semi-solid treatments and forklift pressing (samples RDO203#1, RDO205#1 and RDO205#3 from Alloy #1) used in the study are listed in Table 21. Figs. 66-68 show the microstructure of samples RDO203#1, RDO205#1 and RDO205#3, respectively. It is observed that the voids are Type II and tend to connect through liquid phase (under load). It is also observed from Table 21 that the T6 properties are very poor and the number of voids in tensile specimens are relatively large for all three samples. There is not much difference in mechanical properties for water quenched samples (samples RDO203#1 and RDO205#1) and the air cooled sample (sample RDO205#3), which means that the cooling rate after press forging may not greatly affect the T6 properties of this experiment. It is possible that the time before pressing and or quenching may have been excessive (i.e. effectively an air cool).

Two types of voids are found in both parts 0313.2H and 0313.2EX1 (Alloy #1) induction heated and formed at HMM (see Fig.27), as shown in Figure 57-60. They are similar to Type II and III voids found in other A356 aluminum alloy with different semi-solid treatments. Type II voids may result from shrinkage of the liquid. Type II voids are

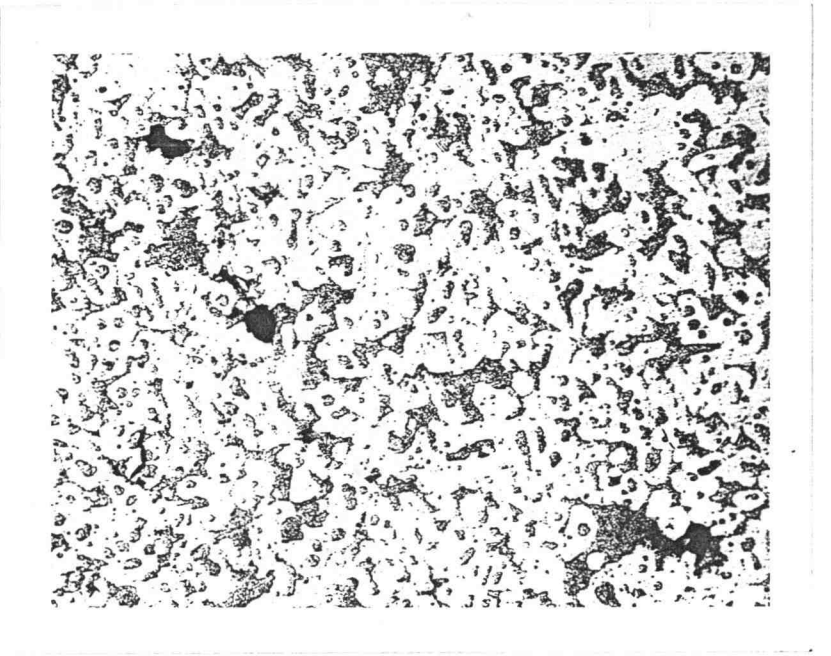

Fig. 66 Microstructure with voids in sample RDO203#1
50 X

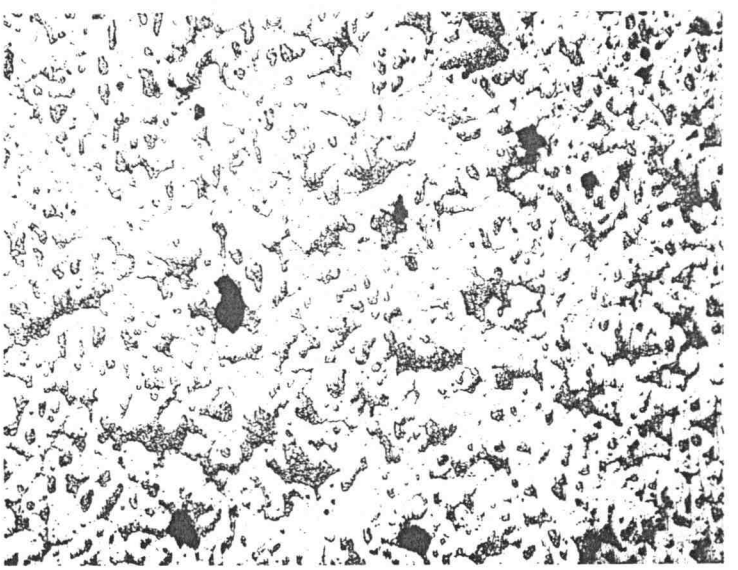

Fig. 67 Microstructure with voids in sample RDO205#1
50 X

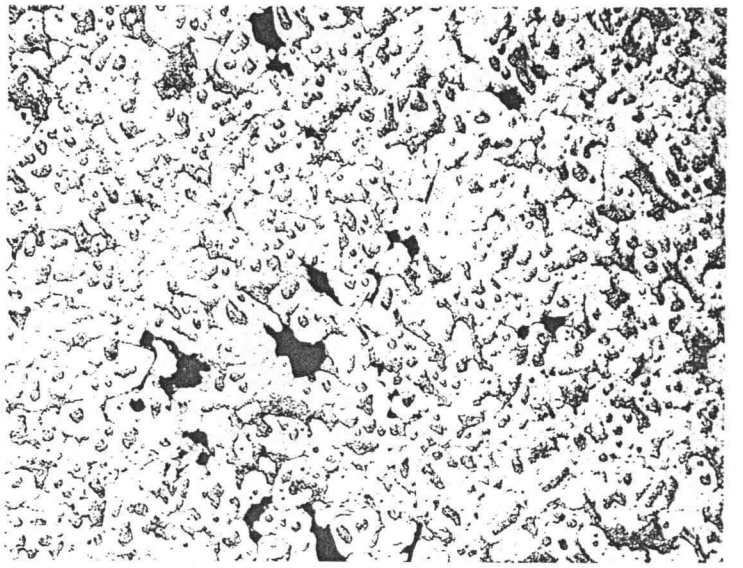

Fig. 68 Microstructure with voids in sample RDO205#3
50 X

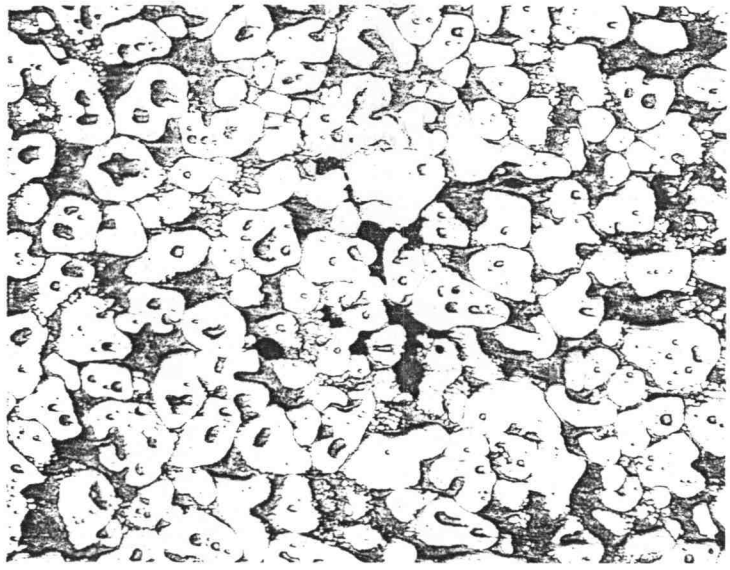

Figure 69. Microstructure with voids in sample 0313.2H

50X

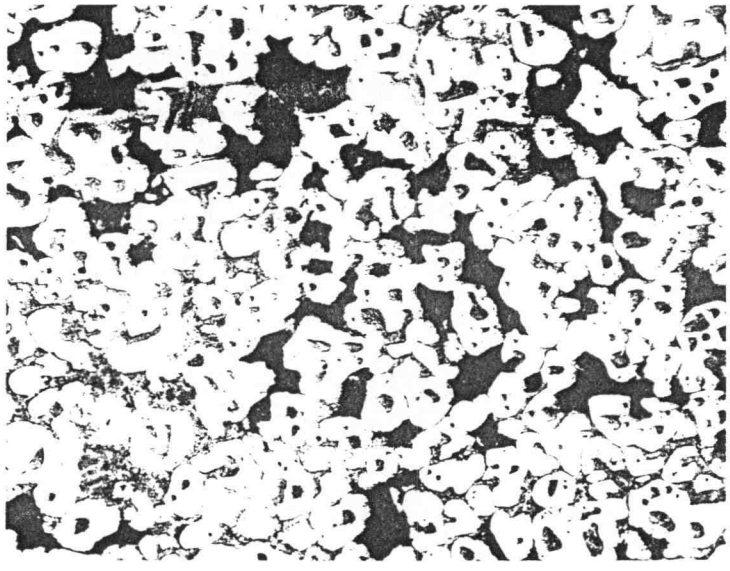

Figure 70. Microstructure with voids in sample 0313.2EX1

50X

Figure 71. Microstructure with voids in sample 0313.2H

200X

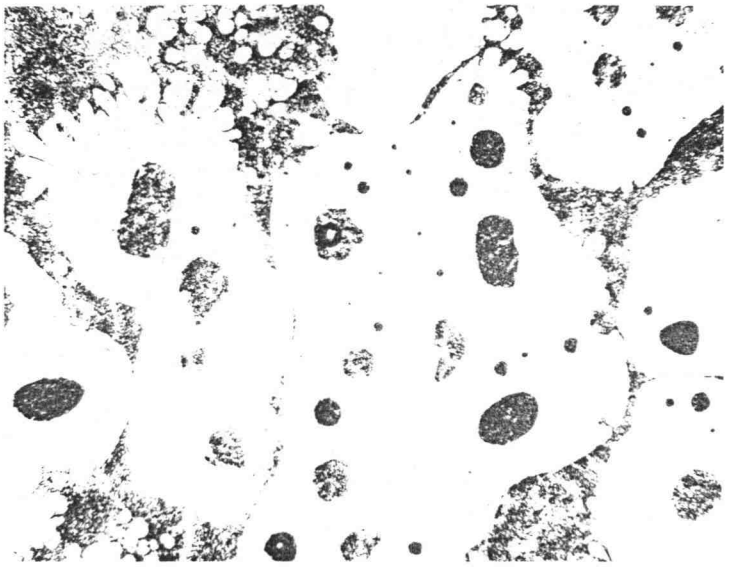

Figure 72. Microstructure with voids in sample 0313.2EX1

200X

observed in Figures 69 and 70. The numbers of Type II voids in parts 0313.2H and 0313.2EX1 are 0.522/mm^2 and 0.073/mm^2, respectively. It is also found that Type II voids are concentrated in the middle area of both parts. Type III voids mainly exist in the entrapped liquid phase and the concentration can be neglected (see Figures 71 and 72) because they are small and may not greatly affect the T6 mechanical properties.

Table 22 shows the T5 and T6 properties of parts 0313.H and 0313.EX1 semi-solid A356 aluminum alloy. It was found that T5 and T6 properties of part 0313.EX1 is better that those of part 0313.H, or the lower void concentration, the better the mechanical properties, which is consistent with earlier results.

Because cooling rate and time may affect the formation and distribution of voids in semi-solid A356 aluminum alloy, the histories of semi-solid treatment in NWA and press forming in HMM can affect the T6 mechanical properties. It is necessary to study the press forming of semi-solid aluminum alloy further.

G. The Effect of Homogenization Treatment on the T6 Properties of Semi-solid A356 Aluminum Alloy

Figures 73-76 show the microstructure of samples of as-cast ingot (Alloy #1) and under three homogenization treatments (see Fig. 28) before semi-solid treatment. It is observed that the as-cast structure may change somewhat after three homogenization treatments. It was found from Figures 74-76 that the number and size of Si particles increase as the homogenization cooling time increases. It was also observed that there is not much microstructural difference in Figure 75 and 76, which implies that homogenization microstructure may not be dramatically affected by the heating rate, but instead by the cooling rate.

Figures 75-80 show the microstructure of samples after semi-solid treatment (kept at 588°C (1090°F) for 20 minutes). It is observed that there is not much difference in the microstructure for all samples of as-cast ingot and under homogenization treatments,

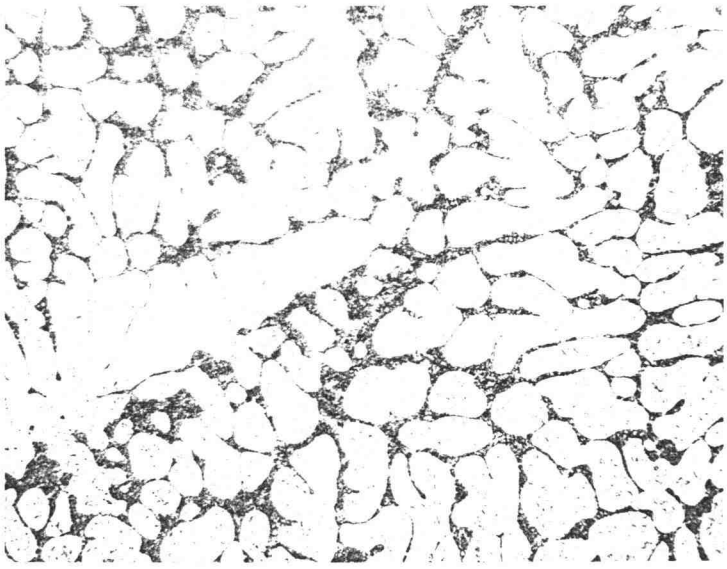

Fig. 73 As-cast A356 (Alloy #1) 400 X

Fig. 74 Under Homogenization Cycle 1 (Alloy #1) 400 X

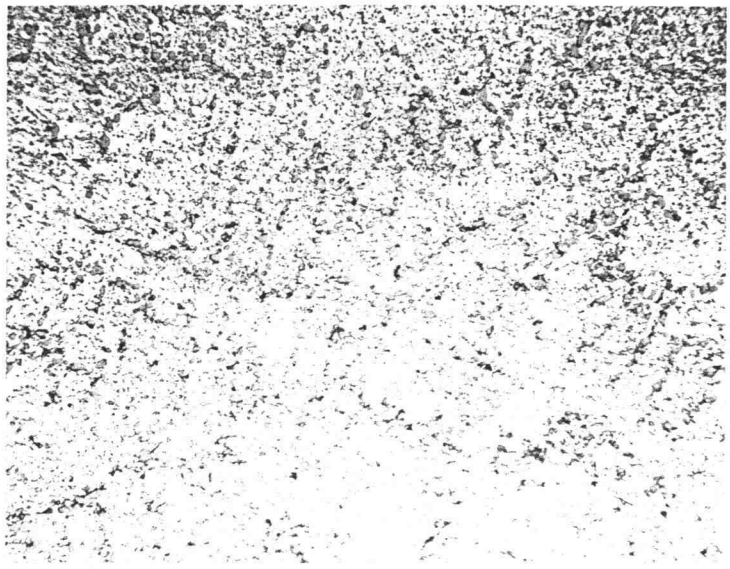

Fig. 75 Under Homogenization Cycle 2
(Alloy #1) 400X

Fig. 76 Under Homogenization Cycle 3
(Alloy #1) 400 X

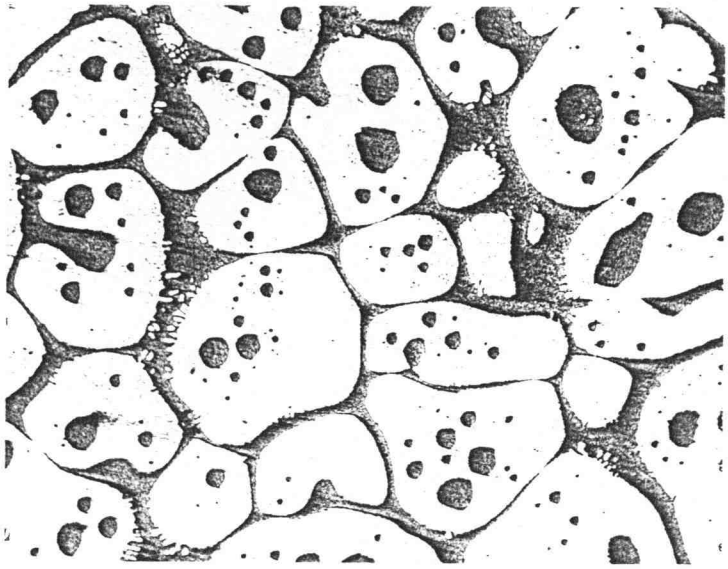

Fig. 77 As-cast + Semi-solid Treatment Cycle11 (Alloy #1) 100X

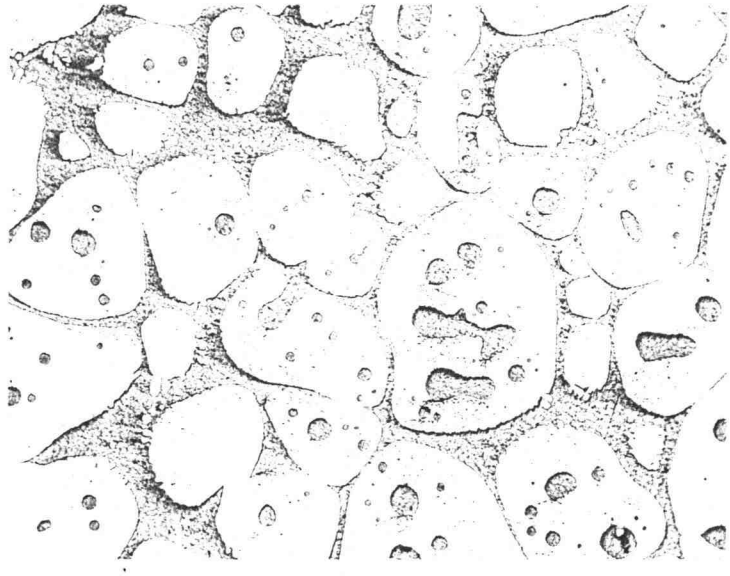

Fig. 78 Homogenization Cycle 1 + Semi-solid Treatment Cycle 11 (Alloy #1) 100 X

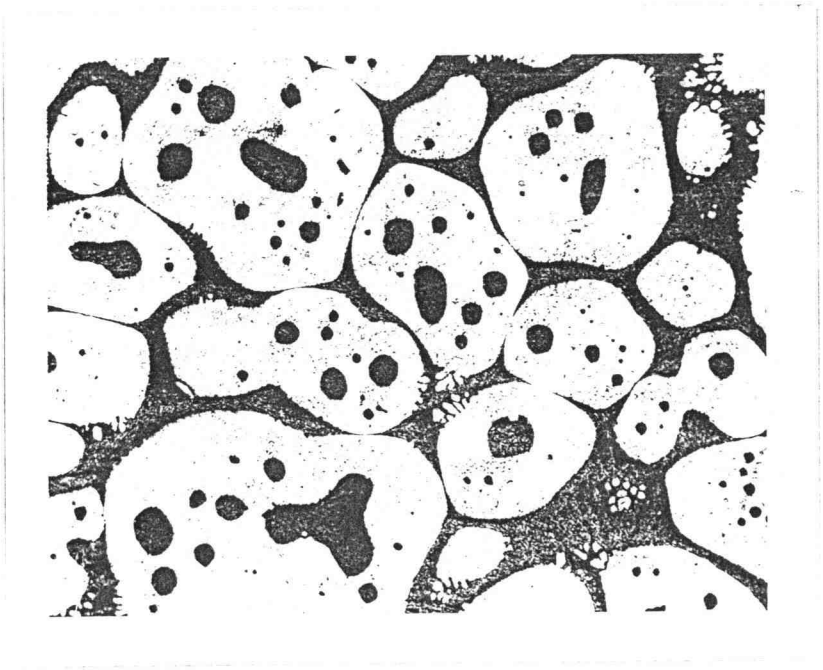

Fig. 79 Homogenization Cycle 2 + Semi-solid Treatment Cycle 11 (Alloy #1) 100X

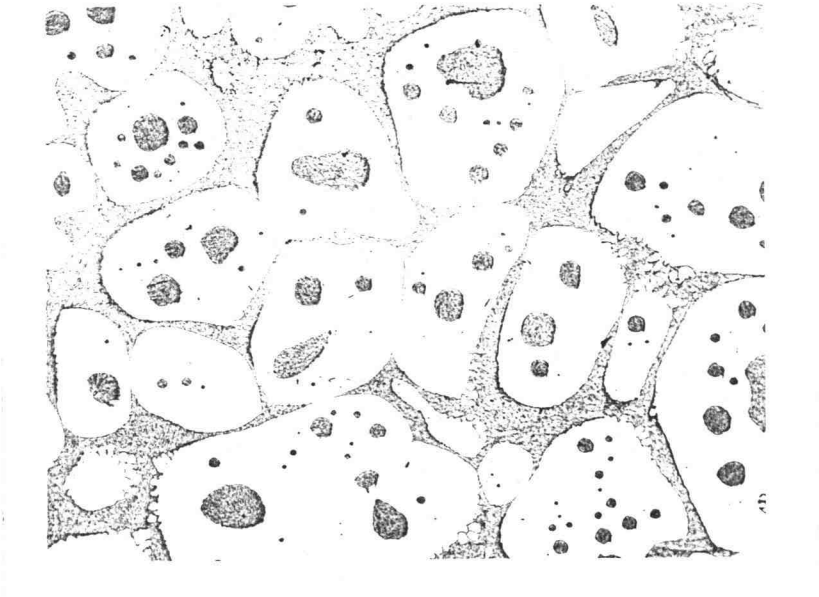

Fig. 80 Homogenization Cycle 3 + Semi-solid Treatment Cycle 11 (Alloy #1) 100 X

Table 22. T5 and T6 properties of semi-solid A356 (Alloy #1) aluminum alloy press formed at HMM.

Sample #	Yield Stress (MPa)	UTS (MPa)	Elongation (%)	Reduction at Area (%)	Heat Treatment	Void conc. #/ mm^2
0313.1H	157	239	5.5	7.5	T5	---
0313.1EX1	161	248	14.0	29.5	T5	---
0313.2H	156	212	3.0	6.0	T5	0.522
0313.2EX1	150	247	14.0	27.0	T5	0.073
0313.3H	236	295	6.0	5.0	T6	---
0313.3EX1	225	305	14.0	27.0	T6	---
0313.4H	233	280	4.5	10.0	T6	---
0313.4EX1	217	301	17.0	28.0	T6	---

Three samples for each test.

which, again, implies that the semi-solid microstructure is not sensitive to the homogenization treatment (heat up rate).

Table 23 shows that the T6 properties of samples after semi-solid treatment (kept at 1090^0F for 5 and 20 minutes) and various homogenization treatments. It is observed that the T6 properties are similar for all samples, which implies that the homogenization cycle(or lack of homogenization) before semi-solid treatment does not greatly affect the T6 properties of semi-solid A356 aluminum alloy in this study.

Table 23 also shows that the T6 properties of samples after the semi-solid treatments (kept at 588°C (1090°F) and 582°C (1080^0F) for 0 minutes, respectively). It is observed that the mechanical properties are relatively poor for both semi-solid treatments. But the homogenization treatment before semi-solid treatment does not affect the T6 properties of semi-solid A356 aluminum alloy, which is consistent to the above results. That is, a minimum time at a temperature (which increases with decreasing temperature), is necessary for proper T6 properties.

H. The Formability Studies of Semi-solid Aluminum Alloys at NWA

The sequences in Table 24 were performed on Alloy #2. It can be observed that there is a range of acceptable formability. In the case of as-cast 356 of Alloy #2 composition, it is between 599 to 602°C (1110 to 1115°F), a fairly small range. Pressing was performed 5-10 sec. after removal from induction furnace, and pressed at 0.7 MPa. Table 25 shows the range of acceptability of formability for A357 Alloy #4. Here, for semi-solid heating procedures as Table 24, 582 to 599°C (1080-1110°F) is the acceptable forming range, somewhat lower than 356, although still a narrow composition range. The temperature measurement was more accurate later due to improved thermocouple positioning.

Some experiments were also performed on modified (lower Si) A356/357 alloysand are listed in Table 26. Alloy #12 has a favorable range of formability of about 612 to

Table 23-1. T6 properties of semi-solid A356 (Alloy #1) aluminum alloy under various homogenization cycle and semi-solid cycle 11.

Sample #	Homogenization Treatment Cycle	Semi-solid Treatment Cycle	Yield Stress (MPa)	UTS (MPa)	Elongation (%)	Reduction Area (%)
Homo1	--------	11	250	311	12.71	18.15
Homo2	1	11	250	314	13.52	21.90
Homo3	2	11	248	311	11.86	19.44
Homo4	3	11	247	314	12.40	20.13

Kept at semi-solid temperature of 588°C (1090°F) for 20 minutes. Three specimens for each test.

Table 23-2. T6 properties of semi-solid A356 (Alloy #1) aluminum alloy under various homogenization cycle and semi-solid cycle 11.

Sample #	Homogenization Treatment Cycle	Semi-solid Treatment Cycle	Yield Stress (MPa)	UTS (MPa)	Elongation (%)	Reduction Area (%)
Homo5	-------	11	256	319	13.72	18.51
Homo6	2	11	256	323	12.98	21.27
Homo7	3	11	256	324	12.37	18.64

Kept at semi-solid temperature of 588°C (1090°F) for 5 minutes. Two specimens for each test.

Table 23 (Continued)

Table 23-3. T6 properties of semi-solid A356 (Alloy #1) aluminum alloy under various homogenization cycle and semi-solid cycle 11.

Sample #	Homogenization Treatment Cycle	Semi-solid Treatment Cycle	Yield Stress (MPa)	UTS (MPa)	Elongation (%)	Reduction Area (%)
Homo8	-------	11	245	283	5.86	10.71
Homo9	3	11	255	294	6.70	10.72

Kept at semi-solid temperature of 588°C (1090°F) for 0 minutes. Two specimens for each test.

Table 23-4. T6 properties of semi-solid A356 (Alloy #1) aluminum alloy under various homogenization cycle and semi-solid cycle 11.

Sample #	Homogenization Treatment Cycle	Semi-solid Treatment Cycle	Yield Stress (MPa)	UTS (MPa)	Elongation (%)	Reduction Area (%)
Homo10	-------	6	121	228	0.32	1.17
Homo11	3	6	123	222	0.35	1.91

Kept at semi-solid temperature of 582°C (1080°F) for 0 minutes. Two specimens for each test.

Table 24. The results of formability of A356 (Alloy #2) perfomed at NWA.

Final T (°C)	RT to 538°C (kW)	574°C to final T (3 min. at 574°C) (kW)	Time at final T (min.)	Comments on Formability
604	70	40	3	excessive
602	70	40	3	acceptable
599	70	20	3	just short of accept.
596	70	20	3	short of accept.
599	70	20	3	not accept.
591	70	20	3	not accept.
588	70	20	3	not accept

Table 25. The results of formability of A357 (Alloy #4) perfomed at NWA.

Final T (°C)	RT to 538°C (kW)	574°C to final T (3 min. at 574°C) (kW)	Time at final T (min.)	Comments
599	70	40	3	too much liquid
593	70	20	3	up limit of accept.
588	70	20	3	accept.
582	70	20	3	accept.
577	70	20	3	not accept.
Additional	A 357 tests			
588	35 to final T	(571-588 °C in 20 sec.) (5 min. to 538°C)		225 sec. total, not accept., too stiff
588	15 to final T	(571-588 °C in 20 sec.) (5 min. to 538°C)		10 min. total, not accept.
591	20 to final T	(7.5 min. to 588°C) (30 sec. at 591°C) (585-591°C 1.5 min.)		9 min. total, accept.

616°C (1133-1140°F); Alloy #11, 615 to 617°C (1139-1143°F); and Alloy #10, 619 to 622°C (1146-1152°F), all fairly narrow ranges of formability. These appear to be less range of fomability than those of the conventional 356/357 alloys. Table 27 shows the formability of A357 (Alloy#4), tested at 585 to 588°C (1085-1090°F) for 0-5 min. "holding" times. The results of Table 25 showed acceptable formability between 1080-1100°F, 3 min. "holding" times. Consistent with these results, Table 27 shows acceptable formability for 1-5 min. holding at 585 to 599°C (1085-1090°F).

Metallography of A357 (Alloy #4) was performed at Northwest Aluminum. The microstructures for 1085°F appeared adequate (spheroidal shape) for all specimens except for that which did not form well, 1085°F for 0 min. It also appeared that the most favorable structure was on the outside of the deformed (0.7 MPa) square semi-solid specimens, with larger amounts of liquid.

The temperature measurements, based on thermocouples at the surface and the internal of the specimen, was suspect and rechecked. The results are shown in Table 28 for A357 (Alloy #4 and Sr-rich Alloy #6). These results indicate that for Alloy #4, best formability, may actually occur above 585°C (1085°F) for 0-4 min.

The following tests were additionally performed as shown in Table 29. This data suggests that the Pechiney (Alloy #8) semi-solid is formable after just a small period of time at 586°C (1086°F). Also, it appears that 25.4 mm x 25.4 mm x 25.4 mm squares from larger ingots are less formable than smaller ingot (i.e. 99 mm vs. 74 mm). 99 mm series ingot are only fair. Larger ingot sizes may be associated with larger grains and less formability. It was also noted that in larger ingot, there is a grain size gradient across the radius and formability is accordingly affected.

Additional tests were also performed on Alloys #5-8 at 586 to 596°C (1086-1104°F), as shown in Table 30, typically for 4 min. After 4 min. at 589°C (1092°F), Pecheney (Alloy #8) is very good, Alloy #6 is not acceptable, while Alloy #7 is acceptable. In fact, Pechiney is good after 0 min. at 589°C (1092°F). Alloy #7 is marginal at 585°C

Table 26. The results of formability of Alloys #10, 11 and 12 (DF93-95) perfomed at NWA.

Alloy #10

Final T (°F)	RT to 1000°F (kW)	1065°F to final T (3 min. at 1065°F) (kW)	Time at final T (min.)	Comments
1152	70	40	3	up limit of accept.
1146	70	40	3	marg. accept
1147	70	40	3	marg. accept

Alloy #11

Final T (°F)	RT to 1000°F (kW)	1065°F to final T (3 min. at 1065°F) (kW)	Time at final T (min.)	Comments
1143	70	40	3	accept.
1139	70	40	3	lower limit of accept.
1132	70	40	3	not accept.

Alloy #12

Final T (°F)	RT to 1000°F (kW)	1065°F to final T (3 min. at 1065°F) (kW)	Time at final T (min.)	Comments
1140	70	40	3	up limit of accept.
1133	70	40	3	lower limit of accept.

Table 27. The results of formability of A357 (Alloy #4) perfomed at NWA.

Final T (°F)	RT to 1090°F (kW)	Time at final T (min.)	Total time to final T (min.)	Comments
1090	20	0	7 min. and 7 sec.	not good
1090	20	1	7 min. and 20 sec.	good
1090	20	2	7 min. and 46 sec.	good
1090	20	3	7 min. and 3 sec.	good
1090	20	4	7 min. and 3 sec.	good
1090	20	5	7 min. and 50 sec.	good
1085	20	0	7 min.	not good
1085	20	1	7 min. and 20 sec.	good
1085	20	2	6 min. and 49 sec.	good
1085	20	3	7 min. and 18 sec.	good
1085	20	4	6 min. and 40 sec.	good
1085	20	5	6 min. and 50 sec.	good

Table 28. The results of formability of A357 (Alloy #4 and #6) perfomed at NWA. (70 kW to 538°C)

Alloy #	Final T (°C)	538°C to 588°C (kW)	Time at final T (min.)	Comments
4	588	20	4	good
6	588	20	4	barely good
6	591	20	4	good
4	588	20	4	not pressed
6	591	20	4	good
4	585	20	4	marginal
4	588	20	0	good but small
6	588	20	0	fail

Table 29. The results of formability of A357 performed at NWA.

Table 29-1. The results of formability of A357 (sample size: 25.4 mm x 25.4 mm x 25.4 mm) perfomed at NWA. (70 kW to 521°C and 20 kW to 556°C)

Alloy #	Final T (°F)	556°C to final T (kW)	Time at final T (min.)	Comments
8	586	15	0	good
8	586	20	0	good
8	586	20	4	good
5	586	20	4	good
6	586	20	4	not good
7	586	20	4	good
7	588	20	4	good
7	586	20	4	not good
7	584	20	4	good
7	586	20	4	good
7	591	20	4	good

Table 29-2. The results of formability of A357 (sample size: 50.8 mm x 50.8 mm x 50.8 mm) perfomed at NWA. (70 kW to 521°C and 20 kW to 556°C)

Alloy #	Final T (°F)	556°C to final T (kW)	Time at final T (min.)	Comment
7	591	20	4	not good

Table 30. The results of formability of A357 (Alloy #5-#8) perfomed at NWA. (70 kW to 521°C and 20 kW to 558°C)

Alloy #	Final T (°C)	558°F to final T (kW)	Time at final T (min.)	Comments
7	586	20	4	marginal
7	588	20	4	just accept.
7	586	20	4	just accept.
7	589	20	4	good
8	589	20	0	good
8	589	20	4	very good
6	589	20	4	not good
6	591	20	4	not accept.
6	593	20	4	barely acceptable
6	596	20	4	marginal
7	596	20	4	accept.
5	596	20	4	better

(1086°F). Alloy #6 is improved at 596°C (1104°F). These results suggest higher formability for Pechiney, less for direct chill cast ingot particularly of larger diameter. These may suggest that there is a size effect. Smaller spheroids associated with better formability was metallography performed.

More extensive tests were performed on Alloy #4, as shown in Table 31. Here, we also correlate mechanical properties with formability and also the amount of semi-solid "sagging", in the semi-solid state. Excessive distortion by sagging may render the semi-solid difficult to "handle" in a manufacturing process. The results of Table 31 suggest that good formability and minimal sag may achieve at 591°C (1096°F) for one to two min. The mechanical properties of these are relatively good, 7.5% El, 265 MPa (38.5 ksi) yield stress and 312 (45.2 ksi) UTS. Favorable formability from 582 to 593°C (1080 to 1100°F) is consistent with earlier tables for similar temperatures and times at or less than 4 min. We note from the table that there is also a correlation between the ductility (and UTS) and the void concentration in the tensile specimens extracted from the formed cubes. The ductility (and UTS) decreases as the void concentration increases. Table 32 shows that for Alloy #7, 587°C (1088°F) at 4 min. is acceptable in terms of sag and formability as is 591°C (1096°F) from 0-2 min. The tensile data shows these to have about 9% El with 325 MPa (47.1 ksi) UTS and 263 MPa (38.2 ksi) yield strength. Again, we observe a strong correlation between porosity and elongation as well as strength. The strength and elongation decrease as the porosity increases, as shown in Fig. 81 and 82. Table 33 shows analogous tests to Table 32 except using Pechiney (electromagnetically stirred) 357. Good formability is observed from 578°C (1072°F), 4 min. to 591°C (1096°F), 0 min. with acceptable sagging within the time and temperature range. The mechanical properties are generally good; with the better properties associated with low void concentration, as expected.

Additional forming experiments were performed on the low silicon alloys, #9-12. These are listed in Table 34. The difference in the formability between the Alloy #9/10 and

Table 31. The T6 properties of squeezed semi-solid A357 (Alloy #4) Aluminum alloy.

Sample #	Atmosphere	Semisolid Treatment Cycle	Time after 573°C (min)	Final tempt. (°C)	Time at 588°C (min)	Cool down	Yield Stress (MPa)	UTS (MPa)	Elongation (%)	Reduction at Area (%)	# voids ave. in tensile specimen ($1/mm^2$)	Formability Comment
RDO438-4	Air	*	---	589	4	Water	263	306	5.81	6.23	0.86	good
RDO438-5	Air	*	---	587	4	Water	265	321	7.88	10.17	0.67	accept
RDO438-6	Air	*	---	584	4	Water	278	323	10.11	9.72	0.29	marginal
RDO438-7	Air	*	---	582	4	Water	266	319	7.29	7.76	0.72	marginal
RDO438-8	Air	*	---	580	4	Water	268	306	4.46	5.12	0.88	not good
RDO438-9	Air	*	---	591	4	Water	260	316	9.18	8.90	0.60	very good/ excellent
RDO438-10	Air	*	---	593	4	Water	263	312	8.68	9.89	0.68	excess sag./ excess liq.
RDO438-11	Air	*	---	591	0	Water	268	321	8.69	9.42	0.66	marg/accept no excess sag
RDO438-12	Air	*	---	591	1	Water	267	315	7.70	10.36	0.69	good/ not excess sag
RDO438-13	Air	*	---	591	2	Water	263	308	7.16	7.95	0.67	good/slightly excess sag

One sample for each test.

T6: Solution treatment at 538°C for 8 hrs and water quenched. Kept in refrigerator for 1 hr. after quenched. Precipitation treatment at 154°C for 12 hrs. before testing.

*: Semi-solid Treatment for samples 4-13 of Wagstaff RDO438 A357 aluminum alloy

RDO438-4: 70KW to 521°C; 30KW to 558°C; 20KW to 589°C for 4 minutes; Squeezed and water quenched.
RDO438-5: 70KW to 521°C; 30KW to 558°C; 20KW to 587°C for 4 minutes; Squeezed and water quenched.
RDO438-6: 70KW to 521°C; 30KW to 558°C; 20KW to 584°C for 4 minutes; Squeezed and water quenched.
RDO438-7: 70KW to 521°C; 30KW to 558°C; 20KW to 582°C for 4 minutes; Squeezed and water quenched.
RDO438-8: 70KW to 521°C; 30KW to 558°C; 20KW to 580°C for 4 minutes; Squeezed and water quenched.
RDO438-9: 70KW to 521°C; 30KW to 558°C; 20KW to 591°C for 4 minutes; Squeezed and water quenched.
RDO438-10: 70KW to 521°C; 30KW to 558°C; 20KW to 593°C for 4 minutes; Squeezed and water quenched.
RDO438-11: 70KW to 521°C; 30KW to 558°C; 20KW to 591°C for 0 minutes; Squeezed and water quenched.
RDO438-12: 70KW to 521°C; 30KW to 558°C; 20KW to 591°CF for 1 minute; Squeezed and water quenched.
RDO438-13: 70KW to 521°C; 30KW to 558°C; 20KW to 591°C for 2 minutes; Squeezed and water quenched.

Table 32. The T6 properties of squeezed NWA semi-solid A357 (Alloy #7) Aluminum alloy.

Sample #	Atmosphere	Semisolid Treatment Cycle	Time after 573°C (min)	Final tempt. (°C)	Time at 588°C (min)	Cool down	Yield Stress (MPa)	UTS (MPa)	Elongation (%)	Reduction at Area (%)	# voids ave in tensile specimen (1/mm²)	Formability Comment
RDO439-1	Air	*	---	580	4	Water	278	330	7.99	9.59	0.33	marg/no good some sag
RDO439-2	Air	*	---	582	4	Water	----	253	0	1.09	1.34	marg/no good sag near max
RDO439-3	Air	*	---	584	4	Water	284	341	8.98	7.65	0.097	marg/no good
RDO439-4	Air	*	---	587	4	Water	261	331	10.75	11.48	0	good/some sag
RDO439-5	Air	*	---	589	4	Water	274	332	10.60	11.26	0	fair/ good some sag
RDO439-6	Air	*	---	591	4	Water	266	325	8.56	9.18	0.11	very good sig sag
RDO439-7	Air	*	---	593	4	Water	255	321	11.82	11.50	0	excess sag good form
RDO439-8	Air	*	---	591	0	Water	254	313	4.28	4.82	0.62	accept
RDO439-9	Air	*	---	591	1	Water	275	330	11.01	11.73	0	accept/ some sag
RDO439-10	Air	*	---	591	2	Water	270	324	9.65	10.41	0.094	fair/good excess sag

One sample for each test.

T6: Solution treatment at 538°C for 8 hrs. and water quenched. Kept in refrigerator for 1 hr. after quenched. Precipitation treatment at 154°C for 12 hrs. before testing.

*: Semi-solid Treatment for samples 1-10 of NWA RDO439 A357 aluminum alloy

RDO439-1: 70KW to 521°C; 30KW to 558°C; 20KW to 580°C for 4 minutes; Squeezed and water quenched.
RDO439-2: 70KW to 521°C; 30KW to 558°C; 20KW to 582°C for 4 minutes; Squeezed and water quenched.
RDO439-3: 70KW to 521°C; 30KW to 558°C; 20KW to 584°C for 4 minutes; Squeezed and water quenched.
RDO439-4: 70KW to 521°C; 30KW to 558°C; 20KW to 587°CF for 4 minutes; Squeezed and water quenched.
RDO439-5: 70KW to 521°C; 30KW to 558°C; 20KW to 589°C for 4 minutes; Squeezed and water quenched.
RDO439-6: 70KW to 521°C; 30KW to 558°C; 20KW to 591°C for 4 minutes; Squeezed and water quenched.
RDO439-7: 70KW to 521°C; 30KW to 558°C; 20KW to 593°C for 4 minutes; Squeezed and water quenched.
RDO439-8: 70KW to 521°C; 30KW to 558°C; 20KW to 591°C for 0 minute; Squeezed and water quenched.
RDO439-9: 70KW to 521°C; 30KW to 558°C; 20KW to 591°C for 1 minute; Squeezed and water quenched.
RDO439-10: 70KW to 521°C; 30KW to 558°C; 20KW to 591°C for 2 minutes; Squeezed and water quenched.

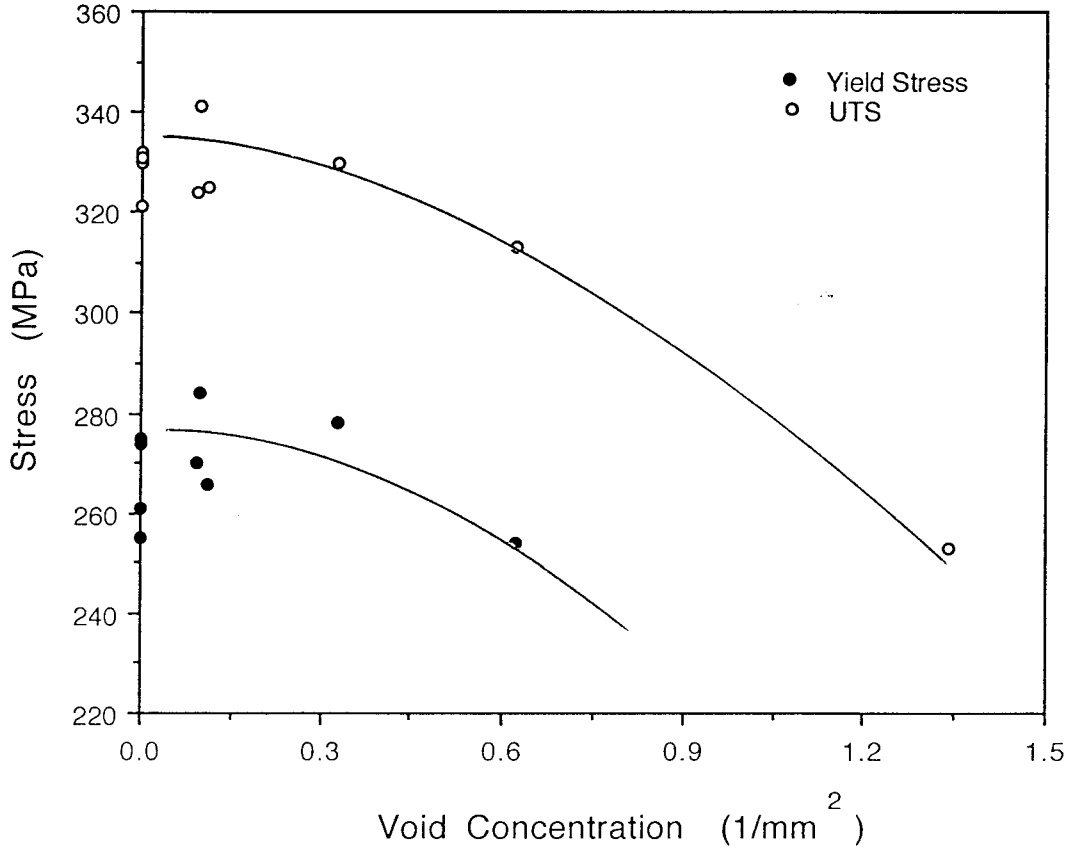

Fig. 81 The relationship between the strength and void concentration of squeezed NWA semi-solid A357 (Alloy #7).

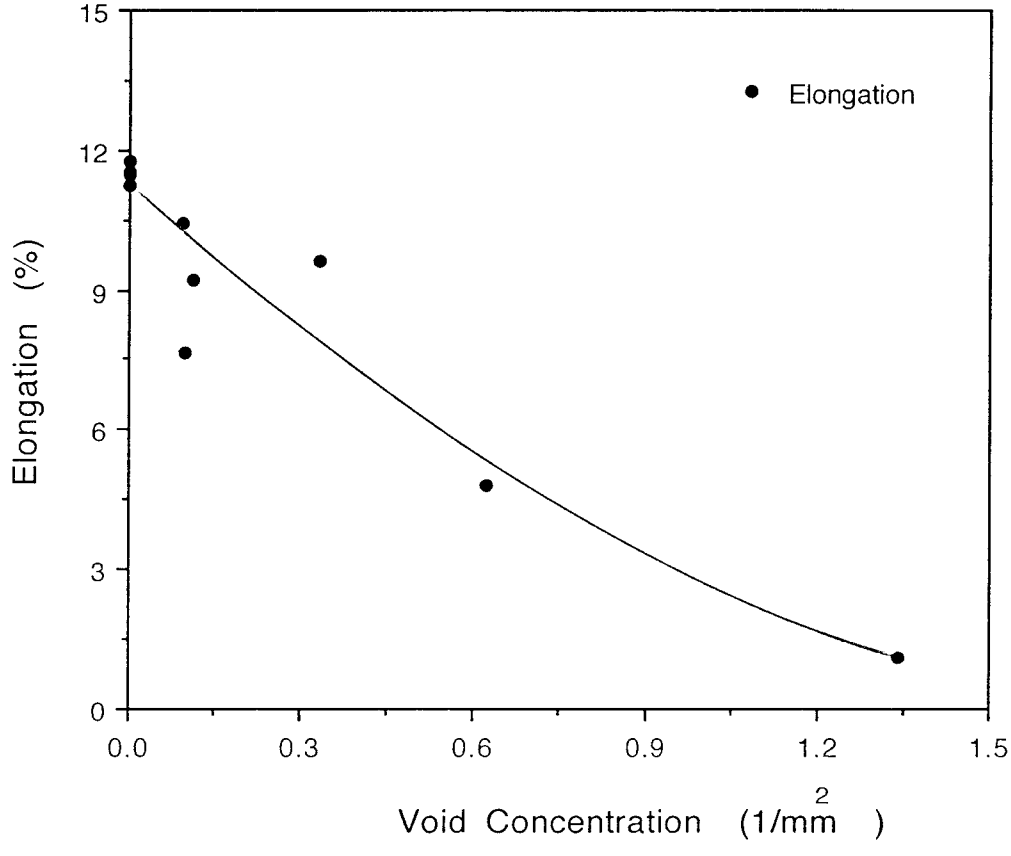

Fig. 82 The relationship between the elongation and void concentration of squeezed NWA semi-solid A357 (Alloy #7).

Table 33. The T6 properties of squeezed semi-solid A357 (Alloy #8) Aluminum alloy.

Sample #	Atmosphere	Semisolid Treatment Cycle	Time after 573°C (min)	Final tempt. (°C)	Time at 588°C (min)	Cool down	Yield Stress (MPa)	UTS (MPa)	Elongation (%)	Reduction at Area (%)	# voids ave. in tensile specimen ($1/mm^2$)	Formability Comment
RDO439-11	Air	*	---	591	0	Water	254	303	13.27	13.27	0	some sag/ excell. form
RDO439-12	Air	*	---	589	0	Water	245	304	12.96	11.05	0	some sag/ excell. form
RDO439-13	Air	*	---	587	0	Water	247	305	8.87	9.21	0.22	very good/ some sag
RDO439-14	Air	*	---	584	0	Water	261	307	6.98	7.46	0.65	good form/ some sag
RDO439-15	Air	*	---	582	0	Water	248	320	12.86	11.69	0	very good/ some sag
RDO439-16	Air	*	---	580	0	Water	248	310	10.18	8.68	0.12	poor/ some sag
RDO439-17	Air	*	---	580	4	Water	260	312	12.20	10.11	0	good form/ excess sag
RDO439-18	Air	*	---	578	4	Water	246	309	9.76	9.19	0.22	good form/ some sag

One sample for each test.

T6: Solution treatment at 538°C for 8 hrs. and water quenched. Kept in refrigerator for 1 hr. after quenched. Precipitation treatment at 154°C for 12 hrs. before testing.

*: Semi-solid Treatment for samples 11-18 of French RDO439 A357 aluminum alloy

RDO439-11: 70KW to 521°C; 30KW to 558°C; 20KW to 591°C for 0 minute; Squeezed and water quenched.

RDO439-12: 70KW to 521°C; 30KW to 558°C; 20KW to 589°C for 0 minute; Squeezed and water quenched.

RDO439-13: 70KW to 521°C; 30KW to 558°C; 20KW to 587°Cfor 0 minute; Squeezed and water quenched.

RDO439-14: 70KW to 521°C; 30KW to 558°C; 20KW to 584°C for 0 minute; Squeezed and water quenched.

RDO439-15: 70KW to 521°C; 30KW to 558°C; 20KW to 582°C for 0 minute; Squeezed and water quenched.

RDO439-16: 70KW to 521°C; 30KW to 558°C; 20KW to 580°C for 0 minute; Squeezed and water quenched.

RDO439-17: 70KW to 521°C; 30KW to 558°C; 20KW to 580°C for 4 minutes; Squeezed and water quenched.

RDO439-18: 70KW to 521°C; 30KW to 558°C; 20KW to 578°C for 4 minute; Squeezed and water quenched.

Table 34. The results of formability of Alloys #9-#12 (DF92-95) perfomed at NWA. (70 kW to 521°C and 30 kW to 556°C)

Alloy #	Final T (°C)	556°C to final T (kW)	Time at final T (min.)	Comments
12	610	20	4	good form/ excess sag
12	607	20	4	not good form/some sag
12	609	20	4	poor form/ sig. sag
12	611	20	2	poor form/ some sag
11	612	20	4	fair form/ sig. sag
11	614	20	4	good/exc.form excess sag
11	610	20	4	fair/marg. form/some sag
11	614	20	2	fair form/ some sag
10	618	20	4	fair form/ small sag
10	620	20	4	good form/ excess sag
10	616	20	4	marg.form/lit tle sag
10	614	20	2	very good form/sig. sag
9	621	20	4	marg. form/ little sag
9	626	20	4	fair/good form/signif. sag
9	628	20	4	very good form/excess sag
9	628	20	2	very good form/sig. sag

the Alloy #11/12 may be related to the grain size, the latter being perhaps a factor of two larger than the former. Some grains in Alloy #11/12 may have been in excess of 200 μm.

Some delayed quench tests were performed as listed in Table 35. This table shows that porosity is associated with slower cooling rates. This is consistent with earlier quenching studies.

Additionally tests were performed on Alloy #7 such that the energy (kw) to 583°C (1081°F) was decreased, thus increasing the time for processing. The formability increased with increasing time to 589°C (1092°F) probably due to longer time above the eutectic thus having the effect of increased time at 589°C (1092°F), increasing formability. This is shown in Table 36.

The Pechiney (Alloy #8) was further studied. The results are listed in Table 37. Basically the quench was delayed various times form 10 to 30 seconds, or an air cool. This was performed for a 0 min. at either a 583 (1082) or 589°C (1092°F) "peak" temperature. Basically, the porosity tends to increase as the hold-time (delay) or cooling time increases. The explanation as to why Alloy #8 tests here are not identical to those in Table 33 (higher yield stress, but lower elongation) is not clear. One possibility is higher hydrogen (see Table 38).

More extensive tests were performed on the ingots of Alloy #13-23. Unlike earlier tests, which were typically 25.4 mm x 25.4 mm x 25.4 mm or 50.8 mm x 50.8 mm x 50.8 mm cube samples extracted from the edge to mid-radius position, whole "hockey puck" ingot samples of these alloys were used to study the formability difference between the outer edge and the center of the ingots because of the different grain sizes. Table 39-40 show the formability test results of as-cast "hockey puck" samples of Alloy #13-22. It is observed that the formability appears to be affected by the forming temperature and time at temperature for a given alloy. The time range of acceptable formability is 2-4 minutes at 588°C (1090°F) for Alloy #13. The temperature range of acceptable formability is 601 -604°C (1114-1120°F) for 2 minutes for Alloy #21, and 561-563°C (1042-1046°F) for 3

Table 35. The results of porosity analysis of Alloys #7 perfomed at NWA. (70 kW to 521°C, 30 kW to 556°C and 20kW to 589°C)

Alloy #	Final T (°F)	Time to squeeze (sec.)	Time delayed to quench (sec.)	Comments
7	589	4	7	nil porosity
7	589	4	15	some porosity
7	589	4	24	some porosity
7	589	4	42	very noticable porosity
7	589	4	air cool	substantial porosity
7	589	not pressed	air cool	significant porosity

Table 36. The effect of heat-up rate on the formability of Alloys #7 perfomed at NWA. (Final temperature is 589°C, idle time at final temperature is 4 min. and power at final temperature is 20 kW)

Alloy (#)	RM to T1 (kW)	T1 to final T (kW)	Total time to final T (min.)	Comments
7	70 kW to 521°C	20 kW to 589°C	2.3	good
7	70 kW to 583°C	20 kW to 589°C	1.5	good
7	50 kW to 583°C	20 kW to 589°C	3.2	better
7	30 kW to 583°C	20 kW to 589°C	4.25	better
7	20 kW to 583°C	20 kW to 589°C	5.5	very good
7	15 kW to 583°C	20 kW to 589°C	9.5	very good
7	14 kW to 587°C	20 kW to 589°C	11.5	excellent

Table 37. The T6 properties of squeezed semi-solid A357 (Alloy #8) Aluminum alloy.

Sample #	Atmosphere	Semisolid Treatment Cycle	Time after 573°C (min)	Final tempt. (°C)	Time at 588°C (min)	Total Time to Quench (sec.)	Cool down	Yield Stress (MPa)	UTS (MPa)	Elongation (%)	Reduction at Area (%)	# voids ave. in tensile specimen ($1/mm^2$)
RDO451-1	Air	*	---	589	0	10	Water	286	312	5.85	6.81	0.51
RDO451-2	Air	*	---	589	0	20	Water	286	310	5.71	5.54	0.73
RDO451-3	Air	*	---	589	0	11	Water	281	287	1.22	1.42	1.43
RDO451-4	Air	*	---	589	0	30	Water	278	305	6.33	6.15	0.50
RDO451-5	Air	*	---	589	0	3	Air Cool	279	287	3.27	4.86	1.11
RDO451-6	Air	*	---	583	0	10	Water	288	320	8.91	7.09	0.35
RDO451-7	Air	*	---	583	0	20	Water	290	322	7.32	7.31	0.47
RDO451-8	Air	*	---	583	0	30	Water	290	316	9.91	8.84	0.41
RDO451-9	Air	*	---	583	0	3	Air Cool	-----	224	0	1.87	1.50

One sample for each test.
T6: Solution treatment at 529°C for 3 hrs and water quenched. Delayed in air for 8 hrs after quenched. Precipitation treatment at 177°C for 7 hrs. before testing.

*: Semi-solid Treatment for samples 1-9 of RDO451 A357 aluminum alloy
RDO451-1: 70KW to 521°C; 30KW to 556°C; 20KW to 589°C for 0 minute; 3 sec. to squeeze.
RDO451-2: 70KW to 521°C; 30KW to 556°C; 20KW to 589°C for 0 minute; 7 sec. to squeeze.
RDO451-3: 70KW to 521°C; 30KW to 556°C; 20KW to 589°C for 0 minute; 3 sec. to squeeze.
RDO451-4: 70KW to 521°C; 30KW to 556°C; 20KW to 589°C for 0 minute; 7 sec. to squeeze.
RDO451-5: 70KW to 521°C; 30KW to 556°C; 20KW to 589°C for 0 minute; air cooled.
RDO451-6: 70KW to 521°C; 30KW to 556°C; 20KW to 583°C for 0 minute; 3 sec. to squeeze.
RDO451-7: 70KW to 521°C; 30KW to 556°C; 20KW to 583°C for 0 minute; 7 sec. to squeeze.
RDO451-8: 70KW to 521°C; 30KW to 556°C; 20KW to 583°C for 0 minute; 7 sec. to squeeze.
RDO451-9: 70KW to 521°C; 30KW to 556°C; 20KW to 583°C for 0 minute; air cooled.

Table 38. The results of hydrogen analysis of some A356 and A357 alloys used in this study.

Alloy #	Bulk Hodrogen (ppm)
2	0.05
4	0.32
8	0.18

Bulk Hydrogen = Total Hydrogen-surface Hydrogen

Table 39. The results of formability of as-cast Alloy #13-20 "hockey puck" samples perfomed at NWA.

Alloy #	Final T (°C)	Heating Process (kW)	Time at final T (min.)	Total Time to quench (sec.)	Formability Comments
13	588	30 to 583°C 16 to 588°C	1	10	unaccept form less sag.
13	588	30 to 583°C 16 to 588°C	1.5	10	marg./unaccept form, less sag.
13	588	30 to 583°C 16 to 588°C	2	10	fair/marg. form some sag.
13	588	30 to 583°C 16 to 588°C	2.5	10	fair form. some sag.
13	588	30 to 583°C 16 to 588°C	3	10	good form. some sag.
13	588	30 to 583°C 16 to 588°C	4	10	very good/ excellent form. some sag.
15	588	30 to 583°C 16 to 588°C	4	10	unaccept form. less sag. very good toward the outer edges.
16	588	30 to 583°C 16 to 588°C	3	10	perimeter easily form, sig. sag.
17	588	30 to 583°C 16 to 588°C	3	10	perimeter easily form, sig. sag.
18	588	30 to 583°C 16 to 588°C	4	10	perimeter easily form, maybe overshot tempt.
20	613	30 to 521°C 15 to 559°C 30 to 613°C	2	10	very good/ excellent form. sig. sag.
20	611	30 to 521°C 15 to 559°C 30 to 611°C	2	10	very good/ excellent form. sig. sag.

Table 40. The results of formability of as-cast Alloy #21-23 "hockey puck" samples perfomed at NWA.

Alloy #	Final T (°C)	Heating Process (kW)	Time at final T (min.)	Total Time to quench (sec.)	Formability Comments
21	606	30 to 521°C 15 to 559°C 30 to 606°C	2	10	excellent form. sig. sag.
21	603	30 to 521°C 15 to 559°C 30 to 603°C	2	10	excellent form. sig. sag. slightly more resistance to form
21	601	30 to 521°C 15 to 559°C 30 to 601°C	2	10	very good form. some sag. slightly more resistance to form
22	566	30 to 563°C 16 to 566°C	3	10	stiff unaccept form. too much melt
22	563	30 to 559°C 16 to 563°C	3	10	better, may be acceptable form
22	561	30 to 558°C 16 to 561°C	3	10	better, may be acceptable form. may still be a little stiff
23	563	30 to 559°C 20 to 563°C	3	10	good form but excess liquid
23	561	30 to 493°C 20 to 561°C	3	10	marginal form

minutes for Alloy #22. It is also observed that the formability at outer edge is usually better than that in the center for the puck samples, which implied perhaps a difference in grain size across the diameter. In order to improve the effect of grain size on the formability of puck ingot samples, either of two heat treatments was performed to obtain uniform grain size before semi-solid treatment : annealing (annealed at 413°C (775°F) for 1 hour, slow cool 27.8°C (50°F) per hour to 260°C (500°F)) or homogenization (homogenizated at 499°C (930°F) for 8 hours). The results of annealed and homogenized puck samples of Alloy #13,14-20 are listed in Table 41-42. It is observed that the formability difference between the center and outer edge of annealed or homogenized puck samples is not completely eliminated compared with as-cast samples, which implied that other factors (i.e., temperature gradient in heating and forming processes) may affect the formability difference of puck samples. Additional formability experiments were also performed on 50.8 mm x 5.08 mm x 50.8 mm and 50.8 mm x 5.08 mm x 25.4 mm samples of Alloy #19. The results listed in Table 43 revealed that there is not significant difference in formability between the two sample sizes, which indicates that the formability is not sensitive to the sample size smaller than 50.8 mm x 5.08 mm x 50.8 mm.

Finally, a part was produced by HMM in Arkansas using both Pechiney and NWA 357 ingot. The ingot diameters were 3.0" and 2.9" respectively, and the composition were similar to Alloy #8 and #7. The results of tensile tests are listed in Table 44. The mechanical properties of the NWA and Pechiney parts are essentially identical. This, of course, suggests that thermal treatment to produce a spheroidal microstructure is an alternative effective method to electromagnetic stirring.

Table 41. The results of formability of Alloy #14-22 annealed "hockey puck" samples perfomed at NWA. (annealed 1 hour at 413°C, slow cool 27.8°C per hour to 260°C)

Alloy #	Final T (°C)	Heating Process (kW)	Time at final T (min.)	Total Time to quench (sec.)	Formability Comments
14	588	30 to 583°C 16 to 588°C	2	10	fair/ marg. form. some sag. edge very soft.
14	588	30 to 583°C 16 to 588°C	3	10	fair form. some sag. Center stiff, perimeter very easily formed
14	588	30 to 583°C 16 to 588°C	4	10	good form. some sag. Center stiff, perimeter very easily formed
20	613	30 to 521°C 15 to 559°C 30 to 613°C	2	10	very good/ excellent form. sig. sag.
20	611	30 to 521°C 15 to 559°C 30 to 611°C	2	10	very good/ excellent form. sig. sag.
21	601	30 to 521°C 15 to 559°C 30 to 601°C	2	10	very good form. some sag. slightly more resistance to form
21	601	30 to 521°C 15 to 559°C 30 to 601°C	4	10	excellent form. some sag.
22	561	30 to 556°C 16 to 561°C	3	10	unacceptable form

Table 42. The results of formability of Alloy #14-23 homogenized "hockey puck" samples perfomed at NWA. (homogenized at 499°C for 8 hours)

Alloy #	Final T (°C)	Heating Process (kW)	Time at final T (min.)	Total Time to quench (sec.)	Formability Comments
14	588	30 to 583°C 16 to 588°C	2	10	fair/ marg. form. some sag.
14	588	30 to 583°C 16 to 588°C	3	10	good form. some sag.
14	588	30 to 583°C 16 to 588°C	4	10	very good form. some sag. Center stiff, perimeter very easily formed
20	613	30 to 521°C 15 to 559°C 30 to 613°C	2	10	very excellent form. sig. sag.
20	611	30 to 521°C 15 to 559°C 30 to 611°C	2	10	excellent form. sig. sag.
21	601	30 to 521°C 15 to 559°C 30 to 601°C	3	10	good/very good form. some/sig.sag.
21	561	30 to 556°C 16 to 561°C	4	10	excellent form. some/sig. sag.
22	563	30 to 559°C 22 to 563°C	3	10	marginal, some shearing.
23	563	70 to 493°C 22 to 552°C 15 to 563°C	4	10	good form but excess liquid

Table 43. The results of formability of as-cast Alloy #19 samples perfomed at NWA.

Alloy #	Final T (°C)	Heating Process (kW)	Time at final T (min.)	Total Time to quench (sec.)	Formability Comments
19*	588	30 to 583°C 16 to 588°C	4	10	fair/good form. some sag.
19*	591	30 to 583°C 16 to 591°C	4	10	good form. some sag.
19**	591	30 to 583°C 16 to 591°C	3	10	fair/good form. some sag.
19**	591	30 to 583°C 16 to 591°C	4	10	very good form. some sag.

*: sample size: 50.8 mm x 5.08 mm x 50.8 mm
**: sample size: 50.8 mm x 5.08 mm x 25.4 mm

Table 44. The T6 properties of casted semi-solid A357 (Alloy #7 and #8) Aluminum alloys.

Sample #	Atmosphere	Semisolid Treatment Cycle	Time after 573°C (min)	Final tempt. (°C)	Time at 588°C (min)	Cool down	Yield Stress (MPa)	UTS (MPa)	Elongation (%)	Reduction at Area (%)	Alloy #	# voids ave. in tensile specimen ($1/mm^2$)
#8 -1'	Air	---	---	---	---	Water	38.6	44.1	13.8	17.96	8	0
#8 -2'	Air	---	---	---	---	Water	37.7	45.3	11.3	15.09	8	0
#8 -3''	Air	---	---	---	---	Water	34.7	40.5	4.53	7.86	8	0.53
#7 -1''	Air	---	---	---	---	Water	43.0	50.4	5.78	9.89	7	0.48
#7 -2'	Air	---	---	---	---	Water	47.9	53.3	9.43	9.62	7	0
#7 -3'	Air	---	---	---	---	Water	46.9	53.2	10.3	12.29	7	0
#7-4'	Air	---	---	---	---	Water	39.2	45.5	12.2	17.33	7	0

Two samples for each test.
*: Flat specimens.
**: Cyclinder specimens.
T6 (for specimens of #8-1, #8-2, #8-3 and #7-2):
Solution treatment at 529°C for 3 hrs and water quenched. Delayed in air for 8 hrs after quenched. Precipitation treatment at 177°C for 7 hrs. before testing.

T6 (for specimens of #7-1 and #7-3):
Solution treatment at 538°C for 8 hrs. and water quenched. Kept in refrigerator for 1 hr. after quenched. Precipitation treatment at 154°C for 12 hrs. before testing.

T6 (for specimens of #7-4):
Solution treatment at 529°C for 4 hrs and water quenched. Delayed in air for 8 hrs after quenched. Precipitation treatment at 154°C for 5 hrs. before testing.

Chapter IV.

CONCLUSIONS

1. A new 6xxx alloy, designated as AA6069 with 2% Mg+Si, 1% Cu, 0.2% Cr and 0.1% V, has been developed for application in hot and cold extrusion and forging.

2. The homogenization studies indicates that the T6 properties of AA6069 are not dramatically sensitive to the changes in heating-rate, soak time and cool-down time for the alloy. However, it appears that the rapid heat-up times and slower cool-down times may provide the best T6 properties.

3. The results of T6 study of AA6069 show that precipitation temperature of 166-177°C may provide a best combination of strength and ductility after a 16-24 hour aging.

4. The tensile test results of cold and hot extrusions of hollow wall, bars, gas canister and high pressure cylinders indicate that the T6 properties ranged from 55-70 ksi (380-490 MPa) UTS, 50-65 ksi (345-450 MPa) yield strength, and 10-18% elongation.

5. The results of fatigue and corrosion-fatigue tests show that the properties of fatigue and corrosion-fatigue of AA6069 T6 extrusions are superior to those of 6061 T6 extrusions.

6. The improved properties are probably the results of increase solute, such as Mg, Si and Cr leading to greater precipitation amounts.

7. The improved properties are probably the result of increase solute, such as Mg, Si and Cu, leading to greater precipitate amounts.

8. Spheroidal semi-solid microstructures are formed in aluminum-silicon alloys (356, 357) by purely thermal treatment. The formation of a semi-solid aluminum-silicon A357 starts from melting at the grain boundaries. The heat-up rate does not greatly affect the subsequent semi-solid microstructure. The cooling rate does not affect the size and shape of the spheroidal solid phase. The semi-solid microstructure obtained in this study is similar to those obtained from continuous stirred casting.

9. The grains of the solid phase of A357 grow but the shape does not greatly change with increasing time at isothermal temperatures of 579°C-588°C (1075°F to 1090°F). The mechanism of coarsening of the solid phase is related to Ostwald ripening and/or coalescence of particles.

10. There are three heat-up stages associated with heating semi-solid A356 and A357 aluminum alloys. Stage I is related to the heating of the alloy in the solid state. Stage II is related to the eutectic reaction. Stage III is related to the heating of the semi-solid slurry. Stage II can be a dominant stage which requires the longest time of the three heat-up stages. An increase of furnace temperature can greatly reduce the time of stage II.

11. The atmosphere (vacuum, air, argon) of the semi-solid treatment does not greatly affect the T6 properties of semi-solid A356 aluminum alloy. The microstructure and T6 properties of semi-solid A356 aluminum alloy do not appear sensitive to the homogenization treatments befor semi-solid treatment.

12. Voids are an important defect in semi-solid A356 and 357 aluminum alloys. Three types of voids are observed in the semi-solid samples. Type I voids, found in the water quenched samples, are surface voids which cause a poor surface quality. Type II voids, found in the air cooled and liquid nitrogen quenched samples may be the shrinkage porosity. Type III voids, mainly existed in the entrapped liquid phase, are relatively small voids and are observed in all air cooled, water quneched, and liquid nitrogen quenched samples. The mechanical properties of A356 aluminum alloy decrease as the number of voids (especially Type II void) increases.

13. Type II, principally, and Type III voids are found in the press formed parts of A356 aluminum alloy. The voids are concentrated in the central volume of the parts which has the lowest cooling rate. T6 properties of A356 press formed parts appear to be influenced by the concentration of Type II voids; the lower the concentration of voids, the better the T6 properties.

14. A356 and A357 aluminum alloys can be effectively formed over a temperature range. The formability of Pechiney stressed semi-solid appears to occur over a wider temperature range and shorter times at the forming temperature. This is due to the pre-formed refined semi-solid structure.

15. The formability of A357 may be improved as the the ingot size decreases. This is because the smaller spheroidal particles are associated with smaller grain size.

16. The results of delayed quench tests indicate that the the porosity of pressed semi-solid aluminum alloys increases as the cooling rate after forming decreases, which is consistent with the results of earlier void studies.

17. The formability studies of A357 "hockey puck" samples that comprise the entire diameter of an ingot reveal that the formability at outer edge is usually better than that in the center for the puck samples. This may be related to the difference in grain size across the diameter and other factors (i.e., temperature gradient in heating and forming processes).

18. The mechanical properties of pressure formed parts of NWA and Pechiney are essential identical, which suggests that thermal treatment to produce a spheroidal microstructure is an effective method as electromagnetic stirring in industrial production.

BIBLIOGRAPHY

1. *Aluminum Standards 1988*, Aluminum Society of America, Washington, DC, 1988.

2. *Aluminum Vol. III Fabrication and Finishing*, Kent R. Van Horn, ASM, Metals Park, OH, 1976.

3. *The Metallurgy of Aluminum and Aluminum Alloys*. Robert J. Anderson (ed.), Henry Carey Baird & Co., Inc. New York, 1925.

4. *Aluminum Vol. I Properties, Physical Metallurgy and phase Diagrams*, Kent R. Van Horn, ASM, Metals Park, OH, 1976.

5. *Aluminum Properties and Physical Metallurgy*, J.E. Hatch (ed.), ASM, Metals Park, OH, 1984.

6. *Aluminum and Its Alloys*, Frank King (ed.), Ellis Horwood, LTD. England, 1987.

7. J.R. Davis, *Aluminum and Aluminum Alloys*, ASM, Metals Park, OH, 1993.

8. W.B. Pearson , *Handbook of Lattice Spacing and Structures of Metals and Alloys*, Vol.2, Pergamon Press, 1967.

9. L.F. Mondolfo (ed.), *Aluminum Alloys: Structure and properties.*, Butter Worths, England, 1976.

10. W. Hume-Rothery and G.V. Raynor, *The Structure of Metals and Alloys,* The Institute of Metals, 1962.

11. L.R. Morris et al., *Formability of Aluminum Sheet Alloys: Aluminum Transformation Technology and Applications.* American Society for Metals, 1982.

12. T.H. Standers, Jr. and J.T. Staley, *Review of Fatigue and Fracture Research on High-Strength Aluminum Alloy, Fatigue and Microstructure,* American Society for Metals, 1979, pp. 467-522.

13. I.J. Polmear, *Light Alloys,* London, Edward Arnold, 1981.

14. W.E. Cooke and R.C. Spooner, *Australian Institute of Metals Journal,* Vol. 9, 64, pp. 80.

15. D. Altenpohl, *Aluminum Viewd From Within, Aluminum-Verlag*, Dusseldorf, 1982.

16. T.F. Bower, H.D. Brody, and M.C. Flemings, *Army Materials Research Agency Contract DA-19-020-ORD-5706A*, Frankford Arsenal, Philadelphia, 1964.

17. D. Altenpohl, *Zeitschrift fur Metallkunde*, Vol. 56, 1965, pp. 653-663.

18. W.L. Fink and L.A. Willey, *Transactions of AIME*, Vol.175, 1948, pp.414-427.

19. J.W. Evancho and J.T. Staley, *Metallurgical Transactions A*, Vol.5, Jan. 1974, pp.43-47.

20. J. Katz, *Metal Progress*, Feb. 1966, pp.70-72.

21. S.E. Axter, Tech Paper CM-80-409 Society of Manufacturing Engineers, 1980.

22. C.E. Bates, *J. Heat Treat.*, Vol. 5 (No.1), 1987, pp. 27-40.

23. T. Croucher, *Heat Treat.*, Vol. 19 (No.12), Dec. 1987, pp. 21-25.

24. J. T. Staley, *Industrial Heating XLIV,* Oct. 1977, pp. 6-9.

25. G.F. Bobart, *J. Heat Treat.,* Vol. 6 (No. 1), 1988, pp. 47-52.

26. I. Kirman, *Metallurgical Transaction A,* Vol. 2, 1971,, pp. 1761-1770.

27. J.T. Staley, *Microstructure and Toughness of High-Strength Aluminum Alloys, ASTM STOP 605,* American Society for Testing and Materials, 1976, pp. 71-103.

28. D.S. Tompson, S.A. Levy, and G.E. Spangler, *Thermomechanical Aging of Aluminum Alloys I and II, Aluminum,* Jan., 1974, pp. 647-649.

29. E. H. Dix, Jr., *Transactions of ASM,* Vol. 35, 1944, pp. 130-155.

30. H.Y. Hunsicker, *Metallurgical Transactions A,* May, 1980, pp. 759-773.

31. J.T. Staley, R.H. Brown, and R. Schmidt, *Metallurgical Transactions A,* Vol. 3, 1972, pp.191-199.

32. G.T. Hahn and A.R. Rosenfield, *Metallurgical Transactions A,* Vol. 6A, April, 1975, pp.653-670.

33. D. B. Spencer,R. Mehrabian and M. C. Flemings, *Metall.Trans. A*, vol.3, 1972, pp 1925-1932.

34. M.P. Kenney, J.A. Courtois, R.D. Evans, G. M. Farrier, C.P. Kyonka, A.A. koch and K.P. Young, *Metals Handbook,9th ed.*, ASM International, Metals Park, OH,1988, vol.15, pp327-338.

35. H. LeHuy, J. Masounave and J. Blain, *J. Mater.Sci.,* vol 20(no.1), Jan 1985, pp105-113.

36. F.C. Bennett, *U.S. Patent 4,116,423,* 1978.

37. K.P. Young, R.G. Riek, J.F. Boylan, R.L. Bye, B.E. Bond and M.C. Flemings, *Trans. AFS,* vol.84, 1976, pp169-174.

38. K.P. Young, R.G. Riek,and M.C. Flemings, *Met.Technol.* vol.6(no.4), April 1979, pp1130-137.

39. B. Toloui amd J.V. Wood, *Biomedical Materials*, vol.55, Materials Reserach Society, 1986.

40. J. Cheng, D. Apelian and R.D. Doherty, *Metall. Trans.A,* vol.17A(no.11) Nov.1986, pp2049-2062.

41. M.C. Flemings, *Metall. Trans.A.* vol.22A, May 1991, pp957-981.

42. R.B. Bird, W.E. Stewart and E.N. Lightfoot. *Transpart Phenomena,* John Wiley and Sons, New York, 1960.

43. A. Vogel, R.D. Doherty and B. Cantor, *Proc. Conf. on Solidification and Casting of Metals,* Sheffiekd, 1977, pp518. Metals Soc. Lond (1979).

44. R.D. Doherty, H.I. Lee and E.A. Feest. *Mater. Sci. Engng.* Vol.65,1984, pp182-189.

45. A. Vogel and B. Cantor, *J. Crystal Growth,* Vol.37, 1976,pp139.

46. R.A. Joly and R. Mehrabian, *J. Mater.Sci.,*Vol.11, 1976, pp1393.

47. R.D. Doherty, Met. Sci., Vol.16, 1982,pp1.

48. H.-I, Lee, R.D. Doherty, E.A. Feest and J.M. Titchmarsh, in *Solidification Technology in the Foundry and Casthous*, Metals Society, London, 1983, pp119.

49. N. Apaydin, K.V. Probhakar and R.D. Doherty, *Mater. Sci. Eng.*, VOl.46, 1980, pp145-150.

50. G. Herrman, H. Gleiter and G. Baro, *Acta Metall.*, No.24, 1976, pp353.

51. G. Herrman, H. Gleiter and G. Baro, *Acta Metall.*, No.25 1977, pp467.

52. R.J. Smeulders, F.H. Mischgofsky and H.J. Frankena, *J. Crystal Growth*, Vol. 76. 1986,pp151-169.

53 H. Garabedian and R.F. Strickland, *J. Crystal Growth*, Vol.22, 1974,pp188-192.

54. A.Vogel, *Met.Sci.*, Vol.12, 1978, pp567-578.

55. T..Z. Kattamis, J.C. Coughlin and M.C. Flemings, *Trans, AIME*, Vol.239, 1967, pp1504-1511.

56. G. Wan and P.R. Sahm. *Acta metall.* Vol.38. No.11,1990, pp 2367-2372.

57. G. Wan and P.R. Sahm. *Acta Metall. Mater.* vol.38, No.6,1990. pp967-972.

58. W. Ostwald, *J. Phys. Chem,* 34, 1990, pp 495.

59. I.M. Lifshitz and V.V. Slyozov, *J. Phys. Chem.* Solids 19, 1960, pp35.

60. C. Wagner, *Z. Elektrochem.* 65, 1961, pp581.

61. H.A. Panes, J. F. Hutton and K. Waltus, *An Introduction to Rheology*, Elsevier Science Publishers, New York, NY, 1989.

62. L. Ratke and W.K Thieringer. *Acta Metall.* 33, 1985, pp1793.

63. D.S. Buist, B. Jackson, I.M. Stempenson, W.F. Ford and J/ White, *Trans. Br. Ceram. Soc.* 64, 1965, pp173.

64. R. Warren, *J. Mater. Sci.* Vol.3, 1968, pp471.

65. R. Warren, *J. Mater. Sci.* Vol.7, 1972, pp1434.

66. R. Warren and M.B. Waldron, *Power Metall.* Vol. 15, 1972, pp166.

67. R. Watanabe and Y. Masuda, *Trans. Japan Inst. Metals*, No.14,1973, pp320.

68. R. Watanabe and Y. Masuda, *Sintering and Catalysis,* (edited by G.C. Kyczyski), pp389, Plenum Press, New York, 1975.

69. T.K. Kang and D.N. Yoon, *Metall. Trans,* A9, 1978, pp433.

70. A.N. Niemi and T.H. Courtney, *J. Mater. Sci.* Vol 16, 1981, pp 226.

71. S. Takajo, W.A. Kaysser and G. Petzow. *Acta Metall.* vol32, No.1, 1984, pp107-113.

72. W.A. Kaysser, S. Takajo and G. Petzow. *Acta Metall.* Vol.32, No.1, 1984, pp115-122.

73. H.-K. Moon, *Ph.D. Thesis*, Massachusetts Institute of Technoloty, Cambridge, MA, 1990.

74. P.A. Joly and R. Meharbian, *J. Mater.Sci.*, Vol. 11, 1976, pp1393-1418.

75. J. M. Molenaar, L. Katgerman, W. H. Kool and R.J. Smeulders, *J. Mater. Sci.*, Vol 21, 1986,pp389-394.

76. T.Z. Kattamis and T.J. Piccine, *Mater.Sci. Eng.*, vol. A131,pp265-272, 1991.

77. A. Shibutani, K. Arihara and Y. Nakamura, *Tetsu-to-Hagane*, Vol.66,1980,pp1550-1556.

78. K. Miwa and R. Ichikawa, *J, Japan, Inst. Met.*, vol.45, 1981, pp853-859.

79. K. Chizawa and S. Fukuoka: *J. Fas. Eng. Univ. Tokyo*, vol. 33(2), 1975, pp149-166.

80. R. Ichikawa snd K. Miwa, *J. Japan, Inst. Met.*, Vol.45, 1981, pp189-193.

81. N. Mori, K. Ogi, and K. Matsuda, *J. Japan. Inst. Met.,*Vol.48, 1984, pp936-944.

82. K. Chizawa and S. Ishizuka,*Trans. Japan. Inst. Met.*,Vol.28(2), 1987, pp145-153.

83. K. Chizawa ,S. Ishizuka and Y, Kinoshita,*Trans. Japan. Inst. Met.*, Vol.29(7), 1988, pp598-607.

84. K. Chizawa ,S. Ishizuka and Y, Kinoshita,*Trans. Japan. Inst. Met.*, Vol.28(2), 1988, pp135-144.

85. M.A. Taha, N. A. Mahallawy, M. Lofty Zamzam and S. El-Mardy, *Solidification Processing 1987*, Institute of Metals, London, pp409-412.

86. H. Lehuy, J. Masounave and J. Blain, *J. Mater. Sci.*, Vol.20, 1985, pp105-113.

87. H.I. Lee, *Ph.D. Thesis*, University of Sussex, Sussex, United Kingdom, 1982.

88. N. Wang, G. Shu and H. Yang: *Proc. Int. Symp. on New Developments in Cast Alloy Technology,* B. Liu and J. Liu eds., Luoyang, P.R.China, 1988.

89. J.P. Gabathular, D. Barras, Y. Krahenbuhl, J.C. Weber, *2nd Int. Conf. on Semi-Solid Processing of Alloys and Composites,* MIT, Cambridge, Mass., USA,1992.

90. S. Bercovici, German Patent no. 2514355,1975.

91. T.A. Engh, *Principals of Metal Refining*, Oxford Science Pub., Oxford, U.K.,1922, pp390-397.

92. L. Backerud, *"Grain Refining and Structure Modification"*, Aluminum Alloy Technology Proceedings, Trondheim, Norway, 1991.

93. G. Wan, T. Witulski, and G. Jirt, *La met. ita.* 86,1994, pp.29-36.

94. W.J. Boettinger et al., Metall. Trans. A, 15, 1984, pp. 55

95. J.L. Kirby, *Aluminum Alloys-Physical and Mechanical Properties*, E.A. Starke, Jr. and T.H. Sanders, Jr., eds., EMAS, West Midlands, U.K., 1986, pp.61-79.

96. H. Yu and D.A. Granger, *Aluminum Alloys-Physical and Mechanical Properties*, E.A. Starke, Jr. and T.H. Sanders, Jr., eds., EMAS, West Midlands, U.K., 1986, pp.17-19.

97. Reynolds Aluminum Co., *Reynolds Aluminum Bulletin No. 279*, March 1983.

98. Koon-Hall Testing Corp., Portland, OR, March 1994.

99. R.S. Kaneko, L. Barkow, and E.W. Lee, *J. Met.*, Vol. 42, 1990, pp.16-18.

100. G. Bhuyan, Powertech, Vancouver, Canada, private communication, August, 1994.

101. Y.S. Yand and C-Y. A. Tsao. *Scri. Metal et Mater.* Vol.30, No.12,1994, pp1541-1546.